Lead, piRNAs, and the Heart: Sex-Specific Molecular and Functional Effects of Developmental Lead Exposure in Mouse Models and Human iPSC-Cardiomyocytes

By

Kimberley E. Sala-Hamrick

A dissertation submitted in partial fulfillment
of the requirements for the degree of
Doctor of Philosophy
(Toxicology)
at the University of Michigan
2026

Doctoral Committee:
Assistant Professor Laurie K. Svoboda, Chair
Associate Professor Justin A. Colacino
Professor Dana C. Dolinoy
Research Assistant Professor Andre Monteiro da Rocha
Research Assistant Professor Bambarendage P.U. Perera

Kimberley Elizabeth Hanna Sala-Hamrick

kimbeliz@umich.edu

ORCID iD: 0000-0002-8870-5296

© Kimberley Elizabeth Hanna Sala-Hamrick 2026

Dedication

For Josh, you continue to inspire me to make a positive difference in this world every day.

Acknowledgements

This work was funded by three years of the Environmental Toxicology and Epidemiology (ETEP) training grant (T32 ES0077062) as well as by National Institutes of Health grants: R35 ES031686**,** P30 ES017885, and K01 ES03204812. Further funding was obtained from the Michigan Biological Research Initiative on Sex Differences in Cardiovascular Disease. ChatGPT (open AI 2024 and 2025 version) was used for coding assistance and language improvement in this manuscript. I would also like to thank University of Michigan Advanced Genomics Core for sample processing for these studies.

I have so much gratitude to offer to so many that made not only my research, but my growth as an individual and a scientist possible. Thank you to my committee for their supervision and encouragement. To Dr. Laurie Svoboda, for her leadership, mentorship, and guidance the past 5 years—you have been a constant source of encouragement and someone I look up to. Dr. Dana Dolinoy, thank you for imparting so much knowledge, wisdom, and inspiration. I hope to be a superwoman like you two one day. Dr. Justin Colacino, and Dr. Pini Perera: your support, leadership, and examples you have set for me have made me into a better scientist and human. Dr. Andre Monteiro da Rocha, thank you for teaching me so much about the heart and helping me troubleshoot lab problems.

Dr. Kai Wang, I cannot thank you enough for your mentorship and patience as we coded together throughout the years. I have learned so much from you not only for aim 1, but also skills that I applied to coding for aims 2 and 3 from you. And thank you for not making fun of me

when I came to you with an issue and it was just missing quotation marks in my code. To Kai's mentor, Dr. Maureen Sartor, thank you for your feedback and guidance on the piRNA sequencing project. And to Minghua Li, thank you for your coding support and I'm excited to work with you more!!

Thank you to all the lab managers that have supported this work. Tamara Jones, thank you for keeping orders organized, lab safety in check, and knowing all the details about just about everything. Anagha Tapaswi, you also know just about everything and I can't thank you enough for your hard work on the RNA sequencing projects done here. Chris Clark, your enthusiasm about science is infectious and I loved our brainstorming sessions. Isabelle Melis, thank you for being such a great lab mate and friend and helping me through so much troubleshooting—while my western blots didn't make it to this thesis they're going to be foundational in my future career (I hope). Team mouse: including but not limited to Junru Pan, Dr. Rachel Morgan, Dr. Katelyn Polemi, Dr. Kari Neier, and Dr. Christine Rygiel, thank you for your time and dedication towards making the mouse projects a success.

To other members of the DoGoodS-Pi Epigenetics Research Group, it has been an honor working with you. Esha Shah, you rocked that 442 replicate— I appreciate your endless curiosity, and I can't wait to see what you do for your defense. Jennifer Smith and Amber Siglin, being able to mentor people like you with your passion and joy for science has been delightful and made me a better mentor and scientist. To other rotating member of the Svoboda lab: Julia Ginter-Berriman, Mikayla Speights, Hannah Joo, Isabel Kluszynski, and Halle Fink, I have learned so much from mentoring you and I hope you enjoyed your experiences as much as I did. Dr. Lauren Ward and Dr. Tomoko Ishikawa: you've been in it with me from the beginning until (almost) the end, and I could not have asked for better cohort mates and lifelong friends. Lauren,

thank you for your endless empathy--I can't promise you I will not ever need you to come over and take care of me and my dishes again. Tomoko, you are so amazing at laboratory work I refer to you as a "machine." You two mean so much to me and I love you both.

The past 5 years, the EHS department and the school of public health have taught me so much and given me the opportunity to grow as a person. Being a leader in DSPMP and ESHA and involved in Black and Pink and working to better the department, local communities, and world has connected me with so many passionate individuals seeking to make a positive difference in the world, you know who you are and I thank you.

Thank you to the List lab at Wayne State University for taking on a young woman curious about science and teaching her the ropes. I didn't realize then it would gain me a family. Thank you to my undergraduate lab, the Hammer lab for laying the groundwork and sparking my curiosity.

Phil, you probably don't know how many morning experiments I would have not gotten done had you not called me to wake me up on early mornings. Thank you for listening to me explain science to you and thank you for bringing to so much joy into my life these past two and a half years.

I am a person with the honor of having many close friends all of whom I will not name but who have given me the fuel I needed to complete this PhD. We all need different forms of social engagements in our lives, and between board game days, to running, to concerts, to bird watching excursions I am lucky to have so many friends that keep me going. Erin, Erica, and Tilly, thank you for continuing to make our 15+ year friendships a priority, for your constant support, and for going on yearly adventures in the summers together. All of you are beautiful humans that have made my life so full.

Bumi and Aang, you are my sweetest boys and I appreciate your need to join my zoom calls. You have played an instrumental role in comforting me throughout my PhD.

Lastly and most importantly, thank you to my family for supporting me throughout my life to follow my passions and giving me the tools I need for success. Dad and Adele, your constant support means so much to me. Kelsey, your drive and passion for making the world better inspires me. I have always and will always look up to you, and I hope to be the kind of professor you are. Mom, thank you for sparking my curiosity about biology from an early age, and for helping me trust the process. I love you so much mom, and you both sparked my interests in science and social justice and gave me the tools and confidence to get my PhD. My family is my rock, and they have allowed me to follow my dreams and never give up. Thank you.

Table of Contents

Dedication ii

Acknowledgements iii

List of Tables x

List of Figures xi

List of Abbreviations xiv

Abstract xvii

Chapter 1: Introduction 1

1.1: Cardiovascular Disease 1

1.2: Lead Exposure and CVD 3

1.3: Epigenetics 7

1.4: Developmental Origins of Health and Disease 8

1.5: Small non-coding RNA 9

1.6: piRNA 10

1.7: piRNA in the Cardiovascular System 12

1.8: Purpose of Proposal 15

1.9: Specific Aims 16

Aim 1 16

Aim 2 18

Aim 3 19

1.10: Innovation 21

1.11: References 24

Chapter 2: Aim 1: Sex-Stratified piRNA Expression Analysis Reveals Shared Functional Impacts of Perinatal Pb Exposure in Murine Hearts* 43

2.1: Abstract 44

2.2: Introduction 45

2.3: Methods 49

2.4: Results 58

2.5: Discussion 73

2.6: Supplementary Materials 82

2.7: Acknowledgements 83

2.8: References 84
Chapter 3: Aim 2: Sex Specific Effects of Perinatal Pb Exposure on Murine Cardiac Gene Expression and Function 97
3.1: Abstract 98
3.2: Introduction 98
3.3: Methods 101
3.4: Results 108
3.5: Discussion 116
3.6: Supplementary Information 122
3.7: Acknowledgements 122
3.8: References 123
Chapter 4: Aim 3: Evaluate Cell Line–Specific Gene Expression Changes and Functional Alterations Induced by Pb Exposure During Differentiation in Human iPSC-Derived Ventricular Cardiomyocytes 132
4.1: Abstract 133
4.2: Introduction 134
4.3: Methods 136
4.4: Results 150
4.5: Discussion 175
4.6: Supplementary Information 185
4.7: Acknowledgements 187
4.8: References 188
Chapter 5: Conclusions 196
5.1: Introduction 196
5.2: Summary of key findings 197
Aim 1 197
Aim 2 198
Aim 3 199
5.3: Comparison of mouse vs. human findings 200
5.4: Sex differences in how the heart responds to Pb exposure 201
5.5: piRNA and epigenetic pathways altered by Pb exposure 202
5.6: Functional alterations by developmental Pb exposure 203
5.7: Relation to the Developmental Origins of Disease 205
5.8: Public health and policy implications 206
5.9: Future directions 207
5.10: Concluding Remarks 208

5.11: References 210

List of Tables

Table 2.1: Summary of piRNA expression in control hearts identified by sodium periodate exclusion, including combined and sex-stratified piRNA assessment. 59

Table 2.2: piRNA changes (p-value <0.05 and log fold change (FC) >1 or < -1) associated with perinatal Pb exposure in the mouse heart. 63

Table 3.1: Significantly altered gene ontology pathways for 4-month-old mice perinatally exposed to Pb. 109

Table 4.1: Reagents in EB20 Media 140

Table 4.2: Primer Information 143

Table 4.3: Action potential parameters 149

Table 4.4: Ca transient parameters 150

Table 4.5: Differentially expressed genes by Pb exposure in female iPSCs undergoing differentiation into ventricular cardiomyocytes. 157

Table 4.6: Unbiased top 30 GOBP, GOMF, and GOCC pathway alterations across days and doses. 160

Table 4.7: Median BMCs per day. 164

Table 4.8: Upregulated and downregulated BMC genes per day. 164

Table 4.9: Top 30 GO Terms for BMC modeled data. ` 168

List of Figures

Figure 1.1: Schematic of Research Plan 16

Figure 2.1 : Experimental design for perinatal mouse Pb exposure and sequencing analysis pipeline. 51

Figure 2.2: Combined and sex-stratified baseline heart piRNA expression. 60

Figure 2.3: Genomic annotations and repetitive regions for expression of baseline heart piRNAs. 61

Figure 2.4: Potential changes in expression of heart piRNAs from mice developmentally exposed to Pb. 64

Figure 2.5: Genomic annotations and repetitive regions for expression of heart piRNAs with potential changes in expression in mice developmentally exposed to Pb. 66

Figure 2.6: Gene ontology analysis for piRNAs potentially altered by developmental Pb exposure. 69

Figure 2.7: Assessment of potential mRNA targets. 70

Figure 2.8: Sex-specific changes in *Piwil* expression in 10-month samples. 71

Figure 2.9: ECC gene read counts in hearts from mice at weaning and adult mice. 72

Supplemental Figure 2.10: Piwil expression with perinatal Pb exposure at different time points and by sex. 83

Figure 3.1: Experimental design for perinatal exposure mouse model and analysis. 103

Figure 3.2: PCA plots of 4-month-old RNA Seq data. 108

Figure 3.3: Significantly changed relevant pathways in 4-month-old mice perinatally exposed to Pb. 112
Figure 3.4: Normalized read count assessment of ECC genes reveals potential sex specific change in *Ryr2*. 113
Figure 3.5: Echocardiograms of adult mice perinatally exposed to Pb. 115
Figure 3.6 Overlaps in HFrEF gene signatures. 116
Figure 4.1: Protocol for differentiation of iPSCs into ventricular cardiomyocytes. 138
Figure 4.2: Epigenetic and pluripotency marker changes in iPSCs exposed to Pb. 151
Figure 4.3: *DNMT* and *TET* expression changes throughout differentiation. 152
Figure 4.4: *PIWIL* expression is dynamic throughout differentiation in both cell lines. 153
Figure 4.5: Comparison of *PIWIL* expression levels between human immature heart samples and iPSC-derived ventricular cardiomyocytes. 154
Figure 4.6: PCA plots reveal clustering by day and replicate number but not by Pb treatment. 156
Figure 4.7: Overlap in DEGs by day and dose. 158
Figure 4.8: Pathways related to important cardiac processes were altered by Pb exposure in iPSCs from a female patient differentiating into ventricular cardiomyocytes. 162
Figure 4.9: Best BMC across days of differentiation. 163
Figure 4.10: Overlap in BMC genes per day of differentiation. 165
Figure 4.11: Accumulation plots for all GO (BP, MF, and CC) and Reactome pathways per day of differentiation. 166
Figure 4.12: BMC modeled selected pathway changes. 168
Figure 4.13: Action potential changes in female and male iPSC-derived ventricular cardiomyocytes treated with Pb during differentiation. 170

Figure 4.14: Ca transient changes in female and male iPSC-derived ventricular cardiomyocytes treated with Pb during differentiation. 172
Figure 4.15: Comparison of median conduction velocity changes for each cell line for action potentials and Ca transients. 173
Figure 4.16: No Pb induced changes in ECC genes observed for either cell line at day 15 of differentiation. 175
Supplemental Figure 4.17: Female and male derived iPSC-CM expression of epigenetic enzymes during differentiation. 186
Figure 5.1: Schematic of Research Plan 197

List of Abbreviations

AF: Atrial Fibrillation

Ago: Argonaute Sub Family of Argonaute Proteins

ANOVA: Analysis of Variance

APD: Action Potential Duration

APD80: Action Potential Duration 80% Repolarization

AVCAPIR: Aortic Valve Calcification-Associated piRNA

BMC: Benchmark Concentration

BMR: Benchmark Response

Ca: Calcium

CAD: Coronary Artery Disease

CAVD: Calcific Aortic Valve Disease

CaTD: Ca Transient Duration

CaTD80: Ca Transient Duration at 80% Recovery

CHAPIR: Cardiac Hypertrophy Associated piRNA

CTEPH: Chronic Thromboembolic Pulmonary Hypertension

Cq: Quantification Cycle

CVD: Cardiovascular Disease

dF: Change in Fluorescence

dF/F0: Action Potential or Ca Transient Amplitude

DMCs: Differentially Methylated Cytosines

DMRs: Differentially Methylated Regions

DNMTs: DNA Methyltransferases

ECC: Excitation-Contraction Coupling

F0: Baseline Fluorescence

FDR: False Discovery Rate

HF: Heart Failure

HFpEF: Heart Failure with Preserved Ejection Fraction

HFrEF: Heart Failure with Reduced Ejection Fraction

HIWI/HILI/HIWI2: Human PIWILs

Hz: Beat Frequency for Action Potentials or Ca Transients

Hz SD: Beat Frequency Standard Deviation

iPSC: Induced Pluripotent Stem Cell

iPSC-CM: Induced Pluripotent Stem Cell Derived Cardiomyocyte

KD: Knockdown

KO: Knockout

LINE-1: Long Interspersed Nuclear Elements, 1

LV: Left Ventricle

MI: Myocardial Infarction

miRNA: micro-RNA

MIWI/MILI/MIWI2: Mouse PIWILs

m6A: N6-Methyladenosine

ncRNA: Non-coding RNA

NIEHS: National Institute of Environmental Health Sciences

PCA: Principal Component Analysis

piRNA: PIWI-interacting RNA

PIWI (PIWIL): P-element Induced Wimpy Testis (Like) Protein Subfamily of Argonaute Proteins

Pb: Lead

qRT-PCR: Quantitative Reverse Transcription Polymerase Chain Reaction

siRNA: Small Interfering RNA

smRNA: Small RNA

TaRGET: Toxicant Exposures and Responses by Genomic and Epigenomic Regulators of Transcription

TE: Transposable Element

TETs: Ten-Eleven Translocation Methylcytosine Dioxygenases

Abstract

Cardiovascular disease (CVD) is the leading cause of death worldwide.[1,2] CVDs are often chronic, and symptoms may not appear until advanced stages of disease, making prevention and treatment difficult.[3] Importantly, there are prominent sex differences in manifestations, pathogenesis, and prognosis of CVD.[2,4] While genetic and lifestyle factors are well-known contributors to CVD, the role of environmental pollutants is less defined. Lead (Pb), a common environmental contaminant from industrial emissions and older infrastructure, is strongly associated with adverse cardiovascular outcomes.[5]

One way Pb may contribute to the development of CVD is through epigenetic regulation: changes that control expression of genes without altering the underlying DNA sequence. According to the Developmental Origins of Health and Disease hypothesis, environmental exposures during early development can affect disease risk later in life by disrupting normal epigenetic programming.[6] Perinatal exposure to Pb has been shown to alter DNA methylation in a sex specific manner in cardiac tissue, and these changes were associated with genes important for cardiac development.[7]

PIWI-interacting RNAs, or piRNAs, are a class of small noncoding RNAs that function as part of the epigenetic regulatory system in the germline, and although piRNAs are well characterized in the germline, they have recently been detected in somatic tissues, including the heart, though their function remains poorly understood.[8] Previous work has found altered piRNA

expression related to the development of CVD, but none have studied how environmental exposures may play a role in regulating piRNA in CVD.[9,10]

While both Pb exposure and abnormal piRNA expression have been independently associated with adverse cardiovascular outcomes, no study has looked at the two in relation to one another. The central hypothesis of this project is that early developmental exposure to Pb causes adverse sex specific cardiovascular health outcomes later in life through dysregulation of the piRNA system, molecular pathways, and cardiac function.

Aim 1 (Chapter 2) characterizes a sex stratified baseline map of the piRNA-ome in the mouse heart, finding nearly 19,000 piRNAs mapping disproportionately to exons. Aim 1 further reveals hundreds of unique piRNAs in males and females affected by perinatal Pb exposure, mapping near gene regions controlling essential processes in the heart, including mitochondrial, ribosomal, and heart contraction pathways. Additionally, changes in piRNA-associated *Piwil* expression and expression of excitation contraction coupling genes were found only in male mice.

Aim 2 (Chapter 3) characterizes sex specific perinatal Pb exposure induced changes in molecular pathways and function in mice hearts, finding enrichment of pathways related to heart structure and function in both sexes, mitochondrial function in females, and histone biology in males. Further, echocardiograms point towards male-specific changes in heart structure and function induced by perinatal Pb exposure.

Aim 3 (Chapter 4) assesses how Pb exposure during cardiomyocyte differentiation affects gene expression and function of cardiomyocytes derived from one male and one female patient derived human induced pluripotent stem cell (iPSC) cell line. In the female line, gene and pathway changes related to heart development and mitochondrial structure and function were

dysregulated throughout differentiation. In both cell lines, there were cell line specific disruptions in electrophysiology.

Overall, these projects uncovered a comprehensive understanding of the sex specific impacts of developmental Pb exposure on expression of piRNAs, other pertinent molecular pathways, and function in the heart. Importantly, these early life changes may contribute to the development of CVD later in life.

Chapter 1: Introduction

1.1: Cardiovascular Disease

Cardiovascular disease (CVD) is a group of illnesses affecting the heart and circulatory system, including atherosclerosis, myocardial infarctions, stroke, heart failure, arrhythmias, and heart valve problems.[11] Worldwide, CVD killed 18.6 million people in 2019, with most deaths (85%) resulting from heart attacks or strokes.[1,12] In the United States alone, one person dies every 33 seconds from CVD and in the year 2020 CVD accounted for 1 in every 5 deaths.[13,14] The prevalence of cases of CVD doubled from 1990-2019, and 40.5% of the United States population is expected to have some form of CVD by 2030.[12,15,16] Importantly, one third of worldwide deaths due to CVD are premature, occurring in people under 70 years old.[1] Including costs of health care services, medicines, and loss of productivity due to death, heart disease cost the United States $254.3 billion in 2019-2020.[17]

Men and women exhibit significant differences in manifestations, pathogenesis, and prognosis of CVD.[2,4] Men are more likely to contract occlusive coronary artery disease (CAD) while women are more likely to suffer from nonobstructive CAD or microvascular dysfunction.[4] Further, because men develop CAD earlier and with more severe atherosclerosis, myocardial infarctions (MIs) occur an average of 10 years earlier in men than women.[4] However, mortality from MI is higher in younger women compared to younger men.[18] Contrastingly, men are more likely to die from ischemic sudden death due to arrhythmia.[4] Heart failure (HF) affects more women than men, although women more often have HF with preserved ejection fraction

(HFpEF) and men more often have HF with reduced ejection fraction (HFrEF), meaning women have HF where the heart pumps normally but has difficulty relaxing while men have HF where the heart's pumping is impaired.[14,17,19] Furthermore, women with HF tend to have better clinical outcomes.[20,21] Conversely, age-related atrial fibrillation (AF), the most prevalent heart rhythm disorder, is more common in men than women, but men tend to have better quality of life and are less at risk for adverse events.[22] Women, on the other hand, have lower rates of developmental heart conditions, also known as congenital heart defects (CHDs), compared to men.[23]

Cardiomyocytes, the contractile unit of the heart that make up the majority of a heart's mass, show sex-specific structural and functional defects in CVD.[24] Changes in cardiomyocytes in CVD include pathological hypertrophy (enlarging of the muscle tissue), altered programmed cell death, mitochondrial changes, and impaired electrical activity causing arrythmias.[24–27] Male and female specific cardiomyocytes have been shown to have differences in their excitation-contraction coupling (ECC) pathway, the process by which electrical impulses (action potentials) are linked to muscle contraction.[28] In this process, action potentials trigger the release of calcium (Ca) into the cell, where it binds to troponin, causing actin and myosin filaments to slide and thus creating uniform contraction that forms a heartbeat.[29] Studies have shown that sex hormones regulate intracellular Ca in cardiomyocytes, but other mechanisms, such as epigenetics (see Chapter 1.3) may also be at play.[28]

Despite the significant global burden of CVD, promising improvements have been made in prevention and treatment, prominently through modifications of lifestyle factors. However, the disease is difficult to confront due to its chronic nature in which symptoms may not develop until advanced stages, as often the first sign of disease may be occurrence of heart attack or stroke which may lead to sudden death.[1,3] Both lifestyle and genetic factors may play a role in the

development of CVD, and high blood pressure, high blood cholesterol, smoking, and poor diet are all significant risk factors.[13] CVD often originates as atherosclerosis, or plaque buildup in the arteries, and management of lifestyle factors or medications are often aimed at managing and preventing atherosclerosis.[30]

Less attention has been paid to environmental pollutants as causative agents of CVD compared to other lifestyle risk factors, but studies have shown that the cardiovascular system is highly sensitive to the effects of environmental exposures.[31] Ambient air pollution and the metals arsenic, cadmium, and Pb are the most well studied environmental contaminants affecting the cardiovascular system and are prevalent human exposures.[31] Air pollution and metal exposure have both been implicated in the development and progression of CVD through facilitating the development of atherosclerotic plaques, prompting of ischemic events, causing arrhythmias, or otherwise altering normal cardiovascular functioning.[31]

1.2: Lead Exposure and CVD

Lead (Pb) is a naturally occurring element that is highly toxic to humans and animals.[32] While standards in the past were more lenient, currently both the World Health Organization and Centers for Disease Control agree that there is no safe blood Pb level.[33] It is well understood that even low levels of Pb exposure, particularly in young children, can result in neurological and developmental problems.[32] Pb poisoning resulting from exposure through municipal water systems was prominently exposed by the Flint water crisis but exists throughout the United States and the world.[34,35] In 2021, an estimated 1.5 million deaths globally were attributed to Pb exposure, most significantly due to cardiovascular effects.[36] An earlier study found Pb exposure contributed to 5.5 million adult deaths in 2019 from cardiovascular disease worldwide (10% of global deaths that year).[37,38]

Origins of Pb poisoning include both occupational and environmental sources and Pb exposure is a public health issue in both high- and low-income countries.[35,39] The consumer use of Pb was banned in the United States (US) in 1978, but the problem of Pb pollution persists today from past contamination or current industrial usage.[32] Pb is present in the air, water, soil, and inside homes, and major sources of exposure in the US include paint in older homes, industrial legacy pollution (waste), batteries, and plumbing.[39] It is estimated that Pb is present in 25% of homes in the US.[40] Thus, exposure routes include inhalation, ingestion, or dermal absorption.

While studies have shown there is no safe level of Pb, it is important to consider historical and current exposure ranges. According to the US Occupational Safety and Health Administration (OSHA), workers can be exposed to high Pb levels resulting in a blood Pb level of over 60 μg/dL, causing both acute and chronic health effects.[41] The NIOSH Adult Blood Lead Epidemiology and Surveillance (ABLES) program recommends that worker blood Pb levels be maintained below 20 μg/dL over a twenty-year period or below 10 μg/dL over a forty-year period in order to prevent chronic health effects.[41] However, studies conducted between 1970-2010 have shown that worker blood Pb levels of 14 μg/dL on average for paint based exposure and 42 μg/dL on average for Pb from manufacturing Pb acid batteries, the latter of which was responsible for over 90% of the Pb consumed in the US.[42]

In non-industrial settings, blood Pb levels are generally lower, but continue to be a problem globally, with one third of children worldwide having a blood Pb level at or above 5 μg/dL.[43] Historically, one survey in 1980 in the US found blood Pb levels around 20 μg/dL or higher in homes with damaged Pb paints.[44] In Flint, MI, where corrosive water usage caused Pb to leak from pipes, the percentage of children with elevated blood Pb levels (≥ 5 μg/dL) nearly

doubled.[45,46] While this crisis exposed the problem to the US, Flint is not alone, as almost 3,000 U.S. neighborhoods showed blood Pb levels among tested children at least twice as high as in Flint.[34] As of 2021, CDC reference blood Pb level was lowered from 5 to 3.5 μg/dL.[47] This value is based on the 97.5th percentile of blood Pb distribution among children 1-5 years old in the US, and it represents a threshold to identify children at high risk and prompt follow up actions to help those most vulnerable.

Once in the body, Pb travels through the bloodstream and is distributed throughout the body and is stored in the bones, where it accumulates over time.[35] In adults, 94% of the total body burden of Pb is stored in bone or teeth, while only 73% of children's Pb body burden is stored in these mineralizing tissues.[48] Resorption from bones occurs in the body during osteoporosis, pregnancy, lactation, menopause, and other conditions and thus there is an increase in Pb concentration in the blood during these conditions.[48] Pb can also be transmitted from mother to fetus and from mother to infants through breast milk.[48] The half-life for blood Pb ranges from 1 week to 2 years, varying with age and exposure history.[48] The half-life of Pb stored in bone, on the other hand, is 1 to 2 decades.[48] This means that Pb stored in bone is an endogenous source of Pb that can be released into the body and cause damage well after an exposure has ended.

Studies have found the major target organ of Pb poisoning to be the central nervous system, with symptoms of lack of attention, memory loss, and headache.[40] Pb exposure has been associated with a drop in intelligence quotient (IQ), and even blood Pb levels lower than 5 μg/dL cause a decrease in IQ score.[49] Low-level, non-occupational exposure to Pb (below 10 μg/dL), have been shown to cause neurological and behavioral disorders in children as well as neurological disorders in adults.[50]

Pb exposure association with adverse cardiovascular outcomes has been supported by both prospective and cross-sectional epidemiological studies.[5] These include hypertension, arrythmias, increased risk of mortality from MI, increased incidence and mortality from coronary disease, and increased risk of peripheral arterial disease.[5,51–55] One prospective cohort study of adults found that low level Pb exposure (lower than 5 μg/dL) is an important risk factor in cardiovascular disease mortality, finding an equivalent of 256,000 cardiovascular disease related deaths annually in the United States could be attributable to Pb blood concentrations.[56] It has also been shown that Pb exposure in pregnant mothers may affect cardiac development in offspring, with numerous studies showing associations between maternal Pb levels and risk of congenital heart defects in the fetus.[57–61]

Mechanistically, Pb has been found to stimulate oxidative stress, inflammation, endothelial dysfunction, and proliferation of vascular smooth muscle cells and fibroblasts, all of which can lead to the development of hypertension.[62] In cellular pathways, Pb is known to mimic Ca, given that Pb ions are similar to Ca ions.[63] As highlighted in the previous section, Ca signaling is important in the cardiovascular system, as it controls uniform contraction of the heart via ECC.[64] Pb has been shown to alter intracellular processes involving Ca, including altering Ca homeostasis as well as function of ion channels, receptors, and transporters.[65] These disruptions have been extensively studied in relation to the neurotoxicant properties of Pb but are less well documented in the heart. However, studies have found that through disruption of Ca signaling, Pb exposure can lead to the development of arrhythmias and action potentials that are reduced in amplitude and elongated.[65]

1.3: Epigenetics

Another potential mechanism of action through which Pb exposure may lead to adverse cardiovascular outcomes is through epigenetic regulation. Epigenetics refer to mitotically heritable changes in gene expression without altering the underlying DNA sequence, and can be influenced by environmental factors. The developmental biologist Conrad Waddington coined the word epigenetics in 1942, and in 1957 he proposed the epigenetic landscape, building a metaphor in which a cell is represented by a ball that could follow different paths depending on characteristics of the landscape, signifying different intra or extracellular environmental factors.[66,67] This theory explains why most cells in a body all have the same genotype but different gene expression profiles leading to very different characteristics and functions.

Epigenetics comprises three main elements: modifications to DNA, histone modification, and non-coding RNA, all of which interplay together to control gene expression.[68] All three have been found to be regulated by Pb in the context of neurodevelopmental disorders.[69]

Less work has been conducted on how Pb alters the epigenome in the heart, with the bulk of work focused on alterations of DNA methylation. Briefly, DNA methylation is the transfer of a methyl group onto the C5 position of the cytosine to form 5-methylcytosine (5mC).[70] When present at gene promoters, DNA methylation is repressive, preventing transcription factors from binding and leading to gene silencing.[70] Interestingly, based on findings in hematopoietic stem cells, Ca helps regulate DNA methylation, as Ca dependent proteases Calpain 1 and Calpain 2 regulate protein levels of TET enzymes which help in the process of demethylation, and lower Ca levels increase TET1 and TET2 protein expression, as well as the abundance of a DNA demethylation intermediate 5-hydroxylmethylcytosine (5hmC).[71] Since Pb ions mimic Ca and may disrupt Ca signaling, this may be a mechanism by which Pb potentially alters DNA

methylation in the heart. Accordingly, associations between Pb exposure and DNA hypomethylation, particularly of Long Interspersed Nuclear Elements, 1 (LINE-1) transposable elements (TEs), have been found in various studies.[72–75]

1.4: Developmental Origins of Health and Disease

The Developmental Origins of Health and Disease (DOHaD) hypothesis originated in three studies that found poor nutrition at an early age could influence the development of heart disease later in life.[76–78] Similarly, different exposures, including to Pb, at an early age could lead to CVD later in life. During critical periods of development in the womb or in early life, exposures may modify the epigenome to induce long-lasting changes in programming that may render individuals more susceptible to CVD.[79] Of note, there have been shown to be sex differences in how the early environment induces the development of hypertension and CVD.[80]

DNA methylation plays a critical role during development. As cells undergo differentiation, epigenetic changes help guide this process, and these modifications allow for specific gene expression patterns that influence lineage specification and cell identity.[81] For this to happen, germ cells must be extensively reprogrammed.[81] As sperm and egg cells develop, they establish their own epigenetic patterning.[81] Upon fertilization, the zygote undergoes another wave of demethylation, allowing for cells to be in a pluripotent state which then undergo specific methylation patterns during differentiation.[81] Theoretically, if Pb affects epigenetic modifications, this could have implications for both germ cell development and early embryonic development. Metals, including Pb, have indeed been shown to alter the epigenetics of embryonic stem cells, causing changes in pluripotency and differentiation.[82]

Previous work from our lab discovered that mice treated perinatally (during gestation and lactation) with human exposure relevant levels of Pb were found to have hundreds of sex-

specific differentially methylated cytosines (DMCs) and differentially methylated regions (DMRs) in their heart tissue later in life, some of which were on genes related to cardiac development.[7] These included both hypermethylated regions as well as hypomethylated regions in both male and female mice.[7] Interestingly, these DMCs were found to correspond with unique pathways in males and females upon enrichment analysis, including a few pathways important for normal heart development and function in male DMCs.[7] Thus, Pb induced DNA methylation changes during development may contribute to cardiovascular disease in later life.

1.5: Small non-coding RNA

The majority of the genome (98%) contains non protein coding material, previously thought of as "junk DNA," but in the past few decades studies have shown the many vital processes regulated by RNA transcribed from these non-coding regions.[83,84] Non-coding RNAs (ncRNAs) are comprised of long and short ncRNAs as well as transfer and ribosomal RNAs.[83] There are three main types of small noncoding RNA (smRNA): microRNA (miRNA), small interfering RNA (siRNA), and piRNAs which each operate through distinct mechanisms.

MicroRNAs (miRNAs) have been shown to be dysregulated both by Pb and in CVD. Pb exposure in particulate matter was found to be correlated to expression of microRNAs important in oxidative stress and inflammation pathways.[85] In the heart, miRNA have been shown to be dysregulated in CVD, providing both potential biomarkers of disease and mechanistic links to disease progression with involvement in homeostasis, differentiation, and heart function.[86,87] In particular, miRNAs have been shown to play roles in cardiomyocyte proliferation and cardiac repair mechanisms as well as cardiac remodeling during disease progression.[88,89]

1.6: piRNA

PIWI-interacting RNAs, or piRNAs, are key players in modulating the epigenome. Aim 1 connects piRNA function with the DOHaD hypothesis: piRNA pathways may be affected by early exposures, leading to the development of CVD. piRNAs are well characterized to prevent transposable element (TE) mobilization and thus maintain genomic integrity, and exposures to heavy metals have been shown to regulate TE induced damage.[90] In mouse studies, perinatal exposures to Pb were associated with changes in DNA methylation of transposon-associated loci.[91,92] In addition, some human studies have found associations between Pb exposure and hypomethylation of LINE-1 TEs, and one study found *in utero* exposure to Pb in humans also resulted hypermethylation at LINE-1 TEs at birth.[72–75,93] As piRNAs regulate DNA methylation of transposable elements and these have shown altered methylation profiles caused by Pb, piRNA may represent a potential mechanism by which Pb acts. Taken together, Pb exposure may affect cardiac biology through disruption of piRNA functioning.

piRNA are a class of smRNA first coined in the early 2000s by a group of studies showing a novel distinct smRNA which associate with PIWI proteins in both *Drosophila* and mammals.[94–98] piRNAs are the least well studied RNA species in mammals, and are only found in animals.[9,99] They are short (23-34 nucleotides, generally longer than miRNAs), enriched in the germline, and their canonical function is silencing of transposons via transcriptional or posttranscriptional mechanisms.[100] This function makes them critical for maintaining genomic integrity, as mobile TEs can act as mutagens to coding or regulatory sequences.[101]

Germline piRNAs are well characterized, representing a ubiquitously expressed diverse class of over 500,000 unique piRNA sequences as found in web-accessible databases.[102–105] Unlike miRNAs and siRNAs, which associate with Ago subfamily Argonaute proteins to guide them to

their sites of action, piRNAs associate with the PIWI protein subfamily.[106] They are also generally thought to be longer (23-34 base pairs versus 20-24 base pairs) than the other classes of ncRNAs, although recent work has found that piRNAs may be shorter when expressed in somatic tissue compared to the germline.[8] Also distinct from the other ncRNAs is the presence of 2' O-methylation at their 3' end in piRNA, which confers stability.[107–109] Further, while miRNAs are often conserved between species, piRNAs are not as there are hundreds of thousands of unique piRNAs found within each species.[100]

PIWI (or PIWIL) proteins, on the other hand, are well conserved between species. PIWI stands for p-element induced wimpy testis, first discovered in *Drosophila* germline stem cells in a mutagenesis screen, with mutations causing severe defects in spermatogenesis, thus giving the gene its name.[110] There are three mouse PIWI proteins named MIWI (PIWIL1), MILI (PIWIL2), and MIWI2 (PIWIL4) and four human PIWI proteins named HIWI (PIWIL1), HILI (PIWIL2), HIWI3 (PIWIL3), and HIWI2 (PIWIL4). Functionally, as discovered in Drosophila, PIWIs bind to and guide piRNA transcripts to transposons, where they are required for DNA methylation and transcriptional silencing.[100] PIWIs also play a role in secondary piRNA biogenesis in the germline, binding to piRNA transcripts in the intermediate steps of synthesis and in a "ping pong" amplification mechanism which is also highly conserved across species.[111]

Despite being well characterized in the germline, little is known about piRNA function in somatic tissues.[112] Studies have found both piRNAs and PIWILs present in somatic tissues expressed at significantly lower levels compared to the germline.[8,112] They were first discovered to play important roles in stem cell function and in the development of multiple types of cancer, but more recent studies have found piRNA pathways are also important in fully differentiated somatic tissues.[113–115] piRNAs have been found in a diverse array of tissues, including follicular

cells, epididymis, brain, heart, liver, kidney, pancreas, and skeletal muscle.[8,112,116] Functionally, piRNAs likely play their same role regulating TE expression in somatic tissue, but other roles, including regulation of gene expression, have also been suggested.[113] Emerging data has found piRNAs to be involved in regulating N6-methyladenosine (m6A) modifications of mRNAs, which effects mRNA splicing, nuclear transportation, stability, and translation, and piRNA mediated m6A has been shown in both studies of tumor progression as well as CVD.[117–119]

1.7: piRNA in the Cardiovascular System

Somatic roles of piRNA, including in the cardiovascular system, are just beginning to be uncovered. The first evidence of piRNAs playing specific roles in heart tissue was found in the sea slug where certain piRNAs were found at high levels in the heart compared to the germline.[120] After this, piRNAs have been found to be involved in distinct cardiac mechanisms, including cardiac repair, cardiac differentiation, and CVD.[9,10,121–124]

Endogenous cardiac regeneration is very low and so models of cardiac repair are important in developing potential treatment strategies for damage induced by myocardial infarctions or heart failure.[123] piRNA may represent one potential avenue for the development of such therapies.[125] PIWI knockdown was first found to impair whole organism regeneration, including circulatory system regeneration in ascidians (sea squirts).[122] Further, particular piRNAs were found to be differentially expressed in different types of cardiac progenitor cells, implying piRNAs could play functional roles in cardiomyocyte proliferation and regeneration.[123] The piRNAs expressed in these cardiac progenitor cells were found to be associated with inhibition of LINE-1 transposons (presumably through silencing via DNA methylation) and activation of AKT signaling, a powerful survival and repair signal.[123] LINE-1 inhibition is associated with decreased negative repercussions post ischemic damage of the heart through activation of

AKT.[126] Dysregulation of AKT signaling in the heart is associated with several adverse cardiovascular outcomes, including atherosclerosis, cardiac hypertrophy, and vascular remodeling.[127] Therefore, piRNA likely play important roles in regulating cardiac repair and represent a potential treatment avenue in cardiac pathology.

Differential piRNA and PIWIL expression has been found at different stages of cardiac differentiation, suggesting that piRNAs are involved in regulating cardiac differentiation.[124,128] In an *in vitro* analysis of human H9 embryonic stem cells differentiated into cardiomyocytes, investigators found piRNA transcripts (distinguished from miRNA by larger length), of which 241 were detected in pluripotency, 218 in mesoderm and 171 in cardiac cells.[124] Interestingly, this study found that the majority of piRNAs found to be differentially expressed were downregulated as cells were differentiating, suggesting piNRAs may become less important in differentiated cells, and these piRNAs originated from genes involved in essential biological processes in the heart.[124] The majority of piRNAs mapped to unique processes in the developing cardiomyocytes compared to neural progenitor cells, suggesting that they play a unique functional role in cardiac cells.[124] Enriched pathways corresponded to heart development, muscle differentiation, and contraction.[124] The authors of this study suggest piRNA expression fine tunes gene expression to control cardiac differentiation.[124] Further, this work also found differences in expression of PIWIL genes at different stages of differentiation, with a decrease in *PIWIL2* and increase in *PIWIL4* found in cardiac progenitors.[124] Importantly, improper cardiac differentiation can lead to the development of congenital heart defects and these processes can be influenced by environmental exposures.[129] Thus, proper differentiation may be disrupted through modulation of piRNA expression by the environment.

CVD model studies have revealed piRNA involvement in CVD. Models of cardiac hypertrophy, which is related to myocardial ischemia and heart failure, showed increased piRNA expression in rat *in vivo* models of adaptive hypertrophy and decreased piRNA expression in rat-derived *in vitro* models of adaptive hypertrophy.[9] (It is important to note, cardiac hypertrophy can be an adaptive response or a pathological change and differ in underlying molecular mechanisms.[130] In adaptive hypertrophy, cardiomyocytes are enlarged to meet increased demands such as in athletes or during pregnancy, while in pathological hypertrophy, maladaptive remodeling occurs due to stress and leads to heart failure or other CVDs.[130]) Interestingly, the *in vivo* piRNAs were found to be mapped to mRNA regions while the piRNAs found in *in vitro* models mapped to both mRNA and transposon (including LINE-1) regions.[9] This highlights that there is diversity in piRNAs not only present between species but between different model systems, underscoring the complexity of piRNA regulation of heart biology.

One particular piRNA, called Cardiac Hypertrophy Associated piRNA (CHAPIR) has been shown to increase cardiac hypertrophy upon overexpression and decrease cardiac hypertrophy upon KD or KO in *in vitro* and *in vivo* models, respectively.[118] These experiments found the mechanism by which this occurs is through blocking of METTL3-mediated N^6-methyladenosine (m^6A) methylation of Parp10 mRNA transcripts, which leads to increased Parp10 expression and downstream effects on cardiac hypertrophy.[118] Thus, piRNA may play a causal role in heart disease by mechanisms other than silencing of transposons.

Another piRNA was discovered in the context of calcific aortic valve disease (CAVD), the most common form of heart valve disease involving the buildup of Ca in the aortic valve which narrows the valve opening.[119] Aortic valve calcification-associated piRNA (AVCAPIR) promotes AVC *in vitro* and *in vivo* through disruption of fat mass and obesity-associated protein-

mediated m^6A demethylation of CD36 mRNA transcripts, the latter of which stabilizes a procalcific protein, thus enhancing the CAVD phenotype.[119]

Epidemiological studies have suggested that piRNA play roles in CVD.[131,132] One study found large differences in expression (both up and downregulation) of piRNAs in heart failure patients.[10] piRNAs were also found to be differentially expressed in patients with chronic thromboembolic pulmonary hypertension (CTEPH).[133] Another study found specific piRNAs present in MI patients.[9] Together, these results indicate opportunity to utilize piRNA either as biomarkers of disease or potentially in CVD therapies.

1.8: Purpose of Proposal

Given that piRNAs have been shown to play roles in cardiac repair, differentiation, and pathologies, and Pb exposure can disrupt proper epigenetic programming during development and is known to be associated with CVD, this work proposes that exposure to Pb during development can lead to CVD later in life through disruption of the piRNA system. However, piRNA dysregulation is only one component of how Pb impacts cardiac development and biology, and so to gain a comprehensive understanding of the molecular and functional consequences of developmental Pb exposure, this project incorporates small RNA sequencing in mice (Aim 1) and transcriptome profiling and cardiac functional assessments in both mice and human iPSC-derived cardiomyocyte models (Aims 2 and 3). Furthermore, given that CVD shows differences in pathology between the two sexes and epigenetic responses to Pb exposure are also sex specific, this work will also examine the influence of sex across all aims. Overall, these projects aim to fill knowledge gaps surrounding Pb exposure's potential to influence the expression of piRNAs, associated epigenetic and gene regulatory pathways, and ultimately cardiac structure and function in a sex specific manner, in pursuit of discovering mechanisms

underlying Pb's potential to increase CVD risk later in life. The schematic below shows an outline of work to fulfill this proposal's goals.

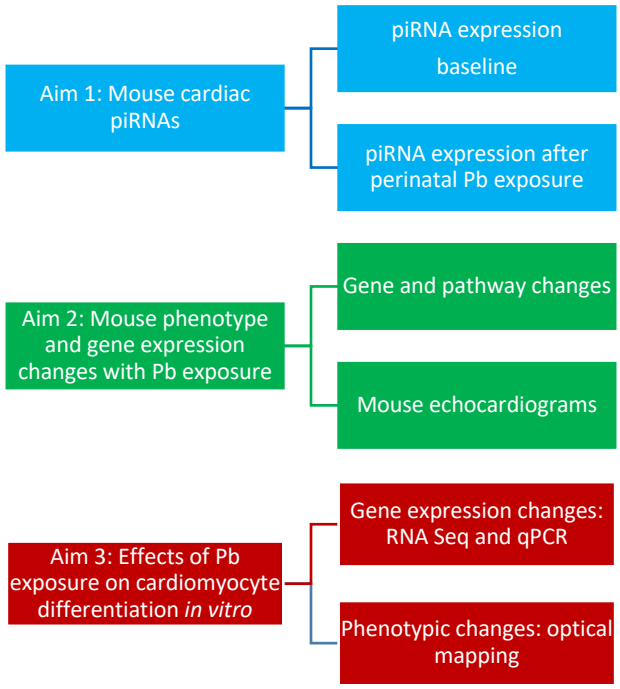


Figure 1.1: Schematic of Research Plan

1.9: Specific Aims

Aim 1

Analyze Sex-Stratified piRNA Expression to Characterize Functional Impacts of Perinatal Pb Exposure in Murine Hearts

Goal: Establish sex-stratified baseline maps of all piRNAs expressed in murine heart tissue and examine effects of perinatal Pb exposure on piRNA expression in murine hearts.

Hypothesis: piRNAs are expressed in the heart, their expression is sex-specific, and their expression is affected by perinatal Pb exposure in a sex-specific manner.

Summary:

The current understanding of piRNA expression in the heart is not well documented, although alterations in piRNA expression have been reported in CVD. Furthermore, Pb exposure is strongly associated with CVD risk, but no studies have investigated Pb's effects on cardiac piRNAs. This study aimed to characterize sex-stratified piRNA expression in the murine heart and assess sex-specific effects of human-relevant maternal Pb exposure on adult offspring cardiac piRNA expression, as well as the expression of piRNA associated machinery.

Virgin female wild-type *a/a* non-agouti mice (derived from a colony for the viable yellow agouti (A^{vy}) strain) 93% identical to the C57BL/6 mice (6-8 weeks old) were randomly assigned to receive control or Pb via drinking water 2 weeks prior to mating, followed by mating with virgin a/a males of the same strain (7-9 weeks old).[134] Pb II acetate trihydrate (32 ppm; Sigma-Aldrich, Milwaukee, WI, USA) was mixed with distilled drinking water, which results in a human-relevant maternal exposure in the 16–60 μg/dL range.[91,135] Pb exposure continued through mating (for both males and females), pregnancy (~3 weeks), and lactation until weaning at 3 weeks of age.[7] After weaning, all offspring received Pb-free water until euthanasia at 3 weeks, 5 months, and 10 months of age. First, smRNA sequencing was performed to generate baseline maps of all piRNA expressed in female and male 5-month-old control murine heart tissue (5-month, n =2 per sex). We used sodium periodate exclusion so that only piRNA was amplified in our samples, as piRNAs are resistant to sodium periodate treatment due to the presence of a unique 3' modification of 2'-O-methylation.[8,108,113] Next, we sequenced smRNA isolated from heart tissue of 5 month old mice exposed to Pb during gestation and lactation. The

expression of piRNA (n= 5 female control and Pb exposed and n = 6 male control and Pb exposed) was compared to baseline maps. Functionality of the specific piRNAs found differentially expressed was assessed through gene ontology analysis to determine differential effects of Pb on piRNA expression as well as sex differences in this effect. Specific genes affected by Pb exposure (potential mRNA targets, piRNA associated *Piwil*s, and ECC genes) were also interrogated by qRT-PCR.

The goal of this aim is to address existing knowledge gaps on our understanding of the piRNA landscape in both control adult heart tissue as well as how developmental Pb exposure affects their expression, with the overarching purpose to understand how this altered piRNA expression may be related to the development of CVD.

Aim 2

Determine the Sex-Specific Effects of Perinatal Pb Exposure on Murine Cardiac Gene Expression and Function

Goal: Examine the sex-specific effects of perinatal Pb exposure on gene and pathway alterations as well as phenotypic changes in adult mouse cardiovascular system.

Aim 2A:

- *Hypothesis: Perinatal Pb exposure alters transcriptional pathways associated with cardiovascular development and disease in a sex specific manner.*

Aim 2A Summary:

While Pb exposure is known to be related to CVD, the underlying sex specific molecular consequences of developmental Pb exposure on the murine heart are unclear. In this aim, we assessed sex-specific molecular pathway changes in midlife in mice perinatally exposed to Pb.

The same perinatal Pb exposure model detailed in aim 1 was used but in a different strain of mice (C57/BL6). Heart tissue was collected at 4 months of age (n=6 per treatment per sex). RNA-Seq analysis was conducted. Sex-stratified gene ontology pathway analysis was performed, and relevant pathways related to heart development, structure, function, and epigenetic and metabolic regulation were selected from significant results.

Aim 2A sought to build on Aim 1 by assessing sex-specific Pb induced changes in cardiac gene expression and relating this to the potential development of cardiac pathologies.

Aim 2B:

- *Hypothesis: Perinatal Pb exposure causes structural and functional changes in the murine heart later in life in a sex specific manner.*

Aim 2B Summary:

To further examine the sex specific effects of developmental Pb exposure on cardiac structure and function, we conducted phenotypic analyses on the same male and female 4-month-old mice perinatally exposed to Pb. Echocardiograms were conducted in at the University of Michigan Physiology Phenotyping Core to assess for sex specific changes in heart structure and function. This included assessing heart rate (bpm), cardiac output (blood pumped in circulation in ml/min), stroke volume (amount of blood pumped out each beat mm^3), mass of ventricles and atria, and interventricular septum thickness and area during diastole and systole (muscle wall separating the left and right ventricles of the heart). Together with the transcriptomic profiling, we sought to paint a picture of how developmental exposure to Pb impacts cardiac processes in a sex specific manner, potentially contributing to the development of cardiac disease states.

Aim 3

Evaluate Cell Line–Specific Gene Expression Changes and Functional Alterations

Induced by Pb Exposure During Differentiation in Human iPSC-Derived Ventricular Cardiomyocytes

Goal: Characterize the dose-specific effects of Pb exposure during differentiation on gene, pathway, and functional alterations in human ventricular cardiomyocytes.

Aim 3A:

- *Hypothesis: Epigenetic regulatory genes as well as genes associated with cardiac development, structure, and function are affected by Pb exposure during differentiation in a cell line specific manner in human iPSC-derived ventricular cardiomyocytes.*

Aim 3A Summary:

Building upon our mouse studies and human literature suggesting early life exposure to Pb can cause adverse cardiovascular outcomes later in life, aim 3A sought to examine how Pb exposure during human cardiomyocyte differentiation alters gene expression of epigenetic machinery and other genes associated with cardiac function.

Expression changes of *PIWIL* and other associated epigenetic machinery were assessed in female and male iPSC derived cardiomyocytes treated with two human relevant doses of Pb (0.5 μM and 5 μM) throughout differentiation (n=3 per cell line). Further, RNA-Seq was conducted in female derived cardiomyocytes, gene ontology pathway analysis was performed, and benchmark dose (BMD) modeling was performed to assess for molecular changes induced by Pb in these cells.

The analysis of epigenetic genes and transcriptomic profiling in aim 3A sought to fill a critical gap in our understanding of how Pb exposure impacts heart cell differentiation, showing how structural, metabolic, and epigenetic regulatory changes may potentially lead to CVD later in life.

Aim 3B:

- *Hypothesis: Pb exposure during differentiation impacts heart cell differentiation and beat characteristics in purified ventricular cardiomyocytes.*

Aim 3B Summary:

To related aim 3A's transcriptomic changes to functional changes that could impact cardiac pathologies, we assessed phenotypes of purified cardiomyocytes exposed to Pb during differentiation.

Functional changes were assessed in differentiated cardiomyocytes derived from one female and one male iPSC line (n=3-4 per cell line) treated with Pb (0.5 μM and 5 μM) throughout differentiation, including changes in Ca transients and action potential properties measured using optical mapping.

No study to date has looked at how Pb exposure during differentiation impacts electrophysiological properties of purified cardiomyocytes. Changes in the beat characteristics long after Pb exposure has ceased may be indicative of long-term functional reprogramming related to cardiac pathologies.

1.10: Innovation

Aim 1:

Compared to other ncRNAs, piRNAs are understudied and the mechanisms by which sex specific somatic piRNA function are yet to be characterized. Further, little is known about piRNA function in the cardiovascular system and how they may contribute to the development of CVD. Previous work has relied on size to distinguish piRNA transcripts from other types of smRNA, while this study will use sodium periodate exclusion, a more rigorous method allowing

for comprehensive characterization of piRNA involved in cardiac cell differentiation and biology. Furthermore, environmental exposures in relation to piRNA expression have not been well studied, and this project is the first to examine the effects of Pb on piRNA dysregulation in relation to the cardiovascular system. Lastly, specific differences in piRNA expression between sexes in the heart have yet to be characterized, as well as the sex-stratified effects of Pb exposure.

Aim 2:

This aim uniquely combines transcriptomic as well as in vivo cardiac phenotyping using a perinatal exposure model of Pb exposure, providing a systems level view of Pb's impact on the heart. It further examines sex specific effects, advancing our understanding of sex as a biological variable. Additionally, many DOHaD studies focus on earlier timepoints, but by examining the mice at midlife we are gaining an understanding of how disruptions of early developmental programming by Pb influence cardiac outcomes in later life, potentially highlighting adverse pathways and outcomes related to the development of CVD.

Aim 3:

As in aim 2, aim 3 integrates epigenetic, transcriptomic, and functional assessments by examining how Pb exposure during differentiation of human derived iPSC lines alters downstream gene and function in human iPSC-derived cardiomyocytes. It uses a new approach methodology and so saves time and costs while providing human relevant data. Modeling the developmental window of human exposure and its potential long term pathological consequences enhances translational relevance. Importantly, it takes the first step of examining sex differences by investigating one male derived and one female derived line. Furthermore, to our knowledge, it is the first study to link Pb exposure during differentiation to electrophysiological disruptions as

purified cardiomyocytes, providing potential insight into mechanisms by which early life exposure may reprogram cardiac function and increase disease susceptibility later in life.

1.11: References

1. World Health Organization. Cardiovascular diseases. Accessed August 9, 2023. https://www.who.int/health-topics/cardiovascular-diseases

2. Gao Z, Chen Z, Sun A, Deng X. Gender differences in cardiovascular disease. *Med Nov Technol Devices*. 2019;4:100025. doi:10.1016/j.medntd.2019.100025

3. Frančula-Zaninović S, Nola IA. Management of Measurable Variable Cardiovascular Disease' Risk Factors. *Curr Cardiol Rev*. 2018;14(3):153-163. doi:10.2174/1573403X14666180222102312

4. Regitz-Zagrosek V, Kararigas G. Mechanistic Pathways of Sex Differences in Cardiovascular Disease. *Physiol Rev*. 2017;97(1):1-37. doi:10.1152/physrev.00021.2015

5. Navas-Acien A, Guallar E, Silbergeld EK, Rothenberg SJ. Lead Exposure and Cardiovascular Disease—A Systematic Review. *Environ Health Perspect*. 2007;115(3):472-482. doi:10.1289/ehp.9785

6. Wadhwa PD, Buss C, Entringer S, Swanson JM. Developmental Origins of Health and Disease: Brief History of the Approach and Current Focus on Epigenetic Mechanisms. *Semin Reprod Med*. 2009;27(5):358-368. doi:10.1055/s-0029-1237424

7. Svoboda LK, Wang K, Jones TR, Colacino JA, Sartor MA, Dolinoy DC. Sex-Specific Alterations in Cardiac DNA Methylation in Adult Mice by Perinatal Lead Exposure. *Int J Environ Res Public Health*. 2021;18(2):577. doi:10.3390/ijerph18020577

8. Perera BPU, Tsai ZTY, Colwell ML, et al. Somatic expression of piRNA and associated machinery in the mouse identifies short, tissue-specific piRNA. *Epigenetics*. 2019;14(5):504-521. doi:10.1080/15592294.2019.1600389

9. Rajan KS, Velmurugan G, Gopal P, et al. Abundant and Altered Expression of PIWI-Interacting RNAs during Cardiac Hypertrophy. *Heart Lung Circ*. 2016;25(10):1013-1020. doi:10.1016/j.hlc.2016.02.015

10. Yang J, Xue FT, Li YY, Liu W, Zhang S. Exosomal piRNA sequencing reveals differences between heart failure and healthy patients. *Eur Rev Med Pharmacol Sci*. 2018;22(22):7952-7961. doi:10.26355/eurrev_201811_16423

11. American Heart Association. What is Cardiovascular Disease? www.heart.org. Accessed August 9, 2023. https://www.heart.org/en/health-topics/consumer-healthcare/what-is-cardiovascular-disease

12. Roth GA, Mensah GA, Johnson CO, et al. Global Burden of Cardiovascular Diseases and Risk Factors, 1990–2019. *J Am Coll Cardiol*. 2020;76(25):2982-3021. doi:10.1016/j.jacc.2020.11.010

13. CDC. Heart Disease Facts. Heart Disease. October 24, 2024. Accessed February 4, 2025. https://www.cdc.gov/heart-disease/data-research/facts-stats/index.html

14. Tsao CW, Aday AW, Almarzooq ZI, et al. Heart Disease and Stroke Statistics—2022 Update: A Report From the American Heart Association. *Circulation*. 2022;145(8):e153-e639. doi:10.1161/CIR.0000000000001052

15.Heidenreich PA, Trogdon JG, Khavjou OA, et al. Forecasting the future of cardiovascular disease in the United States: a policy statement from the American Heart Association. *Circulation*. 2011;123(8):933-944. doi:10.1161/CIR.0b013e31820a55f5

16.Mensah GA, Wei GS, Sorlie PD, et al. Decline in Cardiovascular Mortality: Possible Causes and Implications. *Circ Res*. 2017;120(2):366-380. doi:10.1161/CIRCRESAHA.116.309115

17.2024 Heart Disease and Stroke Statistics: A Report of US and Global Data From the American Heart Association. doi:10.1161/CIR.0000000000001209

18.Vaccarino V, Parsons L, Every NR, Barron HV, Krumholz HM. Sex-based differences in early mortality after myocardial infarction. National Registry of Myocardial Infarction 2 Participants. *N Engl J Med*. 1999;341(4):217-225. doi:10.1056/NEJM199907223410401

19.Scantlebury DC, Borlaug BA. Why are women more likely than men to develop heart failure with preserved ejection fraction? *Curr Opin Cardiol*. 2011;26(6):562-568. doi:10.1097/HCO.0b013e32834b7faf

20.Levy D, Kenchaiah S, Larson MG, et al. Long-term trends in the incidence of and survival with heart failure. *N Engl J Med*. 2002;347(18):1397-1402. doi:10.1056/NEJMoa020265

21.Martínez-Sellés M, Doughty RN, Poppe K, et al. Gender and survival in patients with heart failure: interactions with diabetes and aetiology. Results from the MAGGIC individual patient meta-analysis. *Eur J Heart Fail*. 2012;14(5):473-479. doi:10.1093/eurjhf/hfs026

22. Odening KE, Deiß S, Dilling-Boer D, et al. Mechanisms of sex differences in atrial fibrillation: role of hormones and differences in electrophysiology, structure, function, and remodelling. *EP Eur*. 2019;21(3):366-376. doi:10.1093/europace/euy215

23. Grines CL, Klein AJ, Bauser-Heaton H, et al. Racial and ethnic disparities in coronary, vascular, structural, and congenital heart disease. *Catheter Cardiovasc Interv*. 2021;98(2):277-294. doi:10.1002/ccd.29745

24. Peter AK, Bjerke MA, Leinwand LA. Biology of the cardiac myocyte in heart disease. *Mol Biol Cell*. 2016;27(14):2149-2160. doi:10.1091/mbc.E16-01-0038

25. Cai K, Jiang H, Zou Y, et al. Programmed death of cardiomyocytes in cardiovascular disease and new therapeutic approaches. *Pharmacol Res*. 2024;206:107281. doi:10.1016/j.phrs.2024.107281

26. Fan H, He Z, Huang H, et al. Mitochondrial Quality Control in Cardiomyocytes: A Critical Role in the Progression of Cardiovascular Diseases. *Front Physiol*. 2020;11. doi:10.3389/fphys.2020.00252

27. Antzelevitch C, Burashnikov A. Overview of Basic Mechanisms of Cardiac Arrhythmia. *Card Electrophysiol Clin*. 2011;3(1):23-45. doi:10.1016/j.ccep.2010.10.012

28. Parks RJ, Howlett SE. Sex differences in mechanisms of cardiac excitation–contraction coupling. *Pflugers Arch*. 2013;465(5):747-763. doi:10.1007/s00424-013-1233-0

29. Eisner DA, Caldwell JL, Kistamás K, Trafford AW. Calcium and Excitation-Contraction Coupling in the Heart. *Circ Res*. 2017;121(2):181-195. doi:10.1161/CIRCRESAHA.117.310230

30. Health NRC (US) C on D and. *Atherosclerotic Cardiovascular Diseases*. National Academies Press (US); 1989. Accessed September 21, 2022. https://www.ncbi.nlm.nih.gov/books/NBK218744/

31. Cosselman KE, Navas-Acien A, Kaufman JD. Environmental factors in cardiovascular disease. *Nat Rev Cardiol*. 2015;12(11):627-642. doi:10.1038/nrcardio.2015.152

32. US EPA O. Learn about Lead. February 12, 2013. Accessed February 4, 2025. https://www.epa.gov/lead/learn-about-lead

33. Hanna-Attisha M, Lanphear B, Landrigan P. Lead Poisoning in the 21st Century: The Silent Epidemic Continues. *Am J Public Health*. 2018;108(11):1430. doi:10.2105/AJPH.2018.304725

34. Pell MB, Schneyer J. Reuters finds lead levels higher than Flint's in thousands of locales. Reuters. December 19, 2016. Accessed January 9, 2024. http://www.reuters.com/investigates/special-report/usa-lead-testing/

35. Lead poisoning. Accessed February 4, 2025. https://www.who.int/news-room/fact-sheets/detail/lead-poisoning-and-health

36.Lead exposure - Level 3 risk | Institute for Health Metrics and Evaluation. Accessed February 4, 2025. https://www.healthdata.org/research-analysis/diseases-injuries-risks/factsheets/2021-lead-exposure-level-3-risk

37.Larsen B, Sánchez-Triana E. Global health burden and cost of lead exposure in children and adults: a health impact and economic modelling analysis. *Lancet Planet Health*. 2023;7(10):e831-e840. doi:10.1016/S2542-5196(23)00166-3

38.Jha P, Brown PE, Ansumana R. Counting the global COVID-19 dead. *Lancet Lond Engl*. 2022;399(10339):1937-1938. doi:10.1016/S0140-6736(22)00845-5

39.Obeng-Gyasi E. Sources of lead exposure in various countries. *Rev Environ Health*. 2019;34(1):25-34. doi:10.1515/reveh-2018-0037

40.Rehman K, Fatima F, Waheed I, Akash MSH. Prevalence of exposure of heavy metals and their impact on health consequences. *J Cell Biochem*. 2018;119(1):157-184. doi:10.1002/jcb.26234

41.Lead - Health Effects | OSHA.gov | Occupational Safety and Health Administration. Accessed February 4, 2025. https://www.osha.gov/lead/health-effects

42.Koh DH, Locke SJ, Chen YC, Purdue MP, Friesen MC. Lead exposure in US worksites: A literature review and development of an occupational lead exposure database from the published literature. *Am J Ind Med*. 2015;58(6):605-616. doi:10.1002/ajim.22448

43.The toxic truth | UNICEF. July 30, 2020. Accessed February 6, 2025. https://www.unicef.org/reports/toxic-truth-childrens-exposure-to-lead-pollution-2020

44. Charney E, Sayre J, Coulter M. Increased lead absorption in inner city children: where does the lead come from? *Pediatrics*. 1980;65(2):226-231.

45. Gómez HF, Borgialli DA, Sharman M, et al. Blood Lead Levels of Children in Flint, Michigan: 2006-2016. *J Pediatr*. 2018;197:158-164. doi:10.1016/j.jpeds.2017.12.063

46. Hanna-Attisha M, LaChance J, Sadler RC, Champney Schnepp A. Elevated Blood Lead Levels in Children Associated With the Flint Drinking Water Crisis: A Spatial Analysis of Risk and Public Health Response. *Am J Public Health*. 2016;106(2):283-290. doi:10.2105/AJPH.2015.303003

47. CDC. CDC Updates Blood Lead Reference Value. Childhood Lead Poisoning Prevention. January 31, 2025. Accessed December 8, 2025. https://www.cdc.gov/lead-prevention/php/news-features/updates-blood-lead-reference-value.html

48. Toxicological profile for lead. doi:10.15620/cdc:95222

49. Galiciolli MEA, Lima LS, da Costa N de S, de Andrade DP, Irioda AC, Oliveira CS. IQ alteration induced by lead in developed and underdeveloped/developing countries: A systematic review and a meta-analysis. *Environ Pollut*. 2022;292:118316. doi:10.1016/j.envpol.2021.118316

50. Riva MA, Lafranconi A, D'Orso MI, Cesana G. Lead Poisoning: Historical Aspects of a Paradigmatic "Occupational and Environmental Disease." *Saf Health Work*. 2012;3(1):11-16. doi:10.5491/SHAW.2012.3.1.11

51.Menke A, Muntner P, Batuman V, Silbergeld EK, Guallar E. Blood lead below 0.48 micromol/L (10 microg/dL) and mortality among US adults. *Circulation*. 2006;114(13):1388-1394. doi:10.1161/CIRCULATIONAHA.106.628321

52.Weisskopf MG, Jain N, Nie H, et al. A prospective study of bone lead concentration and death from all causes, cardiovascular diseases, and cancer in the Department of Veterans Affairs Normative Aging Study. *Circulation*. 2009;120(12):1056-1064. doi:10.1161/CIRCULATIONAHA.108.827121

53.Jain NB, Potula V, Schwartz J, et al. Lead levels and ischemic heart disease in a prospective study of middle-aged and elderly men: the VA Normative Aging Study. *Environ Health Perspect*. 2007;115(6):871-875. doi:10.1289/ehp.9629

54.Muntner P, Menke A, DeSalvo KB, Rabito FA, Batuman V. Continued decline in blood lead levels among adults in the United States: the National Health and Nutrition Examination Surveys. *Arch Intern Med*. 2005;165(18):2155-2161. doi:10.1001/archinte.165.18.2155

55.Navas-Acien A, Selvin E, Sharrett AR, Calderon-Aranda E, Silbergeld E, Guallar E. Lead, cadmium, smoking, and increased risk of peripheral arterial disease. *Circulation*. 2004;109(25):3196-3201. doi:10.1161/01.CIR.0000130848.18636.B2

56.Lanphear BP, Rauch S, Auinger P, Allen RW, Hornung RW. Low-level lead exposure and mortality in US adults: a population-based cohort study. *Lancet Public Health*. 2018;3(4):e177-e184. doi:10.1016/S2468-2667(18)30025-2

57.Salehi F, Darmiani K, Nakhaee S, et al. Comparison of Blood Lead Concentrations in Mothers of Children with Congenital Heart Disease and Mothers of Healthy Children. *Biol Trace Elem Res*. 2022;200(5):2001-2007. doi:10.1007/s12011-021-02813-z

58.Wang C, Pi X, Yin S, et al. Maternal exposure to heavy metals and risk for severe congenital heart defects in offspring. *Environ Res*. 2022;212(Pt C):113432. doi:10.1016/j.envres.2022.113432

59.Liang Y, Pan Z, Zhu M, et al. Exposure to essential and non-essential trace elements and risks of congenital heart defects: A narrative review. *Front Nutr*. 2023;10:1121826. doi:10.3389/fnut.2023.1121826

60.Ou Y, Bloom MS, Nie Z, et al. Associations between toxic and essential trace elements in maternal blood and fetal congenital heart defects. *Environ Int*. 2017;106:127-134. doi:10.1016/j.envint.2017.05.017

61.Liu Z, Yu Y, Li X, et al. Maternal lead exposure and risk of congenital heart defects occurrence in offspring. *Reprod Toxicol Elmsford N*. 2015;51:1-6. doi:10.1016/j.reprotox.2014.11.002

62.Vaziri ND. Mechanisms of lead-induced hypertension and cardiovascular disease. *Am J Physiol - Heart Circ Physiol*. 2008;295(2):H454-H465. doi:10.1152/ajpheart.00158.2008

63.Kern M, Audesirk G. Stimulatory and inhibitory effects of inorganic lead on calcineurin. *Toxicology*. 2000;150(1-3):171-178. doi:10.1016/s0300-483x(00)00258-4

64. Terrar DA. Calcium Signaling in the Heart. In: Islam MdS, ed. *Calcium Signaling*. Advances in Experimental Medicine and Biology. Springer International Publishing; 2020:395-443. doi:10.1007/978-3-030-12457-1_16

65. Ferreira de Mattos G, Costa C, Savio F, Alonso M, Nicolson GL. Lead poisoning: acute exposure of the heart to lead ions promotes changes in cardiac function and Cav1.2 ion channels. *Biophys Rev*. 2017;9(5):807-825. doi:10.1007/s12551-017-0303-5

66. Waddington CH. The epigenotype. 1942. *Int J Epidemiol*. 2012;41(1):10-13. doi:10.1093/ije/dyr184

67. Goldberg AD, Allis CD, Bernstein E. Epigenetics: A Landscape Takes Shape. *Cell*. 2007;128(4):635-638. doi:10.1016/j.cell.2007.02.006

68. Zhang L, Lu Q, Chang C. Epigenetics in Health and Disease. *Adv Exp Med Biol*. 2020;1253:3-55. doi:10.1007/978-981-15-3449-2_1

69. Mei Z, Liu G, Zhao B, He Z, Gu S. Emerging roles of epigenetics in lead-induced neurotoxicity. *Environ Int*. 2023;181:108253. doi:10.1016/j.envint.2023.108253

70. Moore LD, Le T, Fan G. DNA Methylation and Its Basic Function. *Neuropsychopharmacology*. 2013;38(1):23-38. doi:10.1038/npp.2012.112

71. Hernández-Oliveras A, Zarain-Herzberg A. The role of Ca2+-signaling in the regulation of epigenetic mechanisms. *Cell Calcium*. 2024;117:102836. doi:10.1016/j.ceca.2023.102836

72. Hanna CW, Bloom MS, Robinson WP, et al. DNA methylation changes in whole blood is associated with exposure to the environmental contaminants, mercury, lead, cadmium and

bisphenol A, in women undergoing ovarian stimulation for IVF. *Hum Reprod Oxf Engl*. 2012;27(5):1401-1410. doi:10.1093/humrep/des038

73. Tajuddin SM, Amaral AFS, Fernández AF, et al. Genetic and non-genetic predictors of LINE-1 methylation in leukocyte DNA. *Environ Health Perspect*. 2013;121(6):650-656. doi:10.1289/ehp.1206068

74. Wright RO, Schwartz J, Wright RJ, et al. Biomarkers of lead exposure and DNA methylation within retrotransposons. *Environ Health Perspect*. 2010;118(6):790-795. doi:10.1289/ehp.0901429

75. Li C, Yang X, Xu M, Zhang J, Sun N. Epigenetic marker (LINE-1 promoter) methylation level was associated with occupational lead exposure. *Clin Toxicol*. 2013;51(4):225-229. doi:10.3109/15563650.2013.782410

76. Barker DJ, Winter PD, Osmond C, Margetts B, Simmonds SJ. Weight in infancy and death from ischaemic heart disease. *Lancet Lond Engl*. 1989;2(8663):577-580. doi:10.1016/s0140-6736(89)90710-1

77. Barker DJ, Gluckman PD, Godfrey KM, Harding JE, Owens JA, Robinson JS. Fetal nutrition and cardiovascular disease in adult life. *Lancet Lond Engl*. 1993;341(8850):938-941. doi:10.1016/0140-6736(93)91224-a

78. Barker DJ, Osmond C. Infant mortality, childhood nutrition, and ischaemic heart disease in England and Wales. *Lancet Lond Engl*. 1986;1(8489):1077-1081. doi:10.1016/s0140-6736(86)91340-1

79. Thornburg KL. The programming of cardiovascular disease. *J Dev Orig Health Dis*. 2015;6(5):366-376. doi:10.1017/S2040174415001300

80. Intapad S, Ojeda NB, Dasinger JH, Alexander BT. Sex Differences in the Developmental Origins of Cardiovascular Disease. *Physiology*. 2014;29(2):122-132. doi:10.1152/physiol.00045.2013

81. Messerschmidt DM, Knowles BB, Solter D. DNA methylation dynamics during epigenetic reprogramming in the germline and preimplantation embryos. *Genes Dev*. 2014;28(8):812-828. doi:10.1101/gad.234294.113

82. Kim N, Filipovic D, Bhattacharya S, Cuddapah S. Epigenetic toxicity of heavy metals − implications for embryonic stem cells. *Environ Int*. 2024;193:109084. doi:10.1016/j.envint.2024.109084

83. Wright MW, Bruford EA. Naming "junk": Human non-protein coding RNA (ncRNA) gene nomenclature. *Hum Genomics*. 2011;5(2):90. doi:10.1186/1479-7364-5-2-90

84. Panni S, Lovering RC, Porras P, Orchard S. Non-coding RNA regulatory networks. *Biochim Biophys Acta BBA - Gene Regul Mech*. 2020;1863(6):194417. doi:10.1016/j.bbagrm.2019.194417

85. Bollati V, Marinelli B, Apostoli P, et al. Exposure to metal-rich particulate matter modifies the expression of candidate microRNAs in peripheral blood leukocytes. *Environ Health Perspect*. 2010;118(6):763-768. doi:10.1289/ehp.0901300

86.Mirzadeh Azad F, Arabian M, Maleki M, Malakootian M. Small Molecules with Big Impacts on Cardiovascular Diseases. *Biochem Genet*. 2020;58(3):359-383. doi:10.1007/s10528-020-09948-z

87.Siasos G, Bletsa E, Stampouloglou PK, et al. MicroRNAs in cardiovascular disease. *Hellenic J Cardiol*. 2020;61(3):165-173. doi:10.1016/j.hjc.2020.03.003

88.Eulalio A, Mano M, Ferro MD, et al. Functional screening identifies miRNAs inducing cardiac regeneration. *Nature*. 2012;492(7429):376-381. doi:10.1038/nature11739

89.Chatterjee E, Das S. Non-coding RNAs in cardiac remodeling: diversity in composition and function. *Curr Opin Physiol*. 2022;26:100534. doi:10.1016/j.cophys.2022.100534

90.Morales ME, Servant G, Ade C, Roy-Engel AM. Altering Genomic Integrity: Heavy Metal Exposure Promotes Transposable Element-Mediated Damage. *Biol Trace Elem Res*. 2015;166(1):24-33. doi:10.1007/s12011-015-0298-3

91.Faulk C, Barks A, Liu K, Goodrich JM, Dolinoy DC. Early-life lead exposure results in dose- and sex-specific effects on weight and epigenetic gene regulation in weanling mice. *Epigenomics*. 2013;5(5):487-500. doi:10.2217/epi.13.49

92.Faulk C, Liu K, Barks A, Goodrich JM, Dolinoy DC. Longitudinal epigenetic drift in mice perinatally exposed to lead. *Epigenetics*. 2014;9(7):934-941. doi:10.4161/epi.29024

93.Goodrich JM, Sánchez BN, Dolinoy DC, et al. Quality control and statistical modeling for environmental epigenetics: A study on in utero lead exposure and DNA methylation at birth. *Epigenetics*. 2015;10(1):19-30. doi:10.4161/15592294.2014.989077

94.Vagin VV, Sigova A, Li C, Seitz H, Gvozdev V, Zamore PD. A distinct small RNA pathway silences selfish genetic elements in the germline. *Science*. 2006;313(5785):320-324. doi:10.1126/science.1129333

95.Aravin A, Gaidatzis D, Pfeffer S, et al. A novel class of small RNAs bind to MILI protein in mouse testes. *Nature*. 2006;442(7099):203-207. doi:10.1038/nature04916

96.Grivna ST, Beyret E, Wang Z, Lin H. A novel class of small RNAs in mouse spermatogenic cells. *Genes Dev*. 2006;20(13):1709-1714. doi:10.1101/gad.1434406

97.Lau NC, Seto AG, Kim J, et al. Characterization of the piRNA complex from rat testes. *Science*. 2006;313(5785):363-367. doi:10.1126/science.1130164

98.Girard A, Sachidanandam R, Hannon GJ, Carmell MA. A germline-specific class of small RNAs binds mammalian Piwi proteins. *Nature*. 2006;442(7099):199-202. doi:10.1038/nature04917

99.Houwing S, Kamminga LM, Berezikov E, et al. A Role for Piwi and piRNAs in Germ Cell Maintenance and Transposon Silencing in Zebrafish. *Cell*. 2007;129(1):69-82. doi:10.1016/j.cell.2007.03.026

100.Mani SR, Juliano CE. Untangling the web: The diverse functions of the PIWI/piRNA pathway. *Mol Reprod Dev*. 2013;80(8):632-664. doi:10.1002/mrd.22195

101.Sturm Á, Ivics Z, Vellai T. The mechanism of ageing: primary role of transposable elements in genome disintegration. *Cell Mol Life Sci CMLS*. 2015;72(10):1839-1847. doi:10.1007/s00018-015-1896-0

102.Zhang P, Si X, Skogerbø G, et al. piRBase: a web resource assisting piRNA functional study. *Database J Biol Databases Curation*. 2014;2014:bau110. doi:10.1093/database/bau110

103.Sarkar A, Maji RK, Saha S, Ghosh Z. piRNAQuest: searching the piRNAome for silencers. *BMC Genomics*. 2014;15:555. doi:10.1186/1471-2164-15-555

104.Sai Lakshmi S, Agrawal S. piRNABank: a web resource on classified and clustered Piwi-interacting RNAs. *Nucleic Acids Res*. 2008;36(Database issue):D173-177. doi:10.1093/nar/gkm696

105.Rosenkranz D. piRNA cluster database: a web resource for piRNA producing loci. *Nucleic Acids Res*. 2016;44(D1):D223-230. doi:10.1093/nar/gkv1265

106.Seto AG, Kingston RE, Lau NC. The Coming of Age for Piwi Proteins. *Mol Cell*. 2007;26(5):603-609. doi:10.1016/j.molcel.2007.05.021

107.Kirino Y, Mourelatos Z. Mouse Piwi-interacting RNAs are 2'-O-methylated at their 3' termini. *Nat Struct Mol Biol*. 2007;14(4):347-348. doi:10.1038/nsmb1218

108.Ohara T, Sakaguchi Y, Suzuki T, Ueda H, Miyauchi K, Suzuki T. The 3' termini of mouse Piwi-interacting RNAs are 2'-O-methylated. *Nat Struct Mol Biol*. 2007;14(4):349-350. doi:10.1038/nsmb1220

109.Brennecke J, Aravin AA, Stark A, et al. Discrete Small RNA-Generating Loci as Master Regulators of Transposon Activity in Drosophila. *Cell*. 2007;128(6):1089-1103. doi:10.1016/j.cell.2007.01.043

110.Lin H, Spradling AC. A novel group of pumilio mutations affects the asymmetric division of germline stem cells in the Drosophila ovary. *Development*. 1997;124(12):2463-2476. doi:10.1242/dev.124.12.2463

111.Shoji K, Suzuki Y, Sugano S, Shimada T, Katsuma S. Artificial “ping-pong” cascade of PIWI-interacting RNA in silkworm cells. *RNA*. 2017;23(1):86-97. doi:10.1261/rna.058875.116

112.Yan Z, Hu HY, Jiang X, et al. Widespread expression of piRNA-like molecules in somatic tissues. *Nucleic Acids Res*. 2011;39(15):6596-6607. doi:10.1093/nar/gkr298

113.Ross RJ, Weiner MM, Lin H. PIWI proteins and PIWI–interacting RNAs in the soma. *Nature*. 2014;505(7483):353-359. doi:10.1038/nature12987

114.Reddien PW, Oviedo NJ, Jennings JR, Jenkin JC, Sánchez Alvarado A. SMEDWI-2 is a PIWI-like protein that regulates planarian stem cells. *Science*. 2005;310(5752):1327-1330. doi:10.1126/science.1116110

115.Fagegaltier D, Falciatori I, Czech B, et al. Oncogenic transformation of Drosophila somatic cells induces a functional piRNA pathway. *Genes Dev*. 2016;30(14):1623-1635. doi:10.1101/gad.284927.116

116.Tsuji J, Thomson T, Brown C, et al. Somatic piRNAs and Transposons are Differentially Expressed Coincident with Skeletal Muscle Atrophy and Programmed Cell Death. *Front Genet*. 2021;12. Accessed September 29, 2022. https://www.frontiersin.org/articles/10.3389/fgene.2021.775369

117.Dou Z, Ma XT, Piao MN, Wang JP, Li JL. Overview of the interplay between m6A methylation modification and non-coding RNA and their impact on tumor cells. *Transl Cancer Res*. 2024;13(6):3106-3125. doi:10.21037/tcr-23-2401

118.Gao XQ, Zhang YH, Liu F, et al. The piRNA CHAPIR regulates cardiac hypertrophy by controlling METTL3-dependent N6-methyladenosine methylation of Parp10 mRNA. *Nat Cell Biol*. 2020;22(11):1319-1331. doi:10.1038/s41556-020-0576-y

119.AVCAPIR: A Novel Procalcific PIWI-Interacting RNA in Calcific Aortic Valve Disease | Circulation. Accessed February 7, 2025. https://www.ahajournals.org/doi/10.1161/CIRCULATIONAHA.123.065213?url_ver=Z39.88-2003&rfr_id=ori:rid:crossref.org&rfr_dat=cr_pub%20%200pubmed

120.Rajasethupathy P, Antonov I, Sheridan R, et al. A Role for Neuronal piRNAs in the Epigenetic Control of Memory-Related Synaptic Plasticity. *Cell*. 2012;149(3):693-707. doi:10.1016/j.cell.2012.02.057

121.Zhou Y, Fang Y, Dai C, Wang Y. PiRNA pathway in the cardiovascular system: a novel regulator of cardiac differentiation, repair and regeneration. *J Mol Med*. 2021;99(12):1681-1690. doi:10.1007/s00109-021-02132-9

122.Rinkevich Y, Voskoboynik A, Rosner A, et al. Repeated, Long-Term Cycling of Putative Stem Cells between Niches in a Basal Chordate. *Dev Cell*. 2013;24(1):76-88. doi:10.1016/j.devcel.2012.11.010

123.Vella S, Gallo A, Lo Nigro A, et al. PIWI-interacting RNA (piRNA) signatures in human cardiac progenitor cells. *Int J Biochem Cell Biol*. 2016;76:1-11. doi:10.1016/j.biocel.2016.04.012

124.Greca AL, Scarafía MA, Cañás MCH, et al. PIWI-interacting RNAs are differentially expressed during cardiac differentiation of human pluripotent stem cells. *PLOS ONE*. 2020;15(5):e0232715. doi:10.1371/journal.pone.0232715

125.Zhang K, Li Y, Huang Y, Sun K. PiRNA in Cardiovascular Disease: Focus on Cardiac Remodeling and Cardiac Protection. *J Cardiovasc Transl Res*. 2023;16(4):768-777. doi:10.1007/s12265-023-10353-1

126.Lucchinetti E, Feng J, Silva R da, et al. Inhibition of LINE-1 expression in the heart decreases ischemic damage by activation of Akt/PKB signaling. *Physiol Genomics*. 2006;25(2):314-324. doi:10.1152/physiolgenomics.00251.2005

127.Abeyrathna P, Su Y. The Critical Role of Akt in Cardiovascular Function. *Vascul Pharmacol*. 2015;74:38-48. doi:10.1016/j.vph.2015.05.008

128.Li Y, Zeng A, Li G, et al. Dynamic regulation of small RNAome during the early stage of cardiac differentiation from pluripotent embryonic stem cells. *Genomics Data*. 2017;12:136-145. doi:10.1016/j.gdata.2017.05.006

129.Liu Q, Van Bortle K, Zhang Y, et al. Disruption of mesoderm formation during cardiac differentiation due to developmental exposure to 13-cis-retinoic acid. *Sci Rep*. 2018;8(1):12960. doi:10.1038/s41598-018-31192-0

130.Nakamura M, Sadoshima J. Mechanisms of physiological and pathological cardiac hypertrophy. *Nat Rev Cardiol*. 2018;15(7):387-407. doi:10.1038/s41569-018-0007-y

131.Li M, Yang Y, Wang Z, et al. Piwi-interacting RNAs (piRNAs) as potential biomarkers and therapeutic targets for cardiovascular diseases. *Angiogenesis*. 2021;24(1):19-34. doi:10.1007/s10456-020-09750-w

132.Cheang I, Zhu Q, Liao S, Li X. Current Understanding of piRNA in Cardiovascular Diseases. *Front Mol Med*. 2022;1. Accessed July 6, 2022. https://www.frontiersin.org/articles/10.3389/fmmed.2021.791931

133.Lipps C, Northe P, Figueiredo R, et al. Non-Invasive Approach for Evaluation of Pulmonary Hypertension Using Extracellular Vesicle-Associated Small Non-Coding RNA. *Biomolecules*. 2019;9(11):666. doi:10.3390/biom9110666

134.Svoboda LK, Wang K, Cavalcante RG, et al. Sex-Specific Programming of Cardiac DNA Methylation by Developmental Phthalate Exposure. *Epigenetics Insights*. 2020;13:2516865720939971. doi:10.1177/2516865720939971

135.Svoboda LK, Neier K, Wang K, et al. Tissue and sex-specific programming of DNA methylation by perinatal lead exposure: implications for environmental epigenetics studies. *Epigenetics*. 16(10):1102-1122. doi:10.1080/15592294.2020.1841872

Chapter 2: Aim 1: Sex-Stratified piRNA Expression Analysis Reveals Shared Functional Impacts of Perinatal Pb Exposure in Murine Hearts*

Goal: Establish sex-stratified baseline maps of all piRNAs expressed in murine heart tissue and examine effects of perinatal Pb exposure on piRNA expression in murine hearts.

Hypothesis: piRNAs are expressed in the heart, their expression is sex-specific, and their expression is affected by perinatal Pb exposure in a sex-specific manner.

***Reuse Note:** This chapter is based on a published manuscript and is reused here with permission under the terms of the Creative Commons license. Sala-Hamrick, Kimberley E et al. "Sex-stratified piRNA expression analysis reveals shared functional impacts of perinatal lead (Pb) exposure in murine hearts." *Epigenetics* vol. 20,1 (2025): 2542879. https://doi.org/10.1080/15592294.2025.2542879
© The Authors. This article is licensed under the **Creative Commons Attribution License (CC BY 4.0)**, which permits unrestricted use, distribution, and reproduction in any medium, provided the original work is properly cited. License link: http://creativecommons.org/licenses/by/4.0/

2.1: Abstract

The landscape of PIWI-interacting RNA (piRNA) expression in the heart is poorly understood, particularly regarding sex differences. Altered piRNA expression has been reported in cardiovascular disease (CVD), and although exposure to the metal lead (Pb) is strongly associated with CVD risk, no studies have investigated Pb's effects on cardiac piRNAs. This study aimed to characterize piRNA expression in the murine heart and assess sex-specific effects of human-relevant maternal Pb exposure on adult offspring cardiac piRNA expression. piRNAs were identified from whole mouse hearts using sodium periodate exclusion of small RNA and subsequent sequencing. Control mice expressed 18,956 piRNAs in combined-sex analysis; sex-specific analyses revealed 9,231 piRNAs in female hearts and 5,972 piRNAs in male hearts. Genomic mapping showed 28-41% aligned to introns, while 12-28% mapped to exons. Comparing control and Pb-exposed hearts, we found more potential Pb-induced expression changes in females (847) compared to males (187) (p-value < 0.05 and $|\log FC| > 1$). These piRNAs were significantly enriched near genes involved in biological processes related to heart function and CVD development, including mitochondrial function, energy metabolism, and cardiac muscle structure (FDR < 0.05). We also interrogated our samples for potential mRNA targets, *Piwil*s, and genes related to excitation contraction coupling (ECC), and found Pb induced sex specific changes in *Piwils* and ECC genes. Overall, we characterized combined and sex-stratified piRNA expression in both control and Pb-exposed murine hearts. In addition to providing a foundation for sex-specific piRNA expression in the heart, these findings suggest a novel epigenetic mechanism by which developmental Pb exposure may impact CVD risk later in life. Future studies will link these sex-specific molecular changes to Pb-induced alterations in cardiac function.

2.2: Introduction

Epigenetic modifications, which include DNA methylation, histone modifications, and non-coding RNA (ncRNA), contribute to changes in gene expression without altering the underlying genetic code itself.[1] PIWI-interacting NA (piRNA) are a class of small non-coding RNA (smRNA) first coined in in the early 2000s by a group of studies showing a novel distinct small RNA which associate with PIWI proteins in both *Drosphila* and mammals.[2–6] piRNAs have since been shown to play important roles in maintaining genomic stability in germ cells by controlling DNA methylation of transposable elements and later to control transposable element expression through cleavage of mRNA targets (post-transcriptional gene silencing).[7–9] piRNA have also been shown to alter histone modifications leading to heterochromatin formation as well as to regulate posttranslational modifications of transcription factors.[10] piRNAs are longer in length than other micro RNAs, as germline piRNAs are roughly 21–35 nucleotides.[11] Primary piRNAs have a strong preference for a 5′ uridine signature, and secondary piRNAs have a bias for an adenine signature at position 10.[12,13] piRNAs are also distinct from other forms of small non-coding RNA in that they have a 2'-O-methylation at their 3' terminus which confers stability.[14] This 2'-O-methylation can be harnessed to select for piRNA compared to other small RNA through treatment with sodium periodate, which oxidizes all molecules terminating in 2′,3′-OH groups, preventing linker attachment and thus only allowing RNA with 2'-O-methylation to be sequenced .[15] This method has previously been shown to be effective in identifying somatic piRNA expression and is more rigorous than using size exclusion.[15–17]

Although they are well characterized in the germline, little is known about piRNA function and sex-specificity in somatic tissues, including the heart. In the soma, piRNA were first discovered to play important roles in stem cell function and in the development of multiple

types of cancer.[18–20] More recent studies have found that piRNA pathways are also important in fully differentiated somatic tissues, particularly in the brain, where they have been implicated in neurodegenerative disease.[21] Our recent work has demonstrated that somatic piRNA (albeit shorter in length versus germline piRNA) and associated *Piwils* are expressed in the mouse soma, including the brain, liver, and kidney.[15]

Some work has found altered piRNA expression in the context of cardiovascular disease (CVD).[22,23] piRNAs have been shown to play roles in cardiac repair, differentiation, and pathologies.[22–25] It has been postulated that they also play critical roles in fine tuning gene expression during differentiation of embryonic stem cell derived cardiomyocytes.[25] Disease-specific piRNAs have been implicated in both *in vivo* and *in vitro* rat models of cardiac hypertrophy, as well as in epidemiological studies.[22,23] Interestingly, in models of cardiac hypertrophy, piRNA expression was found to be increased *in vivo*, mapping to mRNA regions, and decreased *in vitro*, mapping to both mRNA and transposon (including LINE-1) regions.[26] This study also found specific piRNAs elevated in myocardial infarction patients.[26] One epidemiological study found large differences in expression (both up and downregulation) of piRNAs in heart failure patients.[23] piRNAs were also found to be differentially expressed in patients with chronic thromboembolic pulmonary hypertension (CTEPH).[27]

Importantly, there are prominent sex differences in manifestations, pathogenesis, and prognosis of CVD, but whether differential piRNA expression underlies these disparities is unclear.[28,29] piRNA display a degree of sex-specific expression in the germline, with zebrafish models showing that over 20% of piRNAs have differential expression between ovaries and testes. [30,31] It is hypothesized that sex differences in piRNA expression arise from variations in transposable element activity due to differences in germ cell development.[32] Comparatively, little

is known about sex-specific piRNA expression in the soma. Other ncRNA including micro RNAs (miRNAs) and long non-coding RNAs (lncRNAs) have been shown as sex-specific mediators or biomarkers of CVD, although this research is in its early stages.[33]

The Developmental Origins of Health and Disease (DOHaD) paradigm states that environmental exposures during critical periods of life (e.g., periconception, gestation, infancy, adolescence) impact the onset of disease in later life, and this has been demonstrated in humans as well as animal models (including mice).[34] Environmental pollutants are known to play roles in the incidence and progression of CVD. Lead (Pb) is a heavy metal and common environmental contaminant released from industrial sources or found in older homes or buildings, and Pb exposure is associated with adverse cardiovascular health outcomes.[35] However, mechanisms of Pb's role in CVD are still being explored, and how sex differences influence this effect has yet to be characterized. Environmental exposure to Pb has been characterized to regulate gene expression through epigenetic modifications in both humans and mice.[36–42] One of the mechanisms by which Pb may contribute to the development of CVD is through altered regulation of the epigenome. Perinatal exposure to Pb has been shown to alter DNA methylation and gene expression in a sex-specific manner in mouse cardiac tissue, and these changes map to pathways important for cardiac development and disease progression.[42–44] Thus, given that piRNAs modulate gene expression through altering DNA methylation, it is important to assess whether Pb exposure impacts piRNA expression.

We also assessed Pb induced changes in *Piwil*s, genes that encode for proteins associated with piRNA functionality. PIWI stands for p-element induced wimpy testis and was first discovered to play roles in spermatogenesis in Drosophila.[45] The three genes that encode for mouse PIWIL proteins are named *Miwi* (*Piwil1*), *Mili* (*Piwil2*), and *Miwi2* (*Piwil4*). PIWILs

function by binding to and guiding piRNA transcripts to transposons, where they help with DNA methylation and transcriptional silencing.[46] Further, they bind to piRNA transcripts in intermediate steps of secondary piRNA biogenesis, called "ping pong" amplification, which is highly conserved across species.[47]

In addition to epigenetic changes, we sought to understand how Pb exposure may alter cardiac function in the mouse heart by assessing changes in excitation contraction coupling genes. Excitation contraction coupling (ECC), is the process by which an electrical stimulus (action potential) leads to an influx of calcium (Ca) in cardiomyocytes, which results in contraction of these cells.[48] In this process, action potentials trigger the release of Ca into the cell, where it binds to troponin-C, which causes a conformational change in the regulatory complex it is bound to that causes troponin-1 to move and expose an actin site.[49] This enables actin to bind to ATPase on a myosin head, which causes ATP hydrolysis, giving energy for a conformational change in actin-myosin complex that causes actin and myosin filaments to slide past each other, thus creating uniform contraction that forms a heartbeat.[49,50]

Notably, there are known sex differences in ECC at baseline, with smaller and slower peak cardiomyocyte contractions in females compared to males in rat models.[48] Fewer studies have examined cardiac ECC sex differences in humans, but one study showed that gender influences cardiac force, with female cardiac biopsy fibers showing higher maximal force in high Ca conditions and male fibers showing higher Ca sensitivity.[51] Further, Pb is known to mimic Ca and through disruption of Ca signaling can lead to cardiac arrythmias.[52] We assessed four ECC genes in this study: *Atp2A2* (SERCA2), which transports Ca from cytosol into sarcoplasmic reticulum, *Cacna1c* (Cav1.2) which transports Ca into cytosol from outside the cell, *Ryr2* (ryanodine receptor), which transports Ca from sarcoplasmic reticulum into cytosol, and *Slec8a1*

(Na Ca exchanger) which transports Ca out of the cell. Importantly, *Atp2A2* and *Ryr2* are subject to demethylation at promoter regions and are consequently expressed at higher levels as the heart develops from fetal to adult stages in both mouse and human models.[53–55] Given their dynamic, epigenetically regulated expression during development, ECC genes could vulnerable to altered epigenetic programming by developmental exposure to Pb.

Overall, the aims of this project were to identify heart-specific piRNAs in male and female mice and characterize longitudinal piRNA expression influenced by perinatal Pb exposure. This work may lead to the use of piRNA as a potential biomarker of disease and opens the door for the potential to use piRNA for interventions to treat CVD.[56]

2.3: Methods

Mouse breeding experiments

Mice (*mus musculus*) used for this study have recently been described.[57,58] All mice for this study were housed at the ULAM (Unit for Laboratory Animal Medicine) of University of Michigan and maintained on regular 12-12 dark-light cycles at 70-73 °F and 50% humidity. Animals were maintained on a phytoestrogen-free modified AIN-93G diet (TD.95092, 7% Corn Oil Diet, (Envigo, Indianapolis, IN, USA). All animals had access to food and drinking water *ad libitum* throughout the experiment and were housed in polycarbonate-free cages. Health checks were carried out daily by lab personnel and ULAM staff. Health checks consisted of a general assessment of appearances (fur coat intact and well-groomed, eyes clear, no signs of fight wounds) and behavior (mobility, nest building, etc.). In addition to checks by lab personnel, a designated animal handler from ULAM checked these cues on a daily basis, and a veterinarian assessed the health status of the mice at least once a week. At 3 weeks, 5 months, and 10 months

of age, all (both control and Pb exposed as outlined below) mice were euthanized with CO_2 asphyxiation followed by a secondary method of euthanasia of bilateral pneumothorax procedure in accordance with rules and regulations set forth by the Institutional Animal Care and Use Committee (IACUC). This study protocol was approved by the University of Michigan IACUC protocol #PRO00009800. ARRIVE guidelines were adhered to for this study.

Mouse exposure paradigm

This perinatal Pb exposure study was done as part of a larger study under the National Institute of Environmental Health Sciences (NIEHS) Toxicant Exposures and Responses by Genomic and Epigenomic Regulators of Transcription (TaRGET II) Consortium.[58] Pb preparation and exposure were conducted exactly as outlined previously.[40] Virgin female wild-type *a/a* non-agouti mice (derived from a colony for the viable yellow agouti (A^{vy}) strain) 93% identical to the C57BL/6 mice (6-8 weeks old) were randomly assigned to receive control or Pb via drinking water 2 weeks prior to mating, followed by mating with virgin a/a males of the same strain (7-9 weeks old; **Figure 2.1**).[57] Pb II acetate trihydrate (32 ppm; Sigma-Aldrich, Milwaukee, WI, USA) was mixed with distilled drinking water, which results in a human-relevant maternal exposure in the 16–60 μg/dL range.[40,59] Pb exposure continued through mating (for both males and females), pregnancy (~3 weeks), and lactation until weaning at 3 weeks of age (**Figure 2.1**).[43] After weaning, all offspring received Pb-free water until euthanasia at 3 weeks, 5 months, and 10 months of age (**Figure 2.1**). Approximately 1-2 male and 1-2 female offspring per litter were euthanized (n=5-6 per sex per exposure; **Figure 2.1**). No formal sample size calculation was performed. Sample sizes were based on standard practice in the laboratory and were consistent with prior publications using similar methods.[60] Animal collection occurred between 1 and 3 pm, with collection order randomized daily.[60] As outlined in previous studies,

one investigator administered treatment and was therefore aware of treatment group allocation, but all investigators completing subsequent molecular assays were blinded to the treatment group until it was analyzed during bioinformatic analysis.[60] All experiments were conducted according to experimental procedures delineated by the NIEHS TaRGET II Consortium.[58,60] Whole, perfused hearts from these mice were snap frozen in liquid nitrogen and stored at -80 °C at the time of euthanasia. The outcome of interest for this study was piRNA expression in the heart for 5-month samples (**Figure 1**), and gene expression analyses at all three time points

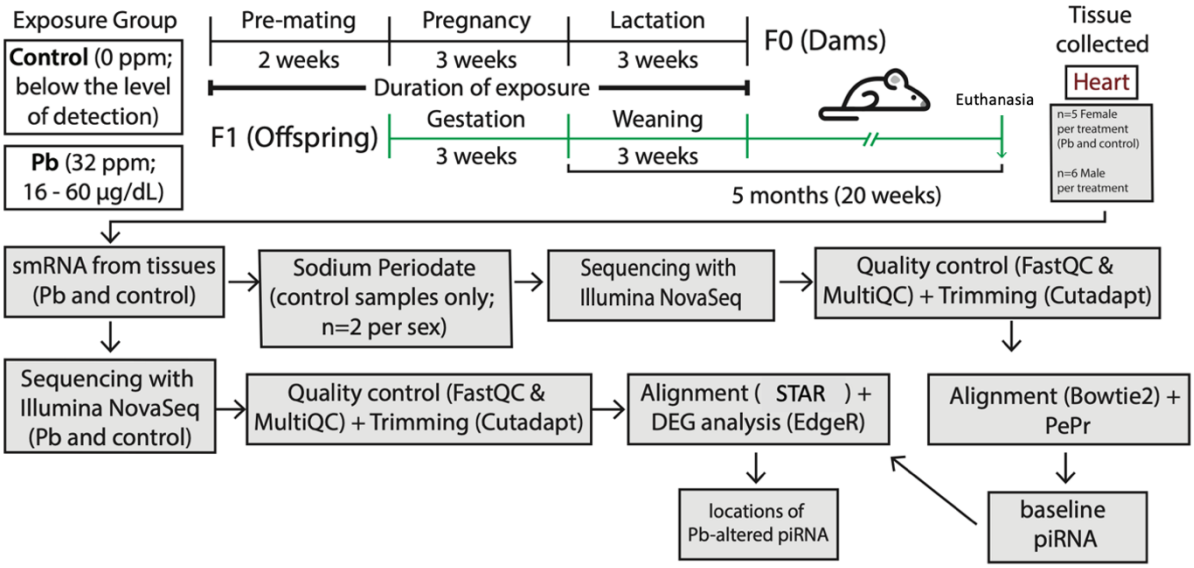


Figure 2.1 : Experimental design for perinatal mouse Pb exposure and sequencing analysis pipeline.

Pb exposure began with female mice two weeks prior to mating and continued through lactation until weaning at 3 weeks of age. After weaning, all offspring received Pb-free water until euthanasia at 5 months of age. Approximately 1-2 male and 1-2 female offspring per litter were euthanized (n=5 female and n=6 male per exposure group). After collecting smRNA from whole heart tissues, sodium periodate treatment was performed on select control hearts (n=2 per sex) to select for baseline piRNA, followed by sequencing on Illumina NovaSeq, quality control

(FastQC and MultiQC) and trimming (Cutadapt), alignment to the genome (Bowtie2), and PePr peak calling to distinguish peaks enriched in the sodium periodate treated samples (piRNA). Another set of smRNA (all collected samples; non-sodium periodate treated; n = 5 female and n =6 male per Pb treatment) was sequenced, underwent quality control (FastQC and MultiQC) and trimming (Cutadapt), alignment to the baseline piRNA generated by previous sequencing using STAR, EdgeR analysis to compare piRNA expression in control vs. Pb-exposed, and the resulting locations of piRNA alterations associated with Pb exposure was used in downstream analyses.

Tissue lysis and smRNA extraction

Heart tissue was cryo-pulverized and small RNA (smRNA) extraction was performed using the AllPrep DNA/RNA Mini Kit (#80204 Qiagen, Aarhus, Denmark) and RNeasy MinElute Cleanup Kit (#74204, Qiagen, Aarhus, Denmark) according to the manufacturer's instructions. The AllPrep kit selects for total RNA, which includes RNAs that are >200 bp, while the RNeasy kit was used to further select for small RNAs that are <200 bp. Sample concentration and quality were assessed using a nanodrop microvolume spectrophotometer (Thermo Fisher Scientific, Waltham, Massachusetts, USA).

Sodium periodate exclusion to select for baseline piRNA assessment

Control heart smRNA samples (n=2 per sex at 5 months, not littermates per sex) were treated with sodium periodate to select for piRNA against other forms of smRNA. piRNAs are resistant to sodium periodate treatment due to the presence of a unique 3' modification of 2'-O-methylation.[15,16,18] Sodium periodate treatment was performed as previously described.[15] Briefly, four separate reactions were set up, each with 400 ng of smRNA (27 µL) with the same amount of borate buffer added (8 µL; generated with 150 mM borax: #T29C533, Alfa Aesar, Ward Hill,

Massachusetts, USA and 150 mM boric acid: #SZBG1380V, Fluka Analytics, Buchs, Switzerland and adjusted to a pH 8.6 using sodium hydroxide: #A4782902, Thermo Fisher Scientific, Waltham, Massachusetts, USA), but three reactions with sodium periodate added (5 µL; #BCBS5360V, Sigma Aldrich, Milwaukee, WI, USA) and the other water (5 µL), and then samples are incubated for 30 minutes. This was followed by an ethanol precipitation, resuspension of smRNA in water, and combination of the three sodium periodate treated smRNA samples into one.

Sequencing of smRNA

smRNA sequencing was performed in two separate batches for this study. For the first, periodate treated (n=2 per sex) and non-treated samples (n=2 per sex) were sequenced (total n=8) at the University of Michigan's Advanced Genomics Core (AGC). Before sequencing, quality control and library preparation were performed by the AGC using TapeStation (RNA ScreenTape #5067-5576 and RNA ScreenTape Sample Buffer #5067-5577, Agilent Technologies, Santa Clara, CA, USA; analysis software 4.1) and SMARTer smRNA-seq kit (#635031, Takara, San Jose, CA, USA). Purification was performed to remove excess adapter present in samples. Sequencing was performed on an Illumina NovaSeq S1 flowcell (200 cycle) ensuring ~38 million reads per sample. For our second batch of sequencing, using non periodate treated samples but including smRNA from hearts of mice that had been treated with Pb (n=5 female per treatment and 6 male per treatment for a total of 22 samples), we followed the same sample preparation procedures as were done for the first batch, and sequenced on an Illumina NovaSeq S4 300 cycle.

Computational analysis: read processing

Reads were analyzed according to a piRNA analysis pipeline established previously.[15] First, raw data quality was assessed using FastQC (v0.11.8) and MultiQC (v1.8). Next, processing of the reads was performed through adapter trimming, size selection (10-45 bp), and quality trimming. After this, Bowtie2 (v2.3.5.1) was used to align reads to the genome, using option -k 1000 –score-min 'C,0,-1' to find the perfect alignments for reads with 100 mapping locations.

Computational analysis: heart-specific piRNA selection

Control samples were used to create baseline maps of piRNA present in the mouse heart. PePr peak calling software (version 1.1.21 with parameters – shiftsize 0 – windowsize 20 – threshold 1E-3 – peaktype sharp) was utilized for pairwise comparison of the filtered alignments from sodium periodate treated and control samples to identify regions overrepresented in periodate treated RNA reads.[61] This step ensures that regions identified are those that are significantly more resistant to the sodium periodate.[61]

Peaks shorter than 20 nucleotides or greater than 45 nucleotides were excluded from subsequent analyses. The website https://csbg.cnb.csic.es/BioinfoGP/venny.html and package eulerr in R were used to create Venn diagrams of expression in different analyses (combined, female, and male) of baseline piRNAs. Genomic annotations were carried out using the Biocondutor package Annotatr (v1.24.0) in R. Full information on genomic annotations can be found here: https://bioconductor.org/packages/devel/bioc/vignettes/annotatr/inst/doc/annotatr-vignette.html .

R package valr (v0.6.8) was used to perform the repeat annotation against the repeat annotation downloaded from the UCSC Genome Browser (https://hgdownload.soe.ucsc.edu/goldenPath/mm10/bigZips/ file: mm10.fa.out.gz), and subsequently the categories were

condensed into themes (ie LTRs, LINEs and SINEs) and other RNA types were omitted from results. The results for both genomic and repeat annotations were plotted using ggplot2.

Computational analysis: piRNA expression upon Pb exposure

To study the effects of Pb exposure, we performed smRNA sequencing (no sodium periodate) and compared results to the baseline piRNA map from control hearts. This alignment was performed using STAR and featureCounts (v2.0.3). Next, differential expression of piRNAs in Pb vs. control treated samples was assessed using generalized linear modeling with EdgeR (v3.40.2) package in R. These results were filtered for significance by p-value (none were significant by FDR) and a |logFC| > 1 and then were plotted using ggplot2 R package. Venn diagram creation, genomic annotations and repeat analysis were performed as described above.

For Gene Ontology analysis of the piRNAs potentially altered by Pb exposure (p-value < 0.05 and |logFC| > 1), the Bioconductor package chipenrich (v2.22.0) was used to perform the gene set enrichment testing, in which piRNA-enriched peaks were assigned to target genes using the nearest transcription start site (TSS) (`locusdef = "nearest_tss"`), and enrichment was evaluated using the `chipenrich` logistic regression model, which adjusts for the number of peaks per gene. The input was piRNAs potentially differentially expressed in Pb treated samples (as determined by edgeR) and GO genesets GOBP (Biological Processes), GOCC (Cellular Compartment), and GOMF (Molecular Function) were used. The results were reduced so that similar processes were narrowed down, filtered for gene sets less than 500 genes, FDR < 0.05, and plotted using ggplot2.

qRT-PCR of potential mRNA targets and Piwils

RNA was extracted from the cyro-pulverized mouse heart samples (n=4 per sex per treatment) described above using the AllPrep DNA/RNA Mini Kit (#80204 Qiagen, Aarhus, Denmark). 500 ng to 1 μg of total RNA was reverse transcribed into cDNA using the iScript cDNA Synthesis Kit (#1708890 BioRad, Hercules, California; the same amount of cDNA was used within each experiment). mRNA expression of mouse genes *Atf2*, *Apbb1, Piwil1, Piwil2,* and *Piwil4,* were quantified using the CFX Real-Time PCR using iTaq Universal SYBR Green Supermix (primers in table below) according to manufacturer's protocols with all samples run in triplicate. mRNA expression was compared using the same method on the same plate to amplification of two reference genes (*β-actin* and *Gapdh*; primer information in table below). Primer efficiency was confirmed using cDNA serial dilutions. All qRT-PCR reactions were carried out for 40 cycles under standard PCR conditions. ΔCq values were calculated by subtracting the Cq triplicate average of a target sample from that of the geometric mean of the reference genes. The relative difference in gene expression was then calculated using $2^{-\Delta Cq}$ and graphed using GraphPad Prism, where unpaired t-tests were used to determine statistical differences between control and treatment groups.

Primer table

Gene name	Primer Information	Company
Atf2	qMmuCID0016589	BioRad, Hercules, California
Apbb1	qMmuCED0039791	BioRad, Hercules, California
Piwil1	F: TGATCAGCGTGAAGCCATTG R: CACCTCGATCATGATTGCCT	Integrated DNA Technologies, Coralville, Iowa

Piwil2	F: CTTCCGGCGGGTAATGAAAC R: GGATACTAGCCGCATAGCCA	Integrated DNA Technologies, Coralville, Iowa
Piwil4	F: GCATGACTGGTGCTCTCAAC R: GCCGCACTCTGTTACACTTT	Integrated DNA Technologies, Coralville, Iowa
β-actin	F: GTGACGTTGACATCCGTAAAGA R: GCCGGACTCATCGTACTCC	Integrated DNA Technologies, Coralville, Iowa
Gapdh	F: TGACCTCAACTACATGGTCTACA R: CTTCCCATTCTCGGCCTTG	Integrated DNA Technologies, Coralville, Iowa

Sequencing of 3-week and 5-month sample RNA

Sequencing of our 3 week and 5 month old sample RNA was performed for a previously published paper from our lab.[62] All RNA handling and sequencing were conducted by the University of Michigan Advanced Genomics Core. RNA quantity was measured with a Qubit fluorometer, and RNA integrity was evaluated using an Agilent 2200 TapeStation. mRNA libraries were prepared with the KAPA mRNA Hyper Prep Kit (Roche) incorporating dual-index adapters. Library size distribution and quality were assessed on the Agilent 2200 TapeStation. Sequencing was performed on an Illumina NovaSeq 6000 platform with an S2 flow cell, generating 50 bp paired-end reads. Each sample yielded an average of ~60 million reads.

Computational analysis: read count analysis of ECC genes

The *RUVr* function from the Bioconductor packages RUVSeq (version 1.32.0) with k=3 was applied to remove any potential batch effects among the 3 week and 5 month samples of the RNA-Seq data within each treatment group.[62,63] Ggplot2 was used to plot normalized read counts for ECC genes at 3 weeks and 10 months of age. Unpaired t tests were used to assess for differences between Pb and control samples.

2.4: Results

Identification of sex-stratified murine heart-specific piRNA using sodium periodate exclusion

To characterize sex-specific cardiac expression of piRNA, we treated smRNA from control mouse hearts (n=4, 2 per sex) with sodium periodate to enrich for piRNA over other smRNA. We used a gold standard sodium periodate method to select for smRNA containing the 2'-O-methylation, sequenced all periodate treated and untreated samples, then utilized the PePr peak calling software to identify the relative enrichment of piRNA in treated vs. untreated samples, and further selected for piRNAs based on their length (20-45 nucleotides).[15,16]

We conducted three assessments of the piRNA sequencing results: combined sex analysis and stratified by sex (female and male). The average number of total million reads was 36.9 in females and 15.9 in males (**Table 2.1**). The alignment rates were between 65-75% for all three assessments, and approximately half of reads mapped to multiple loci for all three analyses (**Table 2.1**). A total of 32,035 enriched regions (representing candidate piRNAs) were present in the heart (for combined sex), with 18,956 of these at transcript lengths between 20-45 nucleotides (**Table 2.1**). In the sex stratified analyses, there were 16,756 female derived enriched regions (9,231 meeting length criteria) and 11,408 male derived enriched regions (5,972 meeting length criteria (**Table 2.1**). Assessing overlaps in expression of piRNA sequences that met

length criteria shown in the Venn Diagram in **Figure 2.2**, 1,386 were found to share expression in all three analyses, with 2,436 unique to only females and 1,768 unique to only males.

Table 2.1: Summary of piRNA expression in control hearts identified by sodium periodate exclusion, including combined and sex-stratified piRNA assessment.

	Average Total Reads (Millions)	**Alignment Rate (%)**	**Mapped to Multiple Loci (%)**	**All enriched peaks**	**piRNA 20 to 45 nucleotides**
Combined	26.38	69.82	54.95	32035	18956
Female	36.89	73.36	58.51	16756	9231
Male	15.87	66.29	51.38	11408	5972

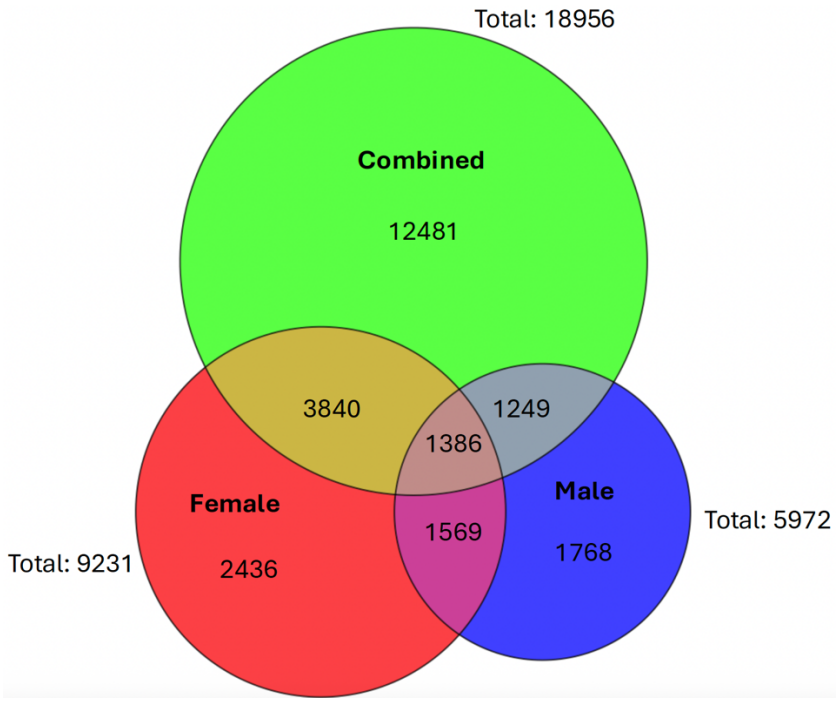


Figure 2.2: Combined and sex-stratified baseline heart piRNA expression.

The Venn diagram shows overlaps in expression of 20-45 nucleotide piRNAs discovered through PePr analysis (**Table 2.1**) from combined (green), female (red), and male (blue) analyses.

Genomic annotations of cardiac piRNAs in adult mice reveal heart-specific locations

We annotated the heart-specific piRNAs to the mouse version mm10 genome and found that the 18,956 piRNAs combined across sexes mapped most frequently to introns, open sea areas, and exons (**Figure 2.3A**). Interestingly, this pattern diverged from what would be expected in a random area of the mm10 genome (shown in yellow in **Figure 2.3A**). This annotation revealed higher proportions of piRNA (for combined sexes, females, and males) mapping to exons (12-15%) and lower proportion of piRNA mapping to introns (38-41%) compared to the expected proportion of exons for a random region of the mm10 genome (4% exonic regions and 49% intronic regions) (**Figure 2.3A**). Sex differences were not seen in genomic annotations.

Analysis of piRNA mapping to known repetitive regions in the genome revealed a lower proportion of piRNAs in long interspersed nuclear elements (LINEs) and similar proportions of piRNAs mapping to long terminal repeat (LTR) retrotransposons compared to the proportion of those repetitive regions in a random region of the genome (LINEs: 4-5% in analysis compared to 38% in a random region; LTRs 18-23% in analysis vs. 25% in a random region) (**Figure 2.3B**). The proportion of piRNAs mapping to SINEs in all three analyses was much higher (65-69% compared to 20% in a random region). **Tables 2.S1** (gene annotations) and **2.S2** (repeat analysis) contain the frequency and proportions labelled on the graphs for **Figures 2.3A** and **2.3B**, respectively.

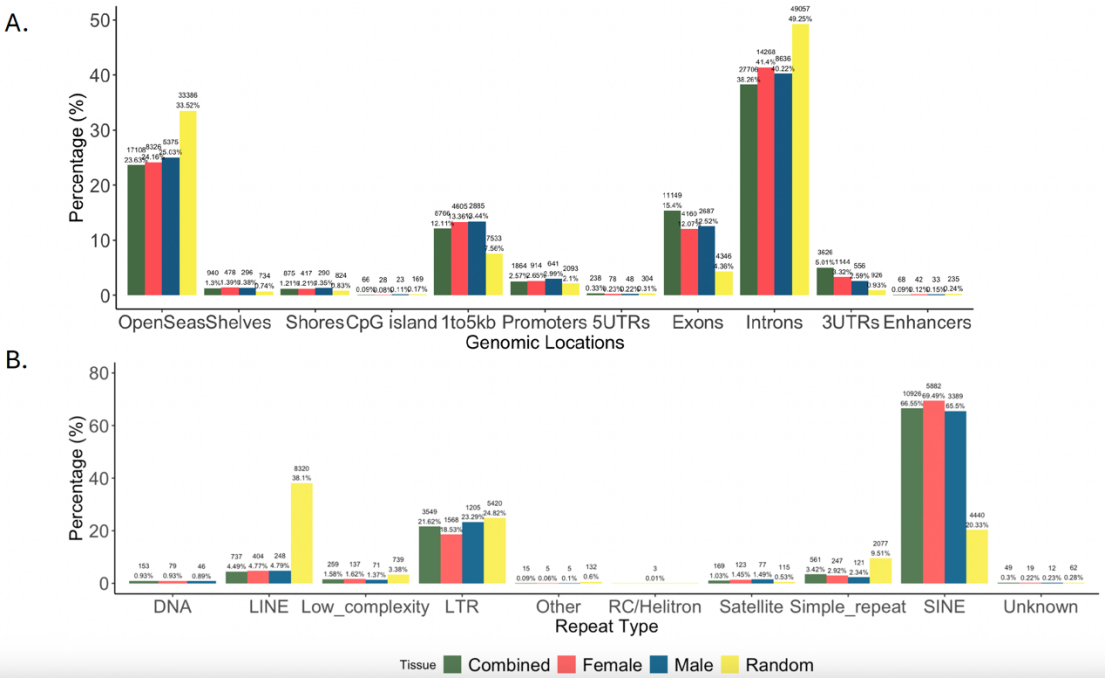


Figure 2.3: Genomic annotations and repetitive regions for expression of baseline heart piRNAs.

Genomic annotations were generated for the regions from which 20-45 nucleotide piRNAs described in Table 1 were derived for combined sex analysis (green), female (red), male (blue),

and a random region of the mm10 genome (yellow) using Annotatr in R (**Figure 2.3A**). The locations annotated included OpenSeas (interCGI), CpG Shelves, CpG Shores, CpG Islands, 1to5kb (upstream of transcription start site), Promoters, 5' UTRs, Exons, Introns, 3'UTRs, and Enhancers. Annotations of repetitive regions were also generated for these piRNAs (**Figure 2.3B**). The repeat annotation was performed by using the R package valr against the repeat annotation downloaded from the UCSC Genome Browser. Types of repetitive regions were condensed into the following categories: DNA, LINE, Low_complexity, LTR, Other, RC/Helitron, Satellite, Simple_repeat, SINE, and Unknown. **Tables 2.S1** (gene annotations) and **2.S2** (repeat analysis) contain the frequency and proportions labelled on the graph for each analysis.

Heart-specific piRNA expression patterns upon perinatal Pb exposure

smRNA from hearts of adult control mice (n=5 females and n=6 males) and mice that had been exposed to Pb during gestation and lactation (n=5 females and n=6 males), all at 5 months of age, were aligned to the 32,035 sequences identified in the combined sex PePr analysis. We included all 32,035 sequences, rather than just those that met the size selection criteria, to ensure that we captured any potential piRNAs that might be present in the broader range of piRNA lengths. While none of the piRNA in Pb-exposed samples were found to be significantly different compared to controls (FDR<0.05), we identified hundreds of potential piRNA expression changes with |log(fold change (FC))| > 1 and p-value < 0.05 (**Table 2.2** and **Figure 2.4**). Using the aforementioned criteria, more potential piRNA expression changes with Pb exposure were identified in the female samples (847) than in males (187) or the combined analysis (301), and only 23 overlapping piRNAs were found between males and females; **Table 2.2** and **Figure 2.4B**). For the combined analysis, of the 301 potentially changed piRNAs found

with exposure, 199 (66.11%) had a greater than two-fold change increase and 102 (33.89%) had a greater than two-fold change decrease (**Table 2.2**). Of the 847 piRNAs changed with Pb exposure in females, 486 (57.38%) had a greater than two-fold change increase and 361 (42.62%) had a greater than two-fold change decrease (**Table 2.2**). Of the 187 piRNAs potentially affected by Pb exposure in males, 122 (65.24%) had a greater than two-fold change increase and 65 (34.76%) had a greater than two-fold change decrease (**Table 2.2**). Overall, the proportion of potentially upregulated versus downregulated piRNAs was relatively consistent across all three groups, with a higher percentage showing increased expression following Pb exposure.

Table 2.2: piRNA changes (p-value <0.05 and log fold change (FC) >1 or < -1) associated with perinatal Pb exposure in the mouse heart.

	Combined	**Female**	**Male**
logFC > 1	199 (66.11%)	486 (57.38%)	122 (65.24%)
logFC < -1	102 (33.89%)	361 (42.62%)	65 (34.76%)
Total	301	847	187

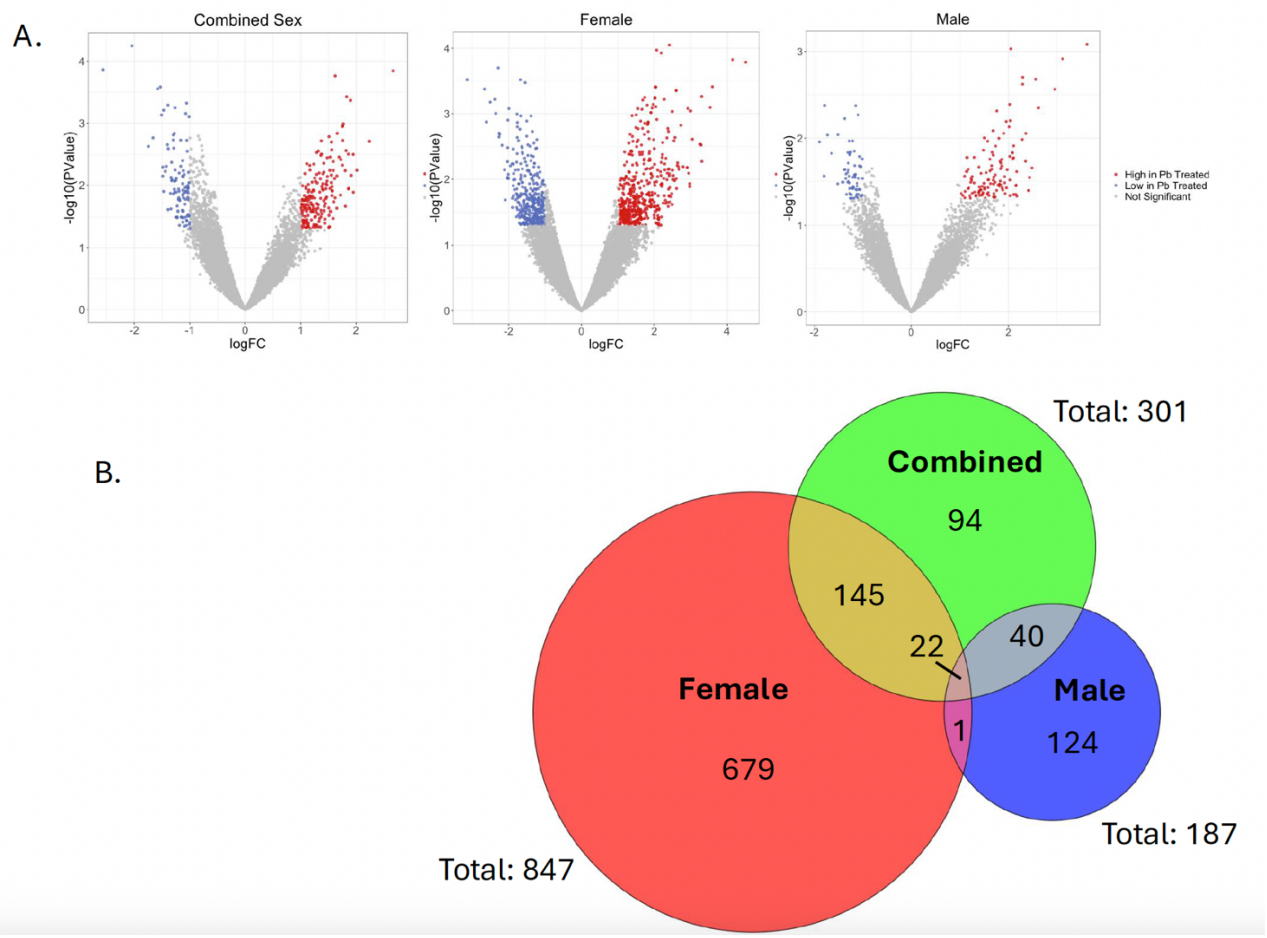


Figure 2.4: Potential changes in expression of heart piRNAs from mice developmentally exposed to Pb.

After mapping piRNAs to the 32,035 peaks in control hearts, edgeR was used to assess for potential changes in expression with Pb exposure compared to control samples in combined sexes, female, and male hearts (potential changes considered at $|logFC| > 1$ and p-value < 0.05). Highlighted regions in blue and red correspond to downregulated and upregulated piRNAs described in **Table 2.2** (log fold change < -1 or >1; **Figure 2.4A**), respectively. The Venn diagram shows overlaps in these piRNAs from combined (green), female (red), and male (blue) analyses (**Figure 2.4B**).

Genomic annotations of heart-specific piRNAs sensitive to Pb exposure

Among the piRNAs potentially altered by Pb exposure (p-value threshold of < 0.05 and $|\log FC| > 1$), we found a higher proportion of piRNAs (from combined sexes, females, and males) mapping to exons (29-36% vs. 4% in a random region) and a lower proportion of piRNAs mapping to introns (20-23% vs. 51% in a random region) compared to those present in a random region of the genome (**Figure 2.5A**). In piRNAs mapping to repetitive regions, a smaller proportion of piRNAs (from combined sexes, females, and males) mapped to LINEs (7-13% vs. 37% in a random region) and a greater proportion of piRNAs mapped to LTRs (32-39% vs. 25% in a random region) compared to a random region of the genome (**Figure 2.5B**). Both the combined (16%) and female (16%) showed similar, lower proportions of SINEs compared to random (22%), while males showed a higher proportion of piRNAs mapping to SINES (25%; **Figure 2.5B**). **Tables 2.S3** (gene annotations) and **2.S4** (repeat analysis) contain the frequency and proportions labelled on the graph for **Figures 2.5A** and **2.5B**, respectively.

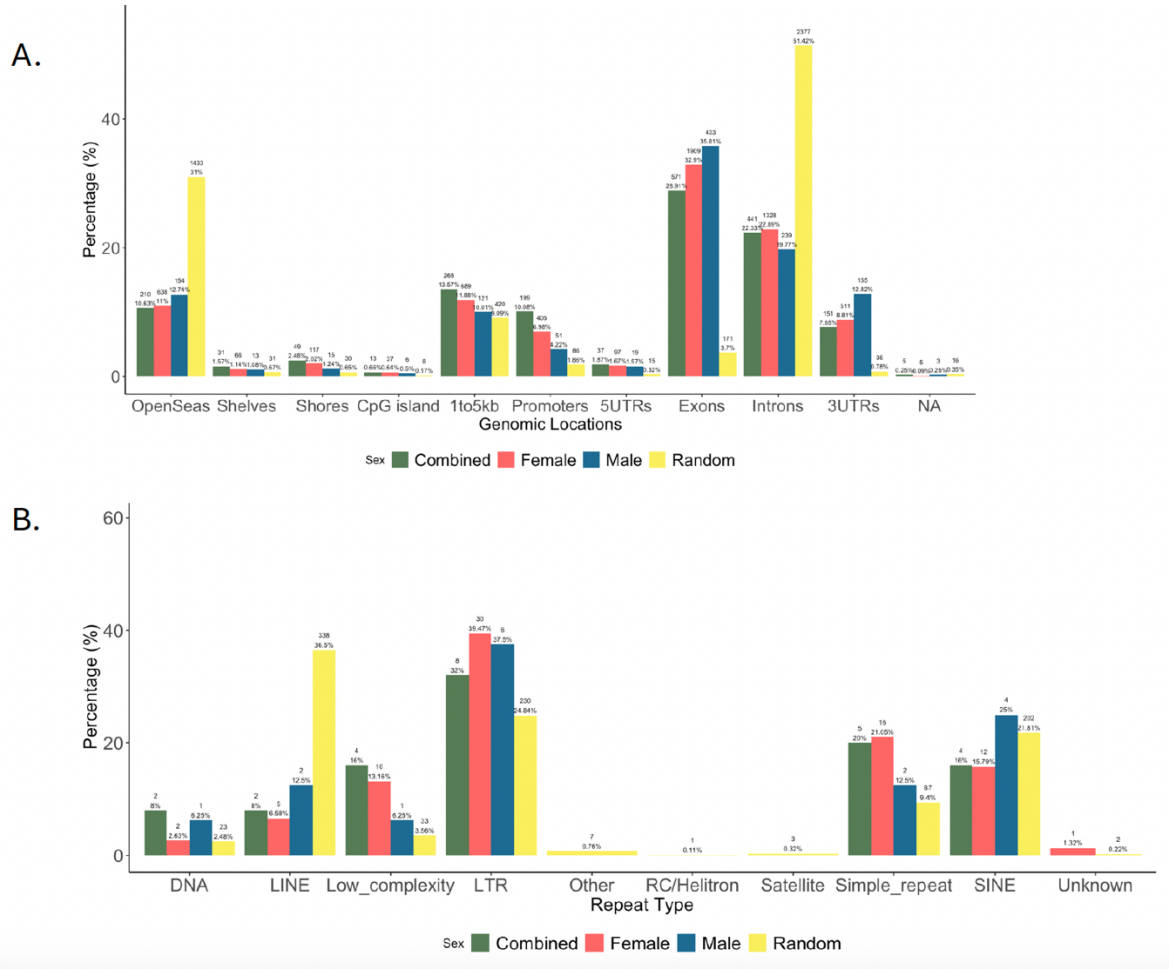


Figure 2.5: Genomic annotations and repetitive regions for expression of heart piRNAs with potential changes in expression in mice developmentally exposed to Pb.

Genomic annotations were generated for regions potential changes in expression of piRNAs by Pb exposure (p-value <0.05 and logFC >1 or < -1) were derived from for combined sex analysis (green), female (red), male (blue), and a random region of the genome (yellow) using Annotatr in R comparing to the mm10 mouse genome (**Figure 2.5A**). The locations annotated included OpenSeas (interCGI), CpG Shelves, CpG Shores, CpG Islands, 1to5kb (upstream of transcription start site), Promoters, 5' UTRs, Exons, Introns, 3'UTRs, and NA (uncategorized). Annotations of repetitive regions were also generated for these piRNAs (**Figure 2.5B**). The repeat annotation was performed by using the R package valr against the repeat annotation downloaded from the

UCSC Genome Browser. Types of repetitive regions were condensed into the following categories: DNA, LINE, Low_complexity, LTR, Other, RC/Helitron, Satellite, Simple_repeat, SINE, and Unknown. **Tables 2.S3** (gene annotations) and **2.S4** (repeat analysis) contain the frequency and proportions labelled on the graph for each analysis.

Gene ontology analysis for heart-specific piRNAs sensitive to perinatal Pb exposure

We performed Gene Ontology overrepresentation analysis for piRNAs potentially altered by Pb exposure (p-value < 0.05 and logFC > ±1) in both sexes combined, females, and males using biological processes (GOBP), cellular compartment (GOCC), and molecular function (GOMF). **Figure 2.6** highlights the biological processes that were significantly differentially expressed (FDR < 0.05) and unique to each sex for piRNAs sensitive to Pb exposure. For GOBP, 48 terms were enriched in the combined analysis, 57 terms were enriched in females, and 39 in males (**Table 2.S5**). Notably, 52 terms were unique to females (not in males) and 34 were unique to males (**Table 2.S5** and **Figure 2.6A**). For GOCC, 16 terms were enriched for the combined analysis, 23 for females, and 20 for males (**Table 2.S6**). Of these, 11 terms were unique to females (not in males) and 8 were unique to males (**Table 2.S6** and **Figure 2.6B**). For GOMF, 4 terms were enriched in the combined analysis, 17 in females, and 9 in males (**Table 2.S7**). Of these, 11 terms were unique to females and 3 were unique to males (**Table 2.S7** and **Figure 2.6C**).

The top 5 GOBP, GOCC, and GOMF terms uniquely enriched for each sex are shown in **Figure 2.6**. These include processes related to heart structure and function for both females and males, such as myofibril assembly (FDR 1.26e-11), striated muscle contraction (FDR 1.26e-11), muscle organ morphogenesis (FDR 9.63e-07), myosin II complex (FDR 1.54e-06), sarcoplasm

(FDR 2.79e-06), and myosin binding (FDR 4.45e-03) for females and sarcomere organization (FDR 2.17e-09) and cardiac muscle contraction (FDR 5.86e-05) for males.

Additionally, processes related to mitochondria were uniquely enriched in both females and males. For females, these included respiratory chain complex (FDR 2.74e-07), mitochondrial matrix (FDR 6.19e-06), and NAD(P)H dehydrogenase (quinone) activity (FDR 5.06e-04). For males, these included autophagy of mitochondrion (FDR 4.89e-05), mitochondrion disassembly (FDR 4.89e-05), outer membrane (FDR 8.91e-08), and integral component of mitochondrial outer membrane (FDR 1.32e-02) for males.

Finally, processes related to energy metabolism were uniquely enriched for both females and males, including generation of precursor metabolites and energy (FDR 1.26e-11), purine-containing compound biosynthetic process (FDR 1.43e-07), carbon-carbon lyase activity (FDR 1.27e-04), and oxidoreduction-driven active transmembrane transporter activity (FDR 4.45e-03) for females and ATPase dependent transmembrane transport complex (FDR 3.22e-03) and protein kinase B binding (FDR 1.13e-02) for males.

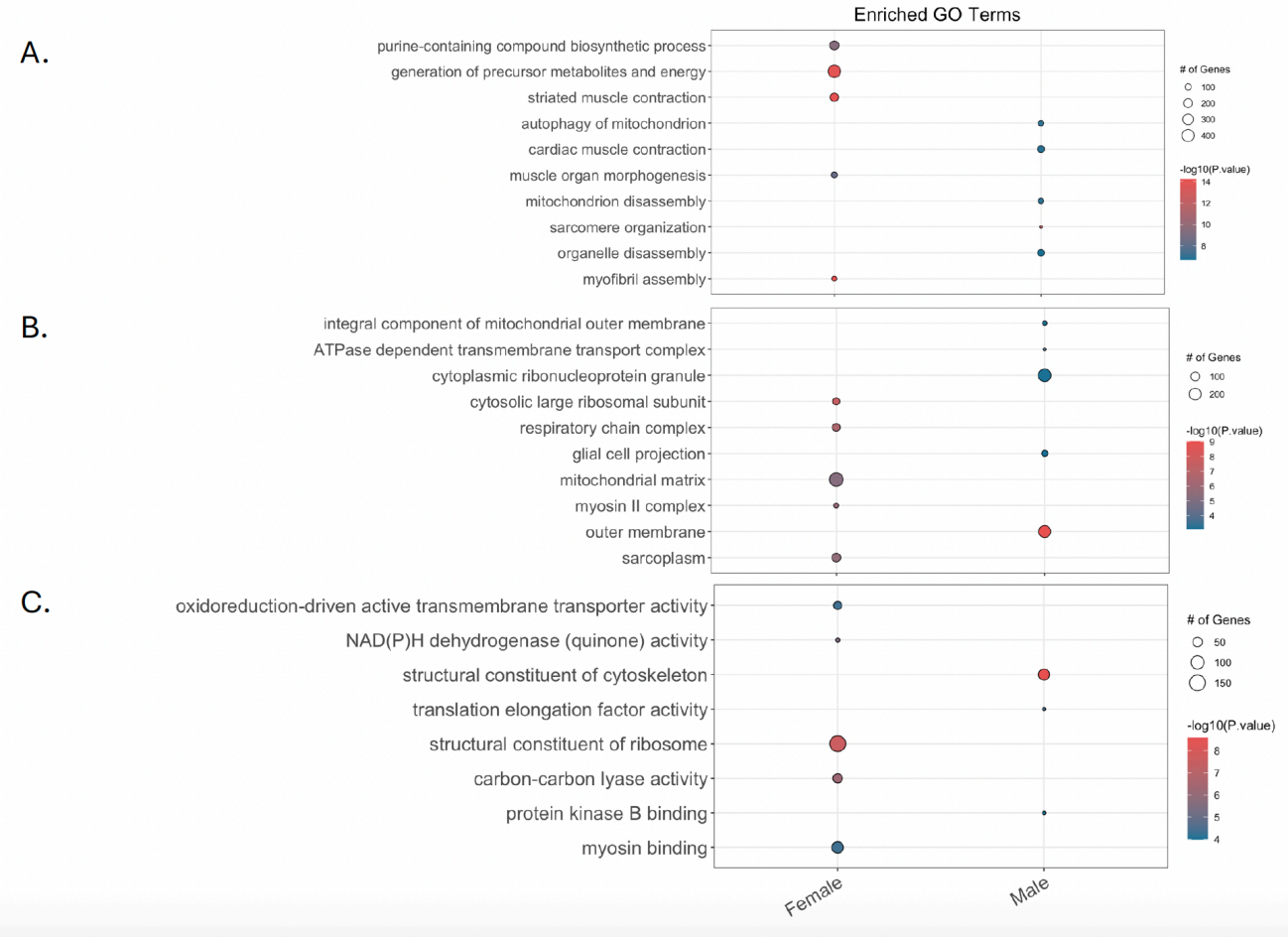


Figure 2.6: Gene ontology analysis for piRNAs potentially altered by developmental Pb exposure.

For combined sex, male, and female analyses, Gene Ontology enrichment was carried out using chipenrich in R for the categories of biological processes (GOBP; **Figure 2.6A**), cellular compartment (GOCC; **Figure 2.6B**), and molecular function (GOMF; **Figure 2.6C**) for piRNAs found to be potentially altered by Pb exposure (p-value <0.05 and logFC >1 or < -1). The top 5 unique GO terms for male and female for all three GO categories are shown here. For all three, GO enrichment was filtered by FDR < 0.05, number of geneset genes is shown by circle size, -log10(p-value) is indicated by red for a more significant value and blue for less significant, and

specific GO terms are listed on the left side. **Tables 2.S5** (GOBP), **2.S6** (GOCC), and **2.S7** (GOMF) contain the full enrichment data for these analyses.

Assessment of potential mRNA targets

Two potential target genes, *Atf2* and *Apbb1*, were selected from the piRNA mapped targets shown in **Table 2.S8** for qRT-PCR analysis. We found Pb exposure did not result in significant gene expression changes in sex-specific or combined analysis (**Figure 2.7**). P-values from unpaired t-tests are shown in each comparison for each gene.

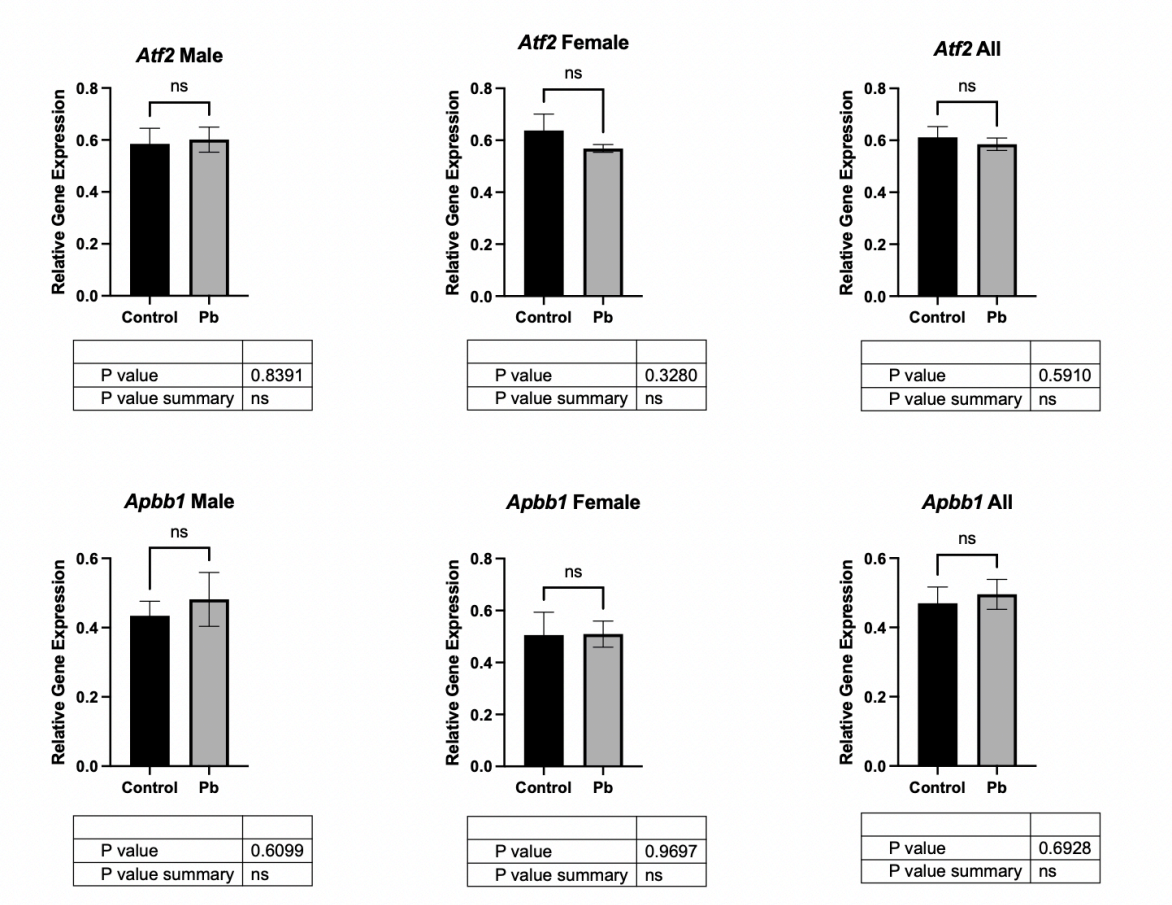


Figure 2.7: Assessment of potential mRNA targets.

mRNA levels (relative gene expression) were assessed for two potential target genes from the same samples in which piRNA analysis was performed. *Atf2* and *Apbb1* were selected from the

piRNA mapped targets shown in **Table 2.S8** for qRT-PCR analysis. Both individual and combined sexes were assessed with no statistical significance for comparison between control and Pb samples. P-values from unpaired t-tests are shown in each comparison for each gene.

Sex-specific Piwil expression changes in heart samples from mice perinatally exposed to Pb

Piwil expression was assessed relative to *β-actin* and *Gapdh* in 10-month-old male and female heart samples from mice treated perinatally with 32 ppm Pb, revealing significant changes in expression with Pb exposure for only male samples (n= 5 to 7 per condition; for males, p-values 0.0003 for 44-fold increase in *Piwil1*, 0.001 for 2-fold decrease in *Piwil2*, and 9.88E-05 for 150-fold increase in *Piwil4*; **Figure 2.8**). No significant changes in *Piwil*s for either sex were observed for 3-week-old and 5-month-old samples (**Supplemental Figure 2.10**).

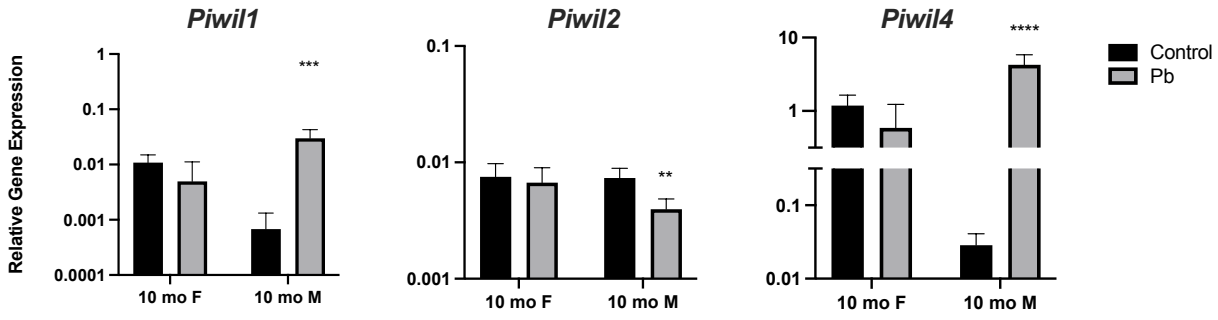


Figure 2.8: Sex-specific changes in *Piwil* expression in 10-month samples.

qRT-PCR was conducted for relative gene expression of *Piwils* (on a log scale) and unpaired t-tests were conducted comparing control to Pb exposed samples. p-values for significant changes shown on the graph were 0.0003 for 44-fold increase in *Piwil1*, 0.001 for 2-fold decrease in *Piwil2*, and 9.88E-05 for 150-fold increase in *Piwil4* for male samples only (n=5-7 per treatment per sex).

Changes in ECC gene expression in weanling and adult heart samples perinatally exposed to Pb

Normalized read counts from RNA-Seq of weanling (3 week old) and adult (5-month old) samples were interrogated for 4 ECC genes: *Atp2a2*, which encodes for a protein that transports Ca from the cytosol into sarcoplasmic reticulum; *Ryr2*, which encodes for a protein that transports Ca from the sarcoplasmic reticulum into the cytosol; *Cacna1c*, which encodes for a protein that transports Ca from extracellular space into the cytosol; and *Slc8a1,* which encodes for a protein that transports Ca out of the cytosol (**Figure 2.9)**. Significant (or nearing significant) upregulation in ECC genes in Pb-exposed weanling (3 week) and adult (5 month) male, but not female, mice was observed (* p-value < 0.05, ** p-value < 0.01, *** p-value < 0.001).

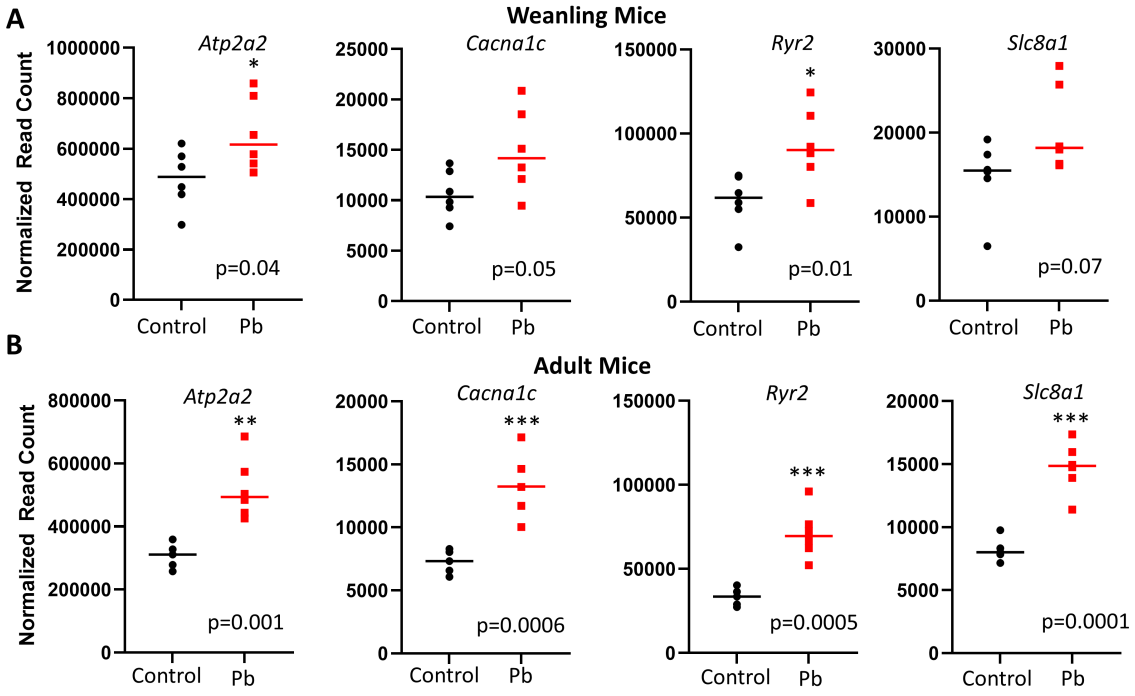


Figure 2.9: ECC gene read counts in hearts from mice at weaning and adult mice. Interrogation of ECC gene read counts for *Atp2a2*, *Cacna1c*, *Ryr2*, and *Slc8a1* demonstrated significant or near significant upregulation in Pb-exposed weanling (A; 3 week) and adult (B; 5

month) male, but not female, mice. (n= 5-7 per treatment per sex; * p-value < 0.05, ** p-value < 0.01, *** p-value < 0.001; female data not shown).

2.5: Discussion

Sex-stratified baseline piRNA expression in murine hearts

Notably, this work is the first to identify 18,956 piRNAs through sodium periodate exclusion in the mouse heart and to characterize sex-specific piRNA effects in adult murine offspring upon perinatal Pb exposure (**Figure 2.1**). Sex-stratified analysis revealed larger numbers of piRNAs expressed from female mice (9,231) compared to male mice (5,972; **Table 2.1**). Of these, 2,436 were found to be uniquely expressed in females and 1,768 unique in males (**Figure 2.2**). These expression profiles may indicate that piRNAs play an important role in the heart. Our previous study found around 40,808 enriched peaks (24,777 piRNA meeting length criteria) expressed in mouse testes, and 5,494 enriched peaks (3,147 piRNA meeting length criteria) in the hippocampus (much more than the brain cortex). [15] Germline piRNAs are well understood to silence transposable element motility, while piRNA function in the hippocampus is still being studied, but it has been suggested they could play roles in brain plasticity and successful aging (proper neurogenesis and maintenance).[64,65] One study of Piwil2 in adult mouse neural progenitor cells found it was dynamically expressed and essential for proper neurogenesis.[65] Aim 3 assesses PIWIL expression and function in differentiation of human iPSC-derived cardiomyocytes to investigate the importance of piRNA and PIWILs in cardiac function.

Another study of piRNAs in human embryonic stem cells undergoing differentiation to cardiomyocytes found 171 piRNAs in cardiac cells mapping to critical biological processes in the heart, using size exclusion for piRNA detection.[25] Although the current study used a different

species as well as samples from whole adult hearts rather than cardiac cells, by also using sodium periodate methods rather than size exclusion, the current study represents a more rigorous and robust method of detecting piRNA.[25]

Possible exonic targeting by piRNAs

Both our baseline piRNA map as well as those altered by Pb (p-value <0.05) showed that piRNAs derived from intronic regions were proportionately expressed at lower levels than expected by chance and exons at higher levels than expected by chance (**Figures 2.3** and **2.5**). Given that the current results indicate a higher proportion of piRNAs map to exons rather than intronic regions, this could point to potential novel mechanisms for both baseline piRNA function in the heart as well as how Pb may alter processes in the heart. In mice, piRNAs have been previously described to play roles in regulation of mRNA in CVD, including regulation of acetylation of transcription factor *Tfec* mRNA involved in cardiomyocyte death after myocardial infarction, suppressing methylation of *Atf7* mRNA to regulate necroptosis in cardiomyocytes, playing a role in advancing cardiac fibrosis through direct inhibition of *Apln* mRNA in cardiac fibroblasts, and regulating cardiac hypertrophy through controlling methylation of *Parp10* mRNA.[66–69] Notably, none of our piRNAs which changed in expression by Pb were found to be mapped to these four specific mRNA targets, although the female data did show expression of piRNA mapping to another transcription factor in the same family as *Atf7*, *Atf2* (**Table 2.S8**).[67,70] We hypothesize that piRNAs we discovered to be changed in expression by Pb and mapping to exonic regions could have roles in the development of CVD. We assessed relative gene expression of two potential exonic targets based on our mapping data in our samples: *Atf2* and *Apbb1,* and found no statistical significance for either gene when comparing Pb vs. control for female, male, and combined samples (**Figure 2.7**). Interestingly, both *Atf2* and *Apbb1* have

multiple isoforms, and qPCR assesses aggregate expression of these. Mapping our differentially expressed piRNAs to the reference genome shows that not all isoforms are targeted, suggesting possible isoform-specific regulation and compensation. This highlights the potential value of conducting isoform-specific analyses to understand the functional relevance of specific piRNAs.

We also looked in our data for the presence of two piRNAs associated with mRNA m6A methylation and cardiac disease in mice, CHAPIR and AVCAPIR, and did not find expression of either at baseline or induced by Pb.[69,71] However, given these were disease-associated piRNAs, they may be undetectable in healthy mice, and this highlights the need to study potential Pb-induced changes in mRNA-targeting piRNAs in models of cardiac pathologies.

One important note is that the piRNAs we identified mapping to exonic regions does not necessarily imply a regulatory function. It is possible that the enrichment in exons reflects the presence of degraded mRNA fragments that were misidentified as piRNAs, leading to potential false positives. Future work is needed to determine whether the piRNAs identified here actively regulate mRNA expression and whether their target genes are involved in cardiovascular disease (CVD).

Pb exposure effects on piRNAs targeting transposable elements

Further, of those piRNAs that originated from intronic regions in control hearts, fewer coincided with LINE expression than expected by chance, and the same effect was observed in the context of Pb exposure (**Figure 2.3B and 2.5B**). However, relatively similar proportions of piRNAs mapping to LTRs were seen in control hearts compared to chance, while a greater proportion of LTRs compared to chance were seen in Pb exposed samples (**Figure 2.3B and 2.5B**). While the exact mechanism of piRNAs mapping to these regions is unclear, this could

imply that Pb exposure affects the functionality of piRNAs in repressing transposable element motility, a well characterized function of piRNAs in the germline that is less well understood in somatic tissue.[7] It is important to note that transposable elements are highly repetitive, and our study limited each read to 10-45 nucleotides and 1000 mapping locations.[72] Therefore, it is possible that some mapping sites were missed, particularly for LINEs.[73]

Sex-stratified characteristics of piRNA expression

Around 38% more piRNAs were discovered through analysis of female control hearts compared to males, and there were many uniquely expressed piRNAs in both female (2,436) and male (1,768) baseline mapping (**Table 2.1** and **Figure 2.2**). Despite these differences, the genomic annotations for piRNAs from control hearts did not show sex specific differences for both genome-wide analysis as well as analysis of repetitive regions (**Figure 2.3**). Taken together, this suggests the potential for functional redundancy despite differences in piRNA expression.

In testes and ovaries, the primary function of piRNAs is the same (to silence transposon expression in germ cells), however differences in timing and type of expression have been found due to differences in oogenesis and spermatogenesis.[74] Further, mutations in essential piRNA pathway genes have been show to result in male sterility but have no effect on female fertility in mice.[75] Therefore, because of biological differences in females and males, piRNA in the heart could be expressed differently but have similar functions.

Research is just beginning to uncover how sex-specific epigenetic changes are related to the development of CVD, and previous work has found that Pb alters DNA methylation in a sex specific manner in the heart.[43] Sequencing of hearts from mice that underwent developmental exposure to Pb revealed a greater number of Pb-altered piRNAs in adult females (847) compared

to age-matched adult males (187), and only 23 piRNAs that overlapped between the two analyses (**Table 2.2** and **Figure 2.4**). The region of genome piRNAs originated from did not vary greatly based on sex, but the mapping to repetitive regions showed some variation based on sex (**Figure 2.5**). Most notably, males showed greater proportions of piRNAs mapping to DNA transposons, LINEs, and SINEs and smaller proportions to low complexity regions and simple repeats (**Figure 2.5**). Therefore, Pb exposure may alter piRNA expression in the heart in a sex-specific manner that has functional consequences.

To further investigate this point, Gene Ontology analysis revealed these piRNAs may be related to unique biological processes in males and females. However, these biological processes have overlapping roles related to heart function. Of the top 5 unique GO terms for GOBP, GOCC, and GOMF for both male and female piRNAs expressed with Pb exposure, processes related to the mitochondria or energy metabolism were enriched (5/13 top pathways for males and 5/15 for females). Given the high energy demands of the heart, mitochondria are critical for normal function, and dysregulation of mitochondrial pathways in the heart are known to be involved in various CVDs including atherosclerosis, ischemia-reperfusion injury, hypertension, diabetes, cardiac hypertrophy, and heart failure mainly through mechanisms of oxidative stress.[76] Pb is known to disrupt energy metabolism and cause oxidative stress, particularly in the brain, but how Pb may affect heart development through oxidative stress is largely unknown.[77,78] Importantly, this GO data suggest that changes in piRNA expression by Pb (p-value < 0.05) may be related to energy metabolism in both sexes, but the specific pathways enriched were distinct in each sex.

Processes related to muscle cell function and structure were enriched in both female (6) and male (2) analyses. For example, myofibril assembly was enriched for females, and

sarcomere organization was enriched for females, with sarcomeres functioning as the unit of contraction within a myofibril. Dysregulation of heart muscle function has been implicated in various CVDs, including cardiomyopathies and heart failure. [79–81] Both female and male pathways also included processes related to ribosomal structure and function (2 for both males and females), alterations of which may be related to the development of CVD.[82]

Pathways with unique functions were also present for both sexes. In males, protein kinase B (Akt) binding was enriched, which has been shown to play roles in heart failure, atherosclerosis, myocardial infarctions, hypertension, and cardiomyopathies.[83] The mapping of piRNAs potentially dysregulated by Pb to regions that regulate distinct pathways with overlapping functional outcomes highlights the notion that while female and male piRNA may originate from different regions, they may play similar roles, as in the germline. Further studies are needed to examine piRNA function in the female and male heart in relation to the origin of piRNA expression.

Sex and age specific alterations in piRNA associated genes

While our piRNAs potentially affected by Pb mapped to similar pathways between the two sexes, we found significant male-specific changes in all three *Piwil*s exclusively in our 10-month samples (**Figure 2.8**). The roles of PIWILs in somatic tissue like the heart are still under scrutiny, but germline PIWILs play a role in maintaining genomic stability through transposon silencing and epigenetic regulation. Therefore, altered expression of *Piwil*s in aging hearts could possibly reflect accelerated cardiac aging or epigenetic stress as a result of developmental Pb exposure. Further, the three mouse PIWI-like proteins have distinct functions in the mouse germline: PIWIL1 (MIWI) functions in later spermatogenesis, primarily in post-transcriptional gene regulation, PIWIL2 (MILI) plays a key role in piRNA biogenesis and post-transcriptional

transposon silencing, and PIWIL4 (MIWI2) is involved in transcriptional silencing through DNA methylation.[84–88] Here, we saw a decline in *Piwil2* expression and an increase in *Piwil*s *1* and *4*, suggesting a possible shift from piRNA production toward enhanced gene silencing activity. The upregulation of *Piwil1* is particularly interesting given the altered piRNAs at 5 months tended to map disproportionately to exons. Taken together, this pattern may reflect a compensatory mechanism to maintain genomic integrity in the aging male heart in response early-life Pb exposure. Future work should examine sex specific mechanisms of PIWILs in the heart both at baseline and in response to Pb.

Sex specific alterations in ECC genes

Of the 4 ECC genes examined by RNA sequencing, we saw significant increases in only male 3-week and 5-month samples (**Figure 2.9**), which were not correlated with changes in the piRNAs mapped to targets (**Table 2.S8**). However, this lack of direct correlation does not exclude the possibility that piRNAs may influence their expression through regulatory mechanisms acting on nearby genomic regions. Contractile dysfunction and arrhythmias in heart failure are often due to defective Ca handling, with reduced expression and activity of SERCA2 (encoded by *Atp2a2***)**, increased expression of NCX (encoded by *Slc8a1*), and potential compensatory decreased activity of Ryr2 all known to be mechanistically involved in disease progression.[89] Given these established roles, the observed upregulation of all four ECC genes in male mice our dataset may reflect early molecular signs of Ca dysregulation that could contribute to later cardiovascular dysfunction. This is especially interesting given that there are sex differences in different types of heart failure, with males tending to have heart failure with reduced ejection fraction (HFrEF). Future work should connect changes in cardiomyocyte Ca handling with the alterations in epigenetics described here.

Study limitations

One major limitation of the present study is that smRNA was isolated from whole heart tissue, which may include fibroblasts, endothelial cells, smooth muscle, blood, and other cell types. Future studies are necessary to define cell type specific piRNAs in the heart. Another limitation of this study is the limited translatability from mice to humans, as previous work suggests that while piRNA associated proteins like PIWILs and piRNA cluster locations are conserved between species, there are major differences in the actual sequences of piRNAs themselves.[11,90,91] Further, only mice at 5 months of age were used for this study, and to understand fully the effects of developmental Pb exposure, additional investigations should look at other time points in the life course, as well as piRNA expressed during cardiac differentiation in *in vitro* models. Of note, while this study suggests potential trends in Pb-induced dysregulation of piRNA expression, none of these changes met the FDR significance threshold, and therefore no conclusions about statistically significant effects can be drawn. Lastly, we used the piRNAs discovered at baseline to assess for expression changes induced by Pb exposure, which limits the detection potential of novel piRNAs induced by Pb exposure.

Future work should also examine the coupling between expression of piRNA and their targets, at baseline and in the context of Pb exposure. A recent paper from our group carried out RNA sequencing and DNA methylation analysis of cardiac genes from the same murine perinatal model of Pb exposure used in this paper, and did not report any significantly differentially expressed genes (DEGs) with Pb exposure at 3 week, 5 month, and 10 month time points.[92] However, this work discovered different temporal gene expression changes in control and Pb exposed hearts that were also unique by sex.[92] This could mean that piRNA differences shown here are reflected by these temporal shifts, and that perhaps we are missing earlier

windows in gene expression changes given the crucial roles piRNA play in development. Furthermore, piRNA could be acting in a post-transcriptional manner thereby regulating protein levels rather than mRNA or affecting expression of TEs which are difficult to capture in traditional RNA sequencing due to their repetitive nature. Further work is required to investigate earlier timepoints (perhaps fetal gene expression changes), proteomics, as well as qPCR verification of potentially targeted TEs, such as LTRs which were identified as piRNA targets related to Pb exposure in this work. Of further interest, the known expression and functionality of the 22 Pb-altered piRNAs in common between our three analyses (**Figure 2.4B**) should be interrogated to understand how Pb exposure mechanistically effects these epigenetic mechanisms in both sexes.

Conclusions

Overall, we characterized sex-stratified piRNA expression in both control and Pb-exposed murine hearts. We found robust expression of piRNA in the heart, many of which mapped to exonic regions, indicating potential future areas of discovery. In addition to providing a foundation for sex-specific piRNA expression in the heart, these findings suggest a novel epigenetic mechanism by which developmental Pb exposure may impact CVD risk later in life. Interestingly, while piRNA and *Piwil* expression differed between females and males, GO analysis revealed that the functional consequences of Pb exposure may be similar. Future studies will link these molecular changes to potential gene or transposable element expression changes as well as Pb-induced alterations in cardiac function.

Author Contributions

All authors provided critical feedback and helped shape the research, analysis and manuscript. KESH and KW analyzed data. KESH made figures and wrote manuscript in consultation with KW, BPUP, MAS, LKS, and DCD.

Disclosure Statement

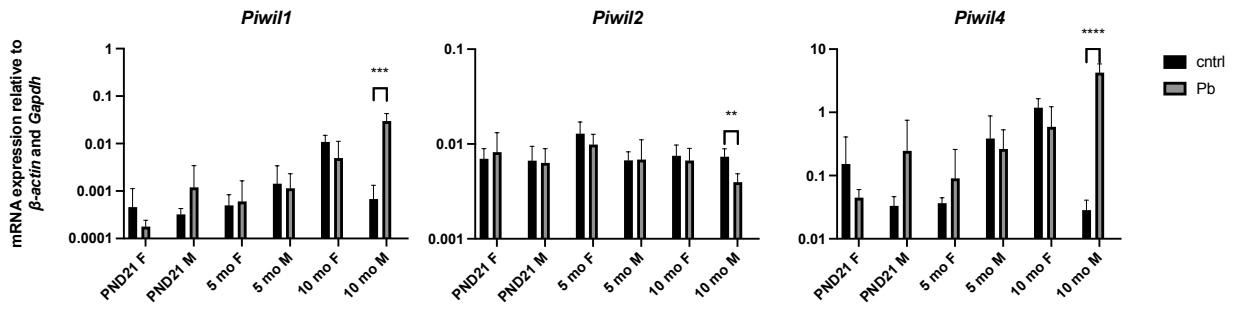
All authors declare that they have no conflicts of interest.

Data Availability Statement

The data supporting the findings of this study are available within the article and its supplementary materials. Sequencing data has been deposited in the NCBI Sequencing Read Archive (SRA) with the accession number PRJNA1257456 and was made available upon publication of this manuscript.

2.6: Supplementary Materials

Supplemental data for this chapter can be found in the figure below and at the repository here: https://doi.org/10.7302/5gs6-2b90



Supplemental Figure 2.10: Piwil expression with perinatal Pb exposure at different time points and by sex.

Piwil1, *2*, and *4* expression on a log scale relative to *B-actin* and *Gapdh* for male and female mice PND21 (3 weeks), 5 months, and 10 months of age. Unpaired t-tests were conducted comparing control to Pb exposed samples, with no changes at any timepoint/sex other than 10 month males (p-values noted in main text; n=5-7 per treatment per sex).

2.7: Acknowledgements

Firstly, I would like to thank Dr. Kai Wang who conducted upstream bioinformatics analysis for this study and trained me in the downstream bioinformatic pipeline. I would also like to thank the DoGoodS-Pi Epigenetics Research Group, including Dr. Kari Neier (Boehringer Ingelheim) and Dr. Christine Rygiel (Illumina) for leading the mouse exposure studies as well as the laboratory manager Tamara Jones (University of Michigan) for her laboratory and administrative support. Additionally, I would like to thank the other authors on the paper that is contained in this aim for their support for this research, analysis, and drafting. I would further like to thank University of Michigan Advanced Genomics Core for sample processing for this study.

2.8: References

1. Dupont C, Armant DR, Brenner CA. Epigenetics: Definition, Mechanisms and Clinical Perspective. *Semin Reprod Med*. 2009;27(5):351-357. doi:10.1055/s-0029-1237423

2. Vagin VV, Sigova A, Li C, Seitz H, Gvozdev V, Zamore PD. A distinct small RNA pathway silences selfish genetic elements in the germline. *Science*. 2006;313(5785):320-324. doi:10.1126/science.1129333

3. Aravin A, Gaidatzis D, Pfeffer S, et al. A novel class of small RNAs bind to MILI protein in mouse testes. *Nature*. 2006;442(7099):203-207. doi:10.1038/nature04916

4. Grivna ST, Beyret E, Wang Z, Lin H. A novel class of small RNAs in mouse spermatogenic cells. *Genes Dev*. 2006;20(13):1709-1714. doi:10.1101/gad.1434406

5. Lau NC, Seto AG, Kim J, et al. Characterization of the piRNA complex from rat testes. *Science*. 2006;313(5785):363-367. doi:10.1126/science.1130164

6. Girard A, Sachidanandam R, Hannon GJ, Carmell MA. A germline-specific class of small RNAs binds mammalian Piwi proteins. *Nature*. 2006;442(7099):199-202. doi:10.1038/nature04917

7. Sun YH, Lee B, Li XZ. The birth of piRNAs: how mammalian piRNAs are produced, originated, and evolved. *Mamm Genome*. 2022;33(2):293-311. doi:10.1007/s00335-021-09927-8

8. Zhang P, Kang JY, Gou LT, et al. MIWI and piRNA-mediated cleavage of messenger RNAs in mouse testes. *Cell Res*. 2015;25(2):193-207. doi:10.1038/cr.2015.4

9. Han BW, Wang W, Li C, Weng Z, Zamore PD. Noncoding RNA. piRNA-guided transposon cleavage initiates Zucchini-dependent, phased piRNA production. *Science*. 2015;348(6236):817-821. doi:10.1126/science.aaa1264

10. Jia DD, Jiang H, Zhang YF, Zhang Y, Qian LL, Zhang YF. The regulatory function of piRNA/PIWI complex in cancer and other human diseases: The role of DNA methylation. *Int J Biol Sci*. 2022;18(8):3358-3373. doi:10.7150/ijbs.68221

11. Ozata DM, Gainetdinov I, Zoch A, O'Carroll D, Zamore PD. PIWI-interacting RNAs: small RNAs with big functions. *Nat Rev Genet*. 2019;20(2):89-108. doi:10.1038/s41576-018-0073-3

12. Marzec M. Size does matter: piRNA and miRNA targeting. *Trends Biochem Sci*. 2022;47(4):287-288. doi:10.1016/j.tibs.2021.12.001

13. Yan Z, Hu HY, Jiang X, et al. Widespread expression of piRNA-like molecules in somatic tissues. *Nucleic Acids Res*. 2011;39(15):6596-6607. doi:10.1093/nar/gkr298

14. Pastore B, Hertz HL, Price IF, Tang W. pre-piRNA trimming and 2'-O-methylation protect piRNAs from 3' tailing and degradation in C. elegans. *Cell Rep*. 2021;36(9):109640. doi:10.1016/j.celrep.2021.109640

15. Perera BPU, Tsai ZTY, Colwell ML, et al. Somatic expression of piRNA and associated machinery in the mouse identifies short, tissue-specific piRNA. *Epigenetics*. 2019;14(5):504-521. doi:10.1080/15592294.2019.1600389

16. Ohara T, Sakaguchi Y, Suzuki T, Ueda H, Miyauchi K, Suzuki T. The 3' termini of mouse Piwi-interacting RNAs are 2'-O-methylated. *Nat Struct Mol Biol*. 2007;14(4):349-350. doi:10.1038/nsmb1220

17. Horwich MD, Li C, Matranga C, et al. The *Drosophila* RNA Methyltransferase, DmHen1, Modifies Germline piRNAs and Single-Stranded siRNAs in RISC. *Curr Biol*. 2007;17(14):1265-1272. doi:10.1016/j.cub.2007.06.030

18. Ross RJ, Weiner MM, Lin H. PIWI proteins and PIWI–interacting RNAs in the soma. *Nature*. 2014;505(7483):353-359. doi:10.1038/nature12987

19. Reddien PW, Oviedo NJ, Jennings JR, Jenkin JC, Sánchez Alvarado A. SMEDWI-2 is a PIWI-like protein that regulates planarian stem cells. *Science*. 2005;310(5752):1327-1330. doi:10.1126/science.1116110

20. Fagegaltier D, Falciatori I, Czech B, et al. Oncogenic transformation of Drosophila somatic cells induces a functional piRNA pathway. *Genes Dev*. 2016;30(14):1623-1635. doi:10.1101/gad.284927.116

21. Wakisaka KT, Imai Y. The dawn of pirna research in various neuronal disorders. *Front Biosci Landmark Ed*. 2019;24(8):1440-1451. doi:10.2741/4789

22. Rajan KS, Velmurugan G, Gopal P, et al. Abundant and Altered Expression of PIWI-Interacting RNAs during Cardiac Hypertrophy. *Heart Lung Circ*. 2016;25(10):1013-1020. doi:10.1016/j.hlc.2016.02.015

23. Yang J, Xue FT, Li YY, Liu W, Zhang S. Exosomal piRNA sequencing reveals differences between heart failure and healthy patients. *Eur Rev Med Pharmacol Sci*. 2018;22(22):7952-7961. doi:10.26355/eurrev_201811_16423

24. Vella S, Gallo A, Lo Nigro A, et al. PIWI-interacting RNA (piRNA) signatures in human cardiac progenitor cells. *Int J Biochem Cell Biol*. 2016;76:1-11. doi:10.1016/j.biocel.2016.04.012

25. Greca AL, Scarafía MA, Cañás MCH, et al. PIWI-interacting RNAs are differentially expressed during cardiac differentiation of human pluripotent stem cells. *PLOS ONE*. 2020;15(5):e0232715. doi:10.1371/journal.pone.0232715

26. Rajan KS, Velmurugan G, Gopal P, et al. Abundant and Altered Expression of PIWI-Interacting RNAs during Cardiac Hypertrophy. *Heart Lung Circ*. 2016;25(10):1013-1020. doi:10.1016/j.hlc.2016.02.015

27. Lipps C, Northe P, Figueiredo R, et al. Non-Invasive Approach for Evaluation of Pulmonary Hypertension Using Extracellular Vesicle-Associated Small Non-Coding RNA. *Biomolecules*. 2019;9(11):666. doi:10.3390/biom9110666

28. Gao Z, Chen Z, Sun A, Deng X. Gender differences in cardiovascular disease. *Med Nov Technol Devices*. 2019;4:100025. doi:10.1016/j.medntd.2019.100025

29. Regitz-Zagrosek V, Kararigas G. Mechanistic Pathways of Sex Differences in Cardiovascular Disease. *Physiol Rev*. 2017;97(1):1-37. doi:10.1152/physrev.00021.2015

30.Zhou X, Zuo Z, Zhou F, et al. Profiling sex-specific piRNAs in zebrafish. *Genetics*. 2010;186(4):1175-1185. doi:10.1534/genetics.110.122234

31.Chen P, Aravin AA. Genetic control of a sex-specific piRNA program. *Curr Biol CB*. 2023;33(9):1825-1835.e3. doi:10.1016/j.cub.2023.03.057

32.Chen P, Kotov AA, Godneeva BK, Bazylev SS, Olenina LV, Aravin AA. piRNA-mediated gene regulation and adaptation to sex-specific transposon expression in *D. melanogaster* male germline. *Genes Dev*. 2021;35(11-12):914-935. doi:10.1101/gad.345041.120

33.Jusic A, Salgado-Somoza A, Paes AB, et al. Approaching Sex Differences in Cardiovascular Non-Coding RNA Research. *Int J Mol Sci*. 2020;21(14):4890. doi:10.3390/ijms21144890

34.Wadhwa PD, Buss C, Entringer S, Swanson JM. Developmental Origins of Health and Disease: Brief History of the Approach and Current Focus on Epigenetic Mechanisms. *Semin Reprod Med*. 2009;27(5):358-368. doi:10.1055/s-0029-1237424

35.Navas-Acien A, Guallar E, Silbergeld EK, Rothenberg SJ. Lead Exposure and Cardiovascular Disease—A Systematic Review. *Environ Health Perspect*. 2007;115(3):472-482. doi:10.1289/ehp.9785

36.Shiek SS, Mani MS, Kabekkodu SP, Dsouza HS. Health repercussions of environmental exposure to lead: Methylation perspective. *Toxicology*. 2021;461:152927. doi:10.1016/j.tox.2021.152927

37. Goodrich JM, Dolinoy DC, Sánchez BN, et al. Adolescent epigenetic profiles and environmental exposures from early life through peri-adolescence. *Environ Epigenetics*. 2016;2(3):dvw018. doi:10.1093/eep/dvw018

38. Yohannes YB, Nakayama SM, Yabe J, et al. Blood lead levels and aberrant DNA methylation of the ALAD and p16 gene promoters in children exposed to environmental-lead. *Environ Res*. 2020;188:109759. doi:10.1016/j.envres.2020.109759

39. Dou JF, Farooqui Z, Faulk CD, et al. Perinatal Lead (Pb) Exposure and Cortical Neuron-Specific DNA Methylation in Male Mice. *Genes*. 2019;10(4):274. doi:10.3390/genes10040274

40. Svoboda LK, Neier K, Wang K, et al. Tissue and sex-specific programming of DNA methylation by perinatal lead exposure: implications for environmental epigenetics studies. *Epigenetics*. 16(10):1102-1122. doi:10.1080/15592294.2020.1841872

41. Wang K, Liu S, Svoboda LK, et al. Tissue- and Sex-Specific DNA Methylation Changes in Mice Perinatally Exposed to Lead (Pb). *Front Genet*. 2020;11:840. doi:10.3389/fgene.2020.00840

42. Svoboda LK, Wang K, Goodrich JM, et al. Perinatal Lead Exposure Promotes Sex-Specific Epigenetic Programming of Disease-Relevant Pathways in Mouse Heart. *Toxics*. 2023;11(1):85. doi:10.3390/toxics11010085

43. Svoboda LK, Wang K, Jones TR, Colacino JA, Sartor MA, Dolinoy DC. Sex-Specific Alterations in Cardiac DNA Methylation in Adult Mice by Perinatal Lead Exposure. *Int J Environ Res Public Health*. 2021;18(2):577. doi:10.3390/ijerph18020577

44. Wang K, Sartor MA, Colacino JA, Dolinoy DC, Svoboda LK. Sex-Specific Deflection of Age-Related DNA Methylation and Gene Expression in Mouse Heart by Perinatal Toxicant Exposures. *bioRxiv*. Preprint posted online April 28, 2024:2024.04.25.591125. doi:10.1101/2024.04.25.591125

45. Lin H, Spradling AC. A novel group of pumilio mutations affects the asymmetric division of germline stem cells in the Drosophila ovary. *Development*. 1997;124(12):2463-2476. doi:10.1242/dev.124.12.2463

46. Mani SR, Juliano CE. Untangling the web: The diverse functions of the PIWI/piRNA pathway. *Mol Reprod Dev*. 2013;80(8):632-664. doi:10.1002/mrd.22195

47. Shoji K, Suzuki Y, Sugano S, Shimada T, Katsuma S. Artificial "ping-pong" cascade of PIWI-interacting RNA in silkworm cells. *RNA*. 2017;23(1):86-97. doi:10.1261/rna.058875.116

48. Parks RJ, Howlett SE. Sex differences in mechanisms of cardiac excitation–contraction coupling. *Pflugers Arch*. 2013;465(5):747-763. doi:10.1007/s00424-013-1233-0

49. CV Physiology | Cardiac Excitation-Contraction Coupling. Accessed September 30, 2025. https://cvphysiology.com/cardiac-function/cf022

50. Eisner DA, Caldwell JL, Kistamás K, Trafford AW. Calcium and Excitation-Contraction Coupling in the Heart. *Circ Res*. 2017;121(2):181-195. doi:10.1161/CIRCRESAHA.117.310230

51. Bening C, Weiler H, Vahl CF. Effects of gender, ejection fraction and weight on cardiac force development in patients undergoing cardiac surgery – an experimental examination. *J Cardiothorac Surg*. 2013;8(1):214. doi:10.1186/1749-8090-8-214

52. Ferreira de Mattos G, Costa C, Savio F, Alonso M, Nicolson GL. Lead poisoning: acute exposure of the heart to lead ions promotes changes in cardiac function and Cav1.2 ion channels. *Biophys Rev*. 2017;9(5):807-825. doi:10.1007/s12551-017-0303-5

53. Rommel C, Hein L. Four Dimensions of the Cardiac Myocyte Epigenome: from Fetal to Adult Heart. *Curr Cardiol Rep*. 2020;22(5):26. doi:10.1007/s11886-020-01280-7

54. Gilsbach R, Schwaderer M, Preissl S, et al. Distinct epigenetic programs regulate cardiac myocyte development and disease in the human heart in vivo. *Nat Commun*. 2018;9:391. doi:10.1038/s41467-017-02762-z

55. Gilsbach R, Preissl S, Grüning BA, et al. Dynamic DNA methylation orchestrates cardiomyocyte development, maturation and disease. *Nat Commun*. 2014;5:5288. doi:10.1038/ncomms6288

56. Perera BPU, Morgan RK, Polemi KM, Sala-Hamrick KE, Svoboda LK, Dolinoy DC. PIWI-Interacting RNA (piRNA) and Epigenetic Editing in Environmental Health Sciences. *Curr Environ Health Rep*. Published online August 2, 2022. doi:10.1007/s40572-022-00372-6

57. Svoboda LK, Wang K, Cavalcante RG, et al. Sex-Specific Programming of Cardiac DNA Methylation by Developmental Phthalate Exposure. *Epigenetics Insights*. 2020;13:2516865720939971. doi:10.1177/2516865720939971

58. Wang T, Pehrsson EC, Purushotham D, et al. The NIEHS TaRGET II Consortium and environmental epigenomics. *Nat Biotechnol*. 2018;36(3):225-227. doi:10.1038/nbt.4099

59. Faulk C, Barks A, Liu K, Goodrich JM, Dolinoy DC. Early-life lead exposure results in dose- and sex-specific effects on weight and epigenetic gene regulation in weanling mice. *Epigenomics*. 2013;5(5):487-500. doi:10.2217/epi.13.49

60. Perera BPU, Wang K, Wang D, et al. Sex and tissue-specificity of piRNA regulation in adult mice following perinatal lead (Pb) exposure. *Epigenetics*. 19(1):2426952. doi:10.1080/15592294.2024.2426952

61. Zhang Y, Lin YH, Johnson TD, Rozek LS, Sartor MA. PePr: a peak-calling prioritization pipeline to identify consistent or differential peaks from replicated ChIP-Seq data. *Bioinforma Oxf Engl*. 2014;30(18):2568-2575. doi:10.1093/bioinformatics/btu372

62. Wang K, Li M, Sartor MA, Colacino JA, Dolinoy DC, Svoboda LK. Perinatal Exposure to Lead or Diethylhexyl Phthalate in Mice: Sex-Specific Effects on Cardiac DNA Methylation and Gene Expression across Time. *Environ Health Perspect*. 2025;133(6):67014. doi:10.1289/EHP15503

63. Risso D, Ngai J, Speed TP, Dudoit S. Normalization of RNA-seq data using factor analysis of control genes or samples. *Nat Biotechnol*. 2014;32(9):896-902. doi:10.1038/nbt.2931

64. Tóth KF, Pezic D, Stuwe E, Webster A. The piRNA Pathway Guards the Germline Genome Against Transposable Elements. *Adv Exp Med Biol*. 2016;886:51. doi:10.1007/978-94-017-7417-8_4

65. Gasperini C, Tuntevski K, Beatini S, et al. Piwil2 (Mili) sustains neurogenesis and prevents cellular senescence in the postnatal hippocampus. *EMBO Rep*. 2022;24(2):e53801. doi:10.15252/embr.202153801

66. Wang K, Zhou L, Liu F, et al. PIWI-Interacting RNA HAAPIR Regulates Cardiomyocyte Death After Myocardial Infarction by Promoting NAT10-Mediated ac4C Acetylation of Tfec mRNA. *Adv Sci*. 2022;9(8):2106058. doi:10.1002/advs.202106058

67. Wang K, Li F, Zhou L, et al. HNEAP Regulates Necroptosis of Cardiomyocytes by Suppressing the m5C Methylation of Atf7 mRNA. *Adv Sci*. 2023;10(34):2304329. doi:10.1002/advs.202304329

68. Chen B, Shi B, Zhou Z, et al. Targeting a cardiac abundant and fibroblasts-specific piRNA (CFRPi) to attenuate and reverse cardiac fibrosis in pressure-overloaded heart failure. *Transl Res*. 2024;0(0). doi:10.1016/j.trsl.2024.01.003

69. Gao XQ, Zhang YH, Liu F, et al. The piRNA CHAPIR regulates cardiac hypertrophy by controlling METTL3-dependent N6-methyladenosine methylation of Parp10 mRNA. *Nat Cell Biol*. 2020;22(11):1319-1331. doi:10.1038/s41556-020-0576-y

70. Meijer BJ, Giugliano FP, Baan B, et al. ATF2 and ATF7 Are Critical Mediators of Intestinal Epithelial Repair. *Cell Mol Gastroenterol Hepatol*. 2020;10(1):23-42. doi:10.1016/j.jcmgh.2020.01.005

71. AVCAPIR: A Novel Procalcific PIWI-Interacting RNA in Calcific Aortic Valve Disease | Circulation. Accessed February 7, 2025.

https://www.ahajournals.org/doi/10.1161/CIRCULATIONAHA.123.065213?url_ver=Z39.88-2003&rfr_id=ori:rid:crossref.org&rfr_dat=cr_pub%20%200pubmed

72.Sexton CE, Han MV. Paired-end mappability of transposable elements in the human genome. *Mob DNA*. 2019;10:29. doi:10.1186/s13100-019-0172-5

73.Lerat E. Identifying repeats and transposable elements in sequenced genomes: how to find your way through the dense forest of programs. *Heredity*. 2010;104(6):520-533. doi:10.1038/hdy.2009.165

74.Quénerch'du E, Anand A, Kai T. The piRNA pathway is developmentally regulated during spermatogenesis in Drosophila. *RNA*. 2016;22(7):1044-1054. doi:10.1261/rna.055996.116

75.Haase AD, Ketting RF, Lai EC, et al. PIWI-interacting RNAs: who, what, when, where, why, and how. *EMBO J*. 2024;43(22):5335-5339. doi:10.1038/s44318-024-00253-8

76.Siasos G, Tsigkou V, Kosmopoulos M, et al. Mitochondria and cardiovascular diseases—from pathophysiology to treatment. *Ann Transl Med*. 2018;6(12):256. doi:10.21037/atm.2018.06.21

77.Ahamed M, Siddiqui MKJ. Low level lead exposure and oxidative stress: Current opinions. *Clin Chim Acta*. 2007;383(1):57-64. doi:10.1016/j.cca.2007.04.024

78.Ji X, Wang B, Paudel YN, et al. Protective Effect of Chlorogenic Acid and Its Analogues on Lead-Induced Developmental Neurotoxicity Through Modulating Oxidative Stress and Autophagy. *Front Mol Biosci*. 2021;8:655549. doi:10.3389/fmolb.2021.655549

79.Gregorio CC, Antin PB. To the heart of myofibril assembly. *Trends Cell Biol*. 2000;10(9):355-362. doi:10.1016/s0962-8924(00)01793-1

80.Lehman SJ, Crocini C, Leinwand LA. Targeting the sarcomere in inherited cardiomyopathies. *Nat Rev Cardiol*. 2022;19(6):353-363. doi:10.1038/s41569-022-00682-0

81.Hamdani N, Kooij V, van Dijk S, et al. Sarcomeric dysfunction in heart failure. *Cardiovasc Res*. 2008;77(4):649-658. doi:10.1093/cvr/cvm079

82.Jiao L, Liu Y, Yu XY, et al. Ribosome biogenesis in disease: new players and therapeutic targets. *Signal Transduct Target Ther*. 2023;8(1):1-22. doi:10.1038/s41392-022-01285-4

83.Chen J, Li Y, Du C, Wei T, Shan T, Wang L. Protein kinases in cardiovascular diseases. *Chin Med J (Engl)*. 2022;135(5):557-570. doi:10.1097/CM9.0000000000001870

84.Reuter M, Berninger P, Chuma S, et al. Miwi catalysis is required for piRNA amplification-independent LINE1 transposon silencing. *Nature*. 2011;480(7376):264-267. doi:10.1038/nature10672

85.Deng W, Lin H. miwi, a murine homolog of piwi, encodes a cytoplasmic protein essential for spermatogenesis. *Dev Cell*. 2002;2(6):819-830. doi:10.1016/s1534-5807(02)00165-x

86.Kuramochi-Miyagawa S, Watanabe T, Gotoh K, et al. DNA methylation of retrotransposon genes is regulated by Piwi family members MILI and MIWI2 in murine fetal testes. *Genes Dev*. 2008;22(7):908-917. doi:10.1101/gad.1640708

87. Aravin AA, Sachidanandam R, Girard A, Fejes-Toth K, Hannon GJ. Developmentally regulated piRNA clusters implicate MILI in transposon control. *Science*. 2007;316(5825):744-747. doi:10.1126/science.1142612

88. Carmell MA, Girard A, van de Kant HJG, et al. MIWI2 is essential for spermatogenesis and repression of transposons in the mouse male germline. *Dev Cell*. 2007;12(4):503-514. doi:10.1016/j.devcel.2007.03.001

89. Scoote M, Poole-Wilson PA, Williams AJ. The therapeutic potential of new insights into myocardial excitation–contraction coupling. *Heart*. 2003;89(4):371-376. doi:10.1136/heart.89.4.371

90. Li Z, Li Z, Zhang Y, et al. Mammalian PIWI–piRNA–target complexes reveal features for broad and efficient target silencing. *Nat Struct Mol Biol*. Published online April 24, 2024:1-10. doi:10.1038/s41594-024-01287-6

91. Shirzad H. PiRNA Biogenesis and Their Role in Human Cancers and Other Diseases: A Narrative Review. *Iran J Public Health*. 2021;50(12):2486-2494. doi:10.18502/ijph.v50i12.7930

92. Wang K, Li M, Sartor MA, Colacino JA, Dolinoy DC, Svoboda LK. Perinatal Exposure to Lead or Diethylhexyl Phthalate in Mice: Sex-Specific Effects on Cardiac DNA Methylation and Gene Expression across Time. *Environ Health Perspect*. 2025;133(6):067014. doi:10.1289/EHP15503

Chapter 3: Aim 2: Sex Specific Effects of Perinatal Pb Exposure on Murine Cardiac Gene Expression and Function

Goal: Examine the sex-specific effects of perinatal Pb exposure on gene and pathway alterations as well as phenotypic changes in adult mouse cardiovascular system.

Aim 2A:

- *Hypothesis: Perinatal Pb exposure alters transcriptional pathways associated with cardiovascular development and disease in a sex specific manner.*

Aim 2B:

- *Hypothesis: Perinatal Pb exposure causes structural and functional changes in the murine heart later in life in a sex specific manner.*

3.1: Abstract

Lead (Pb) exposure is known to be a risk factor for cardiovascular disease (CVD), but how Pb affects the heart through molecular and functional changes is yet to be fully elucidated. Using a murine model of perinatal Pb exposure, we assessed sex-specific transcriptional and functional heart changes in the heart during midlife. Upon RNA-Seq analysis of 4-month mice, we found no Pb induced differentially expressed genes for either sex, but we observed changes caused by Pb related in hundreds of pathways related to cardiac function, development, mitochondria, metabolism, and epigenetics (FDR < 0.05). In particular, pathways related to mitochondrial structure or function were upregulated in female mice, and pathways related to histone biology were upregulated in male mice. Upon interrogating read count data, we found an nearly significant (p-value 0.066) upregulation in *Ryr2*, a gene encoding for a Ca channel important in excitation contraction coupling (ECC) only in female mice. We also assessed sex specific changes in cardiac function by examining echocardiograms in the same 4-month-old mice. We found significant sex specific changes on cardiac structure and function, including decreases in cardiac output, stroke volume, left ventricular mass, and left ventricular volume in males (p-value < 0.05). Together, we discovered that perinatal Pb exposure induces persistent and sex specific changes in gene transcription and heart function, providing the foundation for future mechanistic studies.

3.2: Introduction

Aim 1 highlighted how perinatal Pb exposure leads to sex specific changes in piRNA expression. As previously stated, CVD is highly sexually dimorphic, and studies have shown sex differences in the developmental origins of cardiovascular disease.[1,2] Therefore, Aim 2 aspires to

build on Aim 1 and assess sex-specific changes in changes cardiac gene expression and function in adult mice perinatally exposed to Pb.

Sexually mature, 4 month old mice were used for this study, as changes that may have been induced by Pb during development may not have physiological effects until later in life.[3] Pb remains a persistent environmental hazard throughout the world, and Pb exposure is known to cause cardiovascular disease.[4] Even at low levels, Pb is an important risk factor in the incidence and mortality from cardiovascular disease.[4] One mechanism by which Pb may induce changes in cardiac physiology is through epigenetics, or mitotically heritable changes in gene expression without affecting the underlying DNA sequence, and includes DNA methylation, histone modifications, and non-coding RNA (ncRNA).[5,6]

Our laboratory's earlier work demonstrated that perinatal Pb exposure—encompassing both pre-conception, gestation, and lactation—resulted in widespread, sex-dependent alterations in DNA methylation and piRNA expression (Aim 1) within cardiac tissue later in life.[7,8] These changes included numerous differentially methylated cytosines (DMCs) and regions (DMRs), spanning both hypermethylated and hypomethylated sites in males and females.[7] Pathway enrichment analyses revealed that male- and female-specific DMCs were associated with distinct biological processes, with several male-linked pathways tied to normal cardiac development and function.[7] These findings suggest that Pb-driven epigenetic modifications established during early development may predispose individuals to cardiovascular dysfunction in adulthood.

We conducted RNA-Seq analysis on mice treated perinatally with Pb to assess for gene and pathway changes induced by Pb, paying particular attention to pathways related to cardiac structure and function, development, epigenetics, energy metabolism, and mitochondria. Focus on epigenetics was due to changes seen in previous studies and in Aim 1, and focus on energy

metabolism and mitochondria was assessed because early life exposure to Pb is known to disrupt mitochondrial and metabolic function in the heart.[9,10]

In addition to epigenetic changes, we sought to understand how Pb exposure alters cardiac function in the mouse heart by assessing for changes in excitation contraction coupling genes. Excitation contraction coupling (ECC), is the process by which an electrical stimulus (action potential) leads to an influx of calcium (Ca) in cardiomyocytes, which is converted into contraction of these cells.[11] In this process, action potentials trigger the release of Ca into the cell, where it binds to troponin, causing actin and myosin filaments to slide and thus creating uniform contraction that forms a heartbeat.[12] Notably, there are known sex differences in ECC at baseline, with smaller and slower peak cardiomyocyte contractions in females compared to males in rat models.[11] Further, Pb is known to mimic Ca and through disruption of Ca signaling can lead to cardiac arrythmias.[13] We are assessing four ECC genes in this study: *Atp2A2* (SERCA2), which transports Ca from cytosol into sarcoplasmic reticulum, *Cacna1c* (Cav1.2) which is a channel that allows Ca into cytosol, *Ryr2* (ryanodine receptor), which is a channel that allows Ca from sarcoplasmic reticulum into cytosol, and *Slc8a1* (Na Ca exchanger) which transports Ca out of cell.

Echocardiograms were also conducted on mice perinatally exposed to Pb, which non-invasively provide information on cardiac structure, function, and hemodynamics.[14] This includes assessing heart rate (bpm), cardiac output (blood pumped in circulation in ml/min), stroke volume (amount of blood pumped out each beat mm^3), mass of ventricles and atria, and interventricular septum thickness and area during diastole and systole (muscle separating the left and right ventricle during heart relaxation and contraction). Pb exposure is known to alter echocardiography parameters in both workers chronically exposed as well as a Flemish

population exposed to Pb.[15–18] Furthermore, it is important to interrogate sex differences in these effects as echocardiograms vary by sex.[19]

Overall, the purpose of this aim is to investigate how murine perinatal Pb exposure impacts epigenetics, cardiac gene and pathway dynamics, and cardiac function. With this knowledge, we can better understand how developmental exposure to Pb can lead to cardiovascular disease as well as identify potential biomarkers or therapeutic targets.

3.3: Methods

Mouse breeding experiments

Mice (*mus musculus*) used for this study have recently been described.[20,21] All mice for this study were housed in a University of Michigan School of Public Health facility monitored by the ULAM (Unit for Laboratory Animal Medicine) and maintained on regular 12-12 dark-light cycles at 70-73 °F and 50% humidity. Animals were maintained on a phytoestrogen-free modified AIN-93G diet (TD.95092, 7% Corn Oil Diet, (Envigo, Indianapolis, IN, USA). All animals had access to food and drinking water *ad libitum* throughout the experiment and were housed in polycarbonate-free cages. Health checks were carried out daily by lab personnel and ULAM staff. Health checks consisted of a general assessment of appearances (fur coat intact and well-groomed, eyes clear, no signs of fight wounds) and behavior (mobility, nest building, etc.). In addition to checks by lab personnel, a designated animal handler from ULAM checked these cues on a daily basis, and a veterinarian assessed the health status of the mice at least once a week. At 4 months of age, all (both control and Pb exposed as outlined below) mice were euthanized with CO_2 asphyxiation followed by a secondary method of euthanasia of bilateral pneumothorax procedure in accordance with rules and regulations set forth by the Institutional Animal Care and Use Committee (IACUC). This study protocol was approved by the University

of Michigan IACUC protocol #PRO00009800. ARRIVE guidelines were adhered to for this study.

Mouse exposure paradigm

The same perinatal exposure model as aim 1 was used for this aim, with some key differences in mouse strain and age. Pb preparation and exposure were conducted exactly as outlined previously.[22] Virgin female wild-type C57BL/6 mice (6-8 weeks old) were randomly assigned to receive control or Pb via drinking water 2 weeks prior to mating, followed by mating with virgin males of the same strain (7-9 weeks old; **Figure 3.1**).[20] Pb II acetate trihydrate (32 ppm; Sigma-Aldrich, Milwaukee, WI, USA) was mixed with distilled drinking water, which results in a human-relevant maternal exposure in the 16–60 μg/dL range.[22,23] Pb exposure continued through mating (for both males and females), pregnancy (~3 weeks), and lactation until weaning at 3 weeks of age (**Figure 3.1**).[7] After weaning, all offspring received Pb-free water until euthanasia at 4 months of age (**Figure 3.1**). Approximately 1-2 male and 1-2 female offspring per litter were euthanized (n= 8-12 per sex per exposure **Figure 3.1**). No formal sample size calculation was performed. Sample sizes were based on standard practice in the laboratory and were consistent with prior publications using similar methods.[24] Animal collection occurred between 1 and 3 pm, with collection order randomized daily.[24] As outlined in previous studies, one investigator administered treatment and was therefore aware of treatment group allocation, but all investigators completing subsequent molecular assays were blinded to the treatment group until it was analyzed during bioinformatic analysis.[24] Whole, nonperfused hearts from these mice were snap frozen in liquid nitrogen and stored at -80 °C at the time of euthanasia.

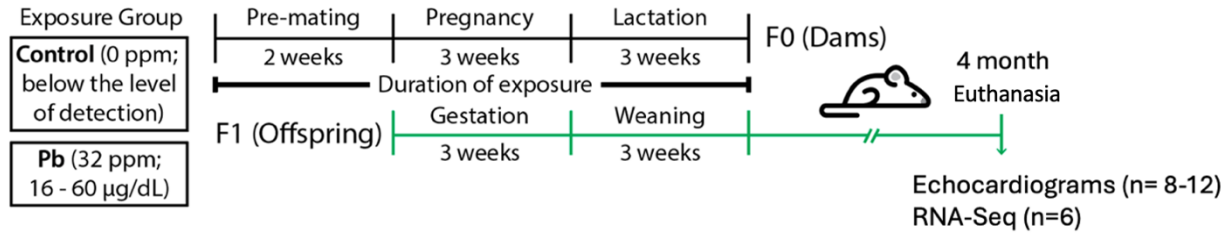


Figure 3.1: Experimental design for perinatal exposure mouse model and analysis.

Pb exposure began with female mice two weeks prior to mating and continued through lactation until weaning at 3 weeks of age. After weaning, all offspring received Pb-free water until euthanasia at 4 months of age. Approximately 1-2 male and 1-2 female offspring per litter were euthanized (n=8-12 per sex per exposure group for echocardiograms and n=6 per sex per exposure group for RNASeq). After euthanasia, RNA was extracted from whole heart tissue for downstream analyses.

Tissue lysis and RNA extraction

Whole heart tissue was cryo-pulverized and RNA extraction was performed using the AllPrep DNA/RNA Mini Kit (#80204 Qiagen, Aarhus, Denmark) according to the manufacturer's instructions with an additional DNAse incubation step (#79254, Qiagen, Aarhus, Denmark). Sample concentration and quality were assessed using a nanodrop microvolume spectrophotometer (Thermo Fisher Scientific, Waltham, Massachusetts, USA).

plexWell cDNA preparation and quality control assessment

RNA sequencing was performed using the plate-based plexWell method (SeqWell), following a modified version of our previously established protocol.[25] For cDNA synthesis, 1 µL of RNA at 10 ng/µL was added to a 96-well plate (Dot Scientific, Cat. #951-PCR-B) and subjected to oligo annealing at 72°C for 10 minutes. Reverse transcription was then carried out at 50°C for 30 minutes, followed by an initial denaturation at 98°C for 3 minutes. Amplification

proceeded through 12 PCR cycles of 98°C for 20 seconds, 67°C for 20 seconds, and 72°C for 6 minutes using a C1000 Thermal Cycler (Bio-Rad, Cat. #1851196). Samples were held at 4°C until purification. cDNA was purified using MAGwise Paramagnetic Beads (SeqWell, Cat. #MG10000), added in a 1:1 volume ratio with a 5-minute binding time. Samples were placed on a magnetic stand, the supernatant was removed, and beads were washed once with 80% ethanol (Spectrum, Cat. #E10258). Elution was performed in 20 µL of 10 mM Tris buffer (Thermo, Cat. #J22638-AE), and samples were stored at –20°C pending quantification.

cDNA concentration was measured using the Quant-iT PicoGreen dsDNA Assay Kit (Thermo, Cat. #P7589) following the manufacturer's instructions. Samples and standards were plated in a 96-well format, and 100 µL of PicoGreen solution was added to each well. After incubation at room temperature in the dark, fluorescence was measured using the SpectraMax M5e and SoftMax Pro software v5.4. A global dilution factor calculator provided by plexWell was used to determine the appropriate cDNA input volume, targeting a minimum of 5 ng per sample.

Library preparation using plexWell and RNA sequencing

For library construction, 6 µL of cDNA at ~1.7 ng/µL per sample was transferred to the sample barcode plate included in the plexWell LP384 Library Preparation Kit (SeqWell, Cat. #LP384X). Each sample was tagged with a unique i7 index using PCR conditions of 55°C for 15 minutes and 68°C for 10 minutes. After indexing, 18 µL of each barcoded sample was pooled, mixed with an equal volume of MAGwise beads, and incubated for 5 minutes to allow binding. Beads were pelleted on a magnetic stand and washed twice with 80% ethanol. Barcoded cDNA was eluted in 40 µL of 10 mM Tris.

Following pooling, sample concentration was re-quantified using the PicoGreen assay to ensure that the final concentration was within the recommended range (3.6–6 ng/μL). The pooled samples were then tagged with an i5 index (pool barcode) through a tagmentation reaction: 55°C for 15 minutes and 68°C for 10 minutes. After tagmentation, samples were purified using the previously described method and eluted in 24 μL of 10 mM Tris.

Final library amplification was conducted with the following thermocycling conditions: 72°C for 10 minutes, 95°C for 3 minutes, followed by 8 cycles of 98°C for 30 seconds, 64°C for 15 seconds, and 72°C for 30 seconds, and a final extension at 72°C for 3 minutes. Amplified libraries were diluted with 205 μL of 10 mM Tris, and 200 μL was purified using 0.8× volume of MAGwise beads. After magnetic separation and two ethanol washes, libraries were eluted in 30 μL of 10 mM Tris and stored at –20°C for short-term use.

Library quality was assessed using the Agilent Bioanalyzer with the High Sensitivity DNA 5000 Kit at the University of Michigan (UM) Advanced Genomics Core. Libraries were sequenced on the Illumina NovaSeq 6000 S4 platform with 151-bp paired-end reads, targeting an average depth of >30 million reads per sample.

Data processing and analysis

Raw reads were demultiplexed using i7 and i5 barcodes. Sequencing data were transferred to the University of Michigan Great Lakes High-Performance Computing Cluster for analysis. Quality control was performed using FastQC and MultiQC.[26,27] Reads were aligned to the mm10 mouse genome reference (splice-aware build) using STAR.[28] Gene-level counts per million

(CPM) were calculated with featureCounts, excluding multi-mapped and multi-overlapping reads.[29]

Computational analysis: DEG and pathway analysis

The R package DESeq2 was used to conduct differential gene expression analysis comparing control to Pb exposed samples. DEG analysis examined genes with padj values of less than 0.05 and absolute log fold change of greater than 1. Principal component analysis (PCA) plots were made using the prcomp function in R.

To assess for pathway enrichment, the LRPath function was utilized as previously described.[30] This function uses logistic regression using the p-value and fold change for each gene to test for enriched or depleted biological categories, and GOBP (biological processes), GOMF (molecular function) and GOCC (cellular compartment) were chosen as the MsigDB gene sets for this analysis.[30] Significant pathways were selected with and FDR cutoff of 0.05. To select for relevant pathways, terms were selected and sorted into 5 categories: cardiac (heart|cardiac|ventric|atrium|muscle|atrial|aorta), mitochondria (mitochondri|respiratory|electron transport|oxidative), metabolism (ATP|glycolysis|fatty acid|glucose|metabolism), development (development|differentiation), and epigenetics (epigenetic|chromatin|histone|methylation|acetylation). Ggplot2 was used to plot dot plots for this data.

Computational analysis: read count analysis of ECC genes

Variance Stabilizing Transformation (VST) in the DESeq2 package was used to normalize read counts of the RNA Sequencing data, and ggplot2 was used to plot normalized read counts for ECC genes. Unpaired t tests were used to assess for differences between Pb and control samples.

Echocardiograms

For 4 month old C57BL/6 control and perinatally exposed mice described above, echocardiography was performed using a Visualsonics 2100 ultrasound machine by the UM Frankel Cardiovascular Center Physiology Phenotyping Core under isoflurane anesthesia as previously described (n= 8-12 per treatment per sex).[31,32] Image acquisition and analysis were performed blinded to the treatment group. M-mode imaging in a parasternal short axis view at the level of the papillary muscles, and two-dimensional long axis imaging were used to calculate ejection fraction, fractional shortening, stroke volume, cardiac output, as well as to make several structural measurements of wall thickness and chamber areas in systole and diastole. Measurements of diastolic function were made using pulsed-wave spectral Doppler analysis of mitral valve inflow patterns (early [E] and late [A] filling waves). Doppler tissue imaging (DTI) was used to measure the early (Ea) and late (Aa) diastolic tissue velocities of the lateral annulus. All parameters were normalized to body weight of each mouse, and both unnormalized and normalized data is presented in **Tables 3.S1** and **3.S2**. For all echocardiogram parameters (both corrected to body weight and unnormalized), a two-way ANOVA with interaction (Sex * Treatment) using Type III sums of squares was performed to assess for changes induced by Pb within and between sexes, followed by pairwise comparisons using estimated marginal means to assess treatment effects within each sex (significant changes considered at p-value < 0.05).

HFrEF gene expression analysis

Venny2.1.0 (https://bioinfogp.cnb.csic.es/tools/venny/) was used to make venn diagrams of overlaps between HFrEF associated genes from a 2024 study of mouse and human single cell heart gene expression and potential differentially expressed genes in this study (p-value < 0.05)

for combined, female, and male mice.[33] Hypergeometric enrichment testing was performed on this data using the phyper() function in R.

3.4: Results

Sex-specific pathway changes in 4-month-old heart samples perinatally exposed to Pb

RNA-Seq was conducted for 4-month samples perinatally exposed to Pb, and PCA plots were made assessing the influence of sex and treatment on variation in the data, showing that sex, but not treatment cluster together (**Figure 3.2**). No genes were found to be significantly differentially expressed by a padj cutoff of 0.05 and |logFC| > 1 (data not shown). Pathway analysis results were filtered by an FDR cutoff of 0.05, and **Table 3.1** shows numbers of significantly altered pathways for combined and sex specific analysis for each GO term. Results were further filtered by relevant pathways into 5 categories: cardiac, development, epigenetics, metabolism, and mitochondria. All results are graphed in **Figure 3.3A**, and specific categories are shown in **Figure 3.3B-F**.

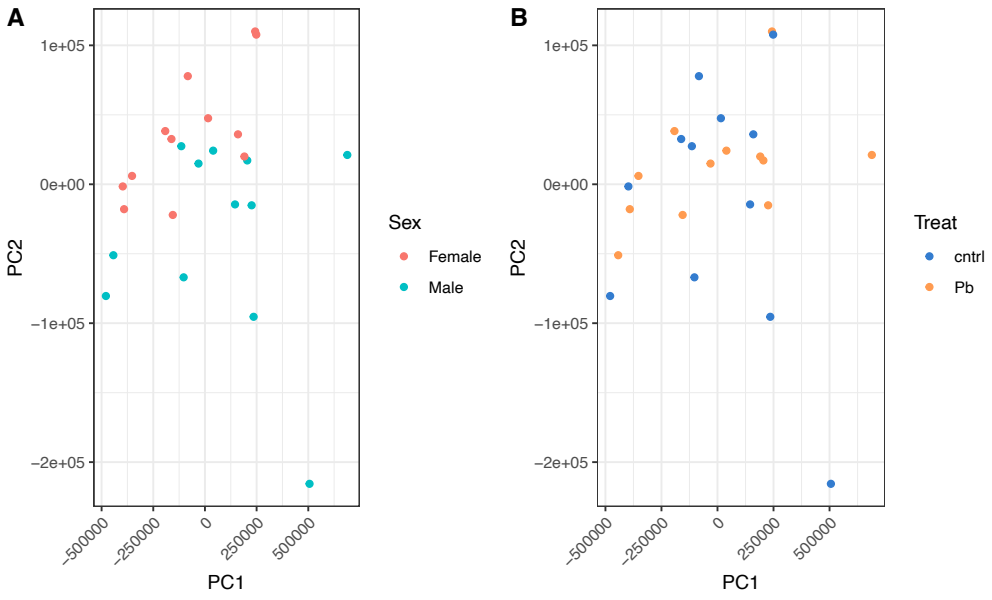


Figure 3.2: PCA plots of 4-month-old RNA Seq data.

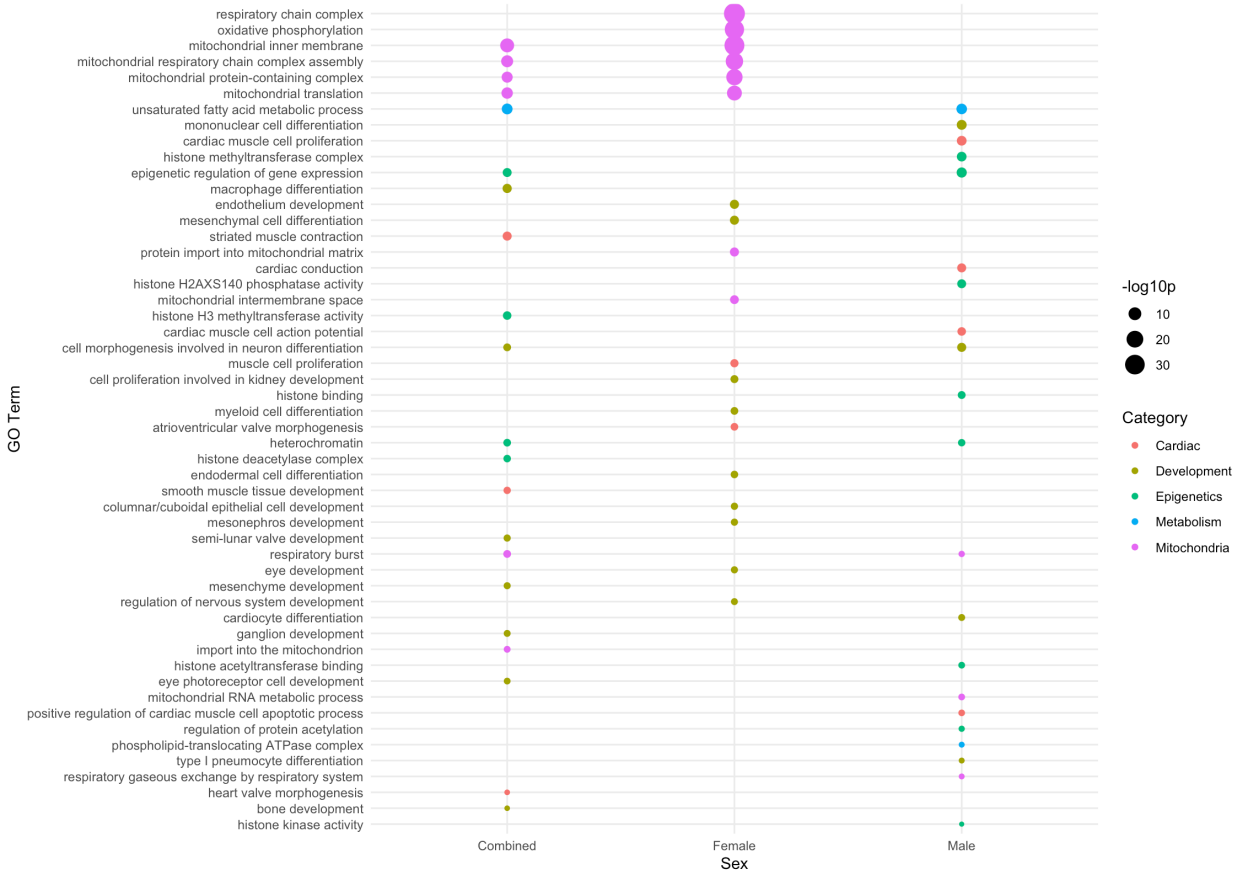
PCA plots were made using the prcomp function and demonstrate variability clustered by sex but not treatment.

	Combined	**Female**	**Male**
GOBP	128	59	122
GOCC	50	29	49
GOMF	43	21	73

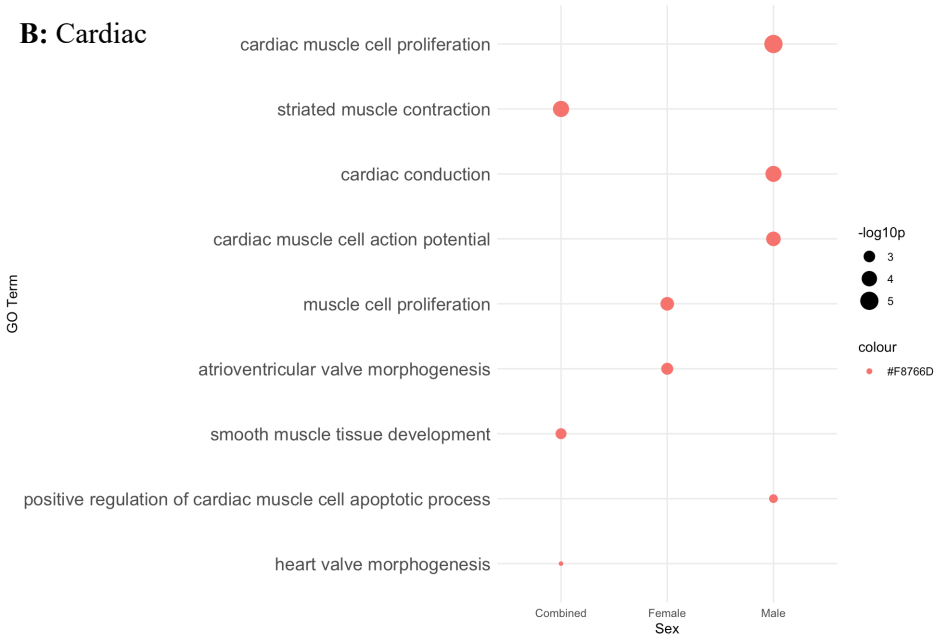
Table 3.1: Significantly altered gene ontology pathways for 4-month-old mice perinatally exposed to Pb.

Three GO categories were assessed: biological processes (BP), cellular compartment (CC), and molecular function (MF) for combined and sex specific analysis. Redundant pathways were reduced in results and filtered by an FDR cutoff of 0.05.

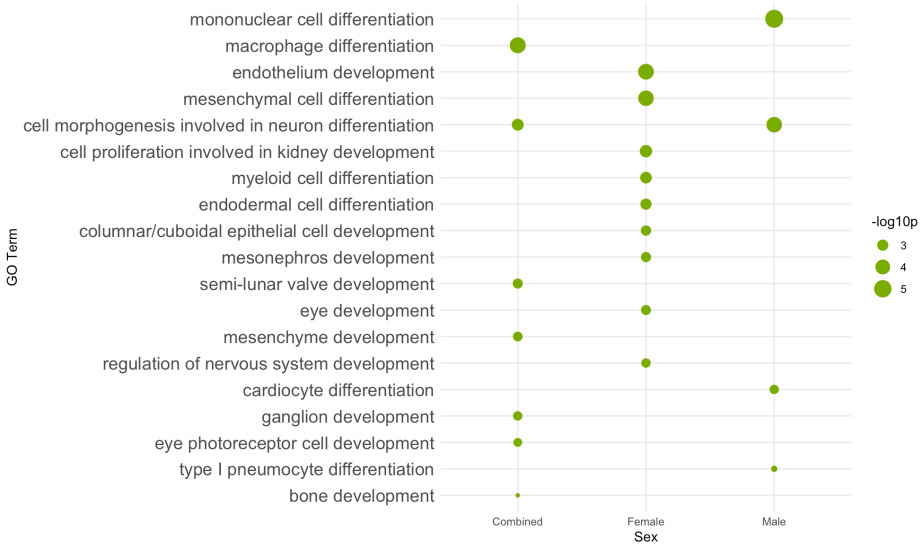
A: All



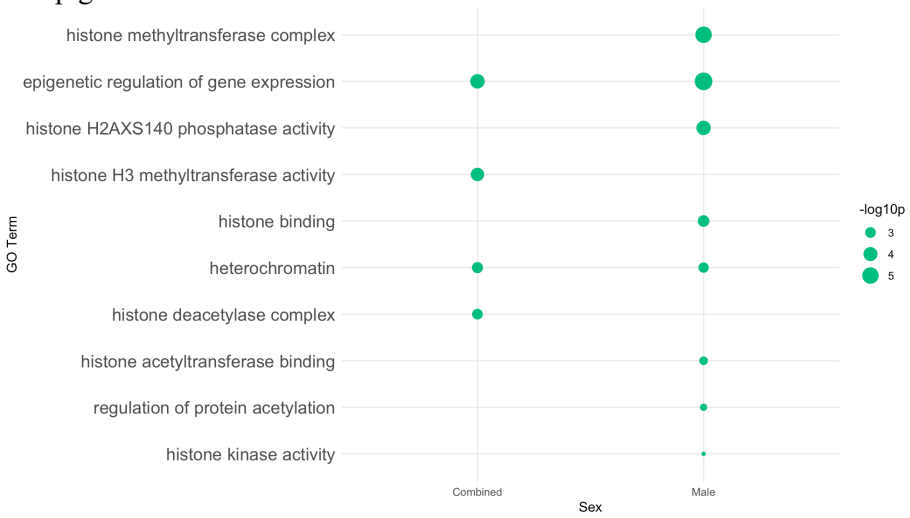
B: Cardiac



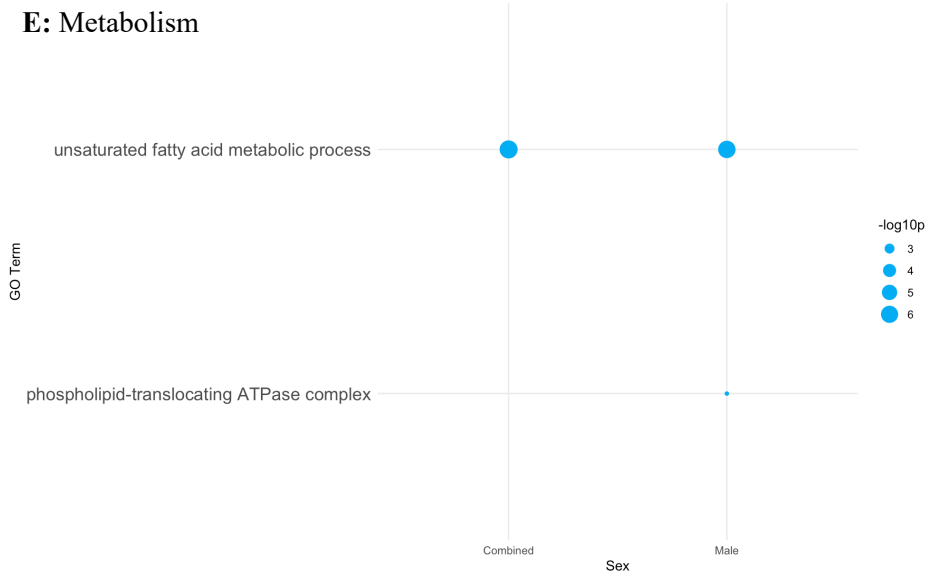
C: Development



D: Epigenetics



E: Metabolism



F: Mitochondria

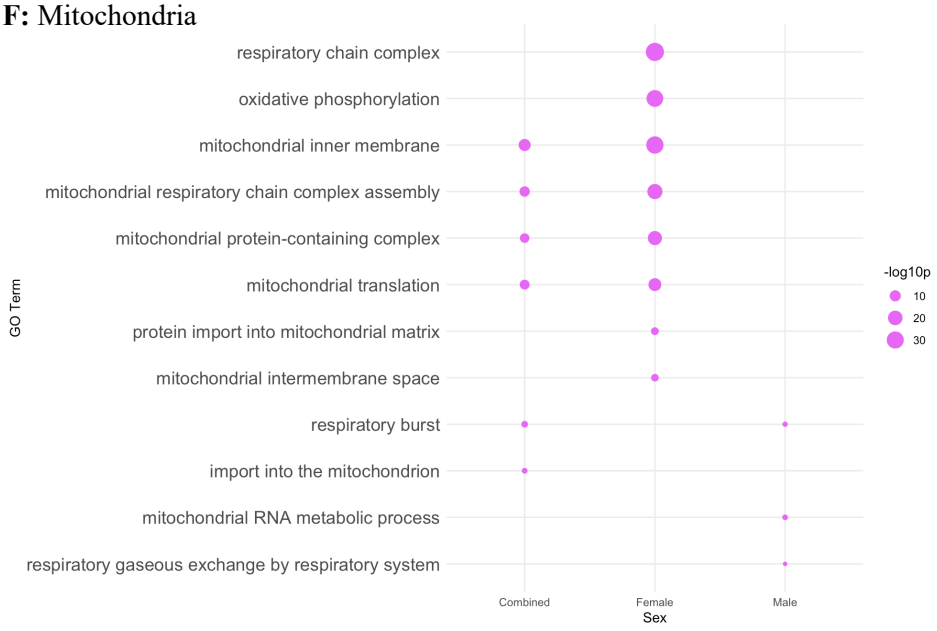


Figure 3.3: Significantly changed relevant pathways in 4-month-old mice perinatally exposed to Pb.

Using LRPath to assess for significantly altered pathways based on differences in gene expression, pathways related to cardiac structure and function (B), development (C), epigenetics (D), metabolism (E), and mitochondria (F), were altered variably in combined and sex specific analyses (all pathways together shown in A).

ECC gene alterations

Specific gene normalized read counts were assessed for ECC (*Atp2A2, Cacna1c, Ryr2,* and *Slc8a1)*, epigenetic, and heart development genes, and none showed significant alterations, although for females, *Ryr2* showed an increase in expression with Pb exposure approaching significance with a p-value of 0.066 for females, 0.25 for males, and 0.063 for the combined sex analysis. (**Figure 3.4**).

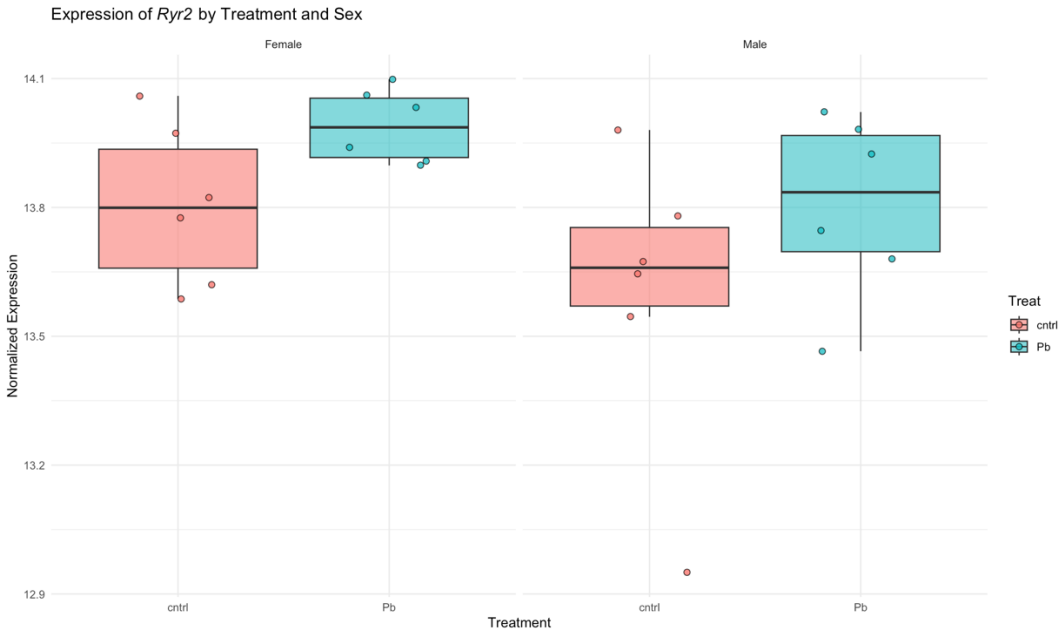
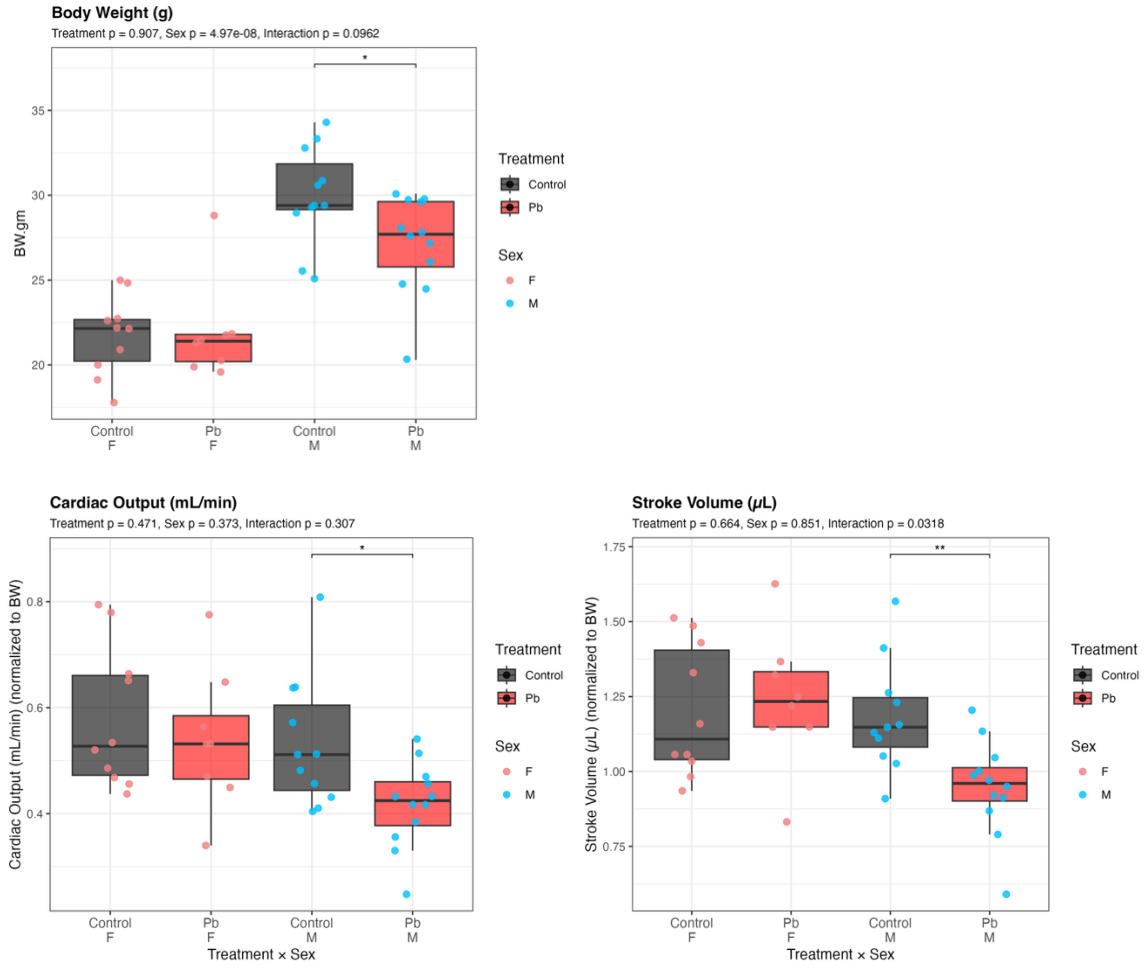


Figure 3.4: Normalized read count assessment of ECC genes reveals potential sex specific change in *Ryr2*.

Normalized read counts were assessed for female and male sample ECC gene changes, and for one gene, *Ryr2*, Pb exposed vs. control female showed a change approaching significance (female p-value: 0.066 , male p-value: 0.25, combined p-value: 0.063).

Echocardiograms of 4-month-old mice perinatally exposed to Pb

Echocardiography studies in 4-month-old mice showed several significant effects of Pb on cardiac structure and function, including reduced body weight, cardiac output, stroke volume, left ventricular mass, and left ventricular volume in males (n=8-12 per group, $p<0.05$, two-way ANOVA; all other parameters corrected to body weight; **Figure 3.5**). However, while post-hoc simple-effects revealed significant decreases in these four parameters only in males, the Treatment × Sex interaction only reached significance for stroke volume (interaction p-value = 0.032). Therefore, sex differences can only be supported for stroke volume. Other echocardiography data can be found in **Figure 3.S1** (unnormalized) and **Figure 3.S2** (normalized to body weight) in the supplementary materials.



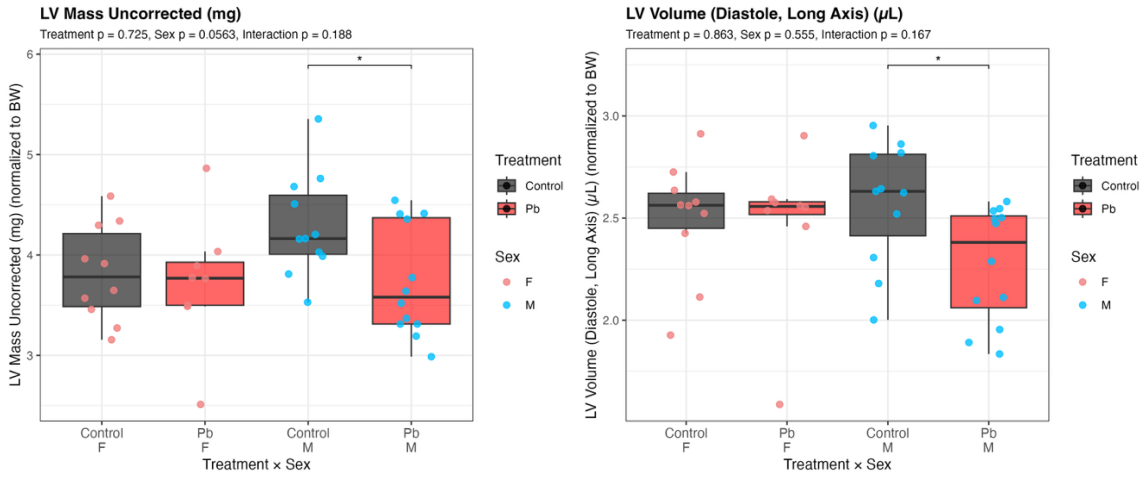


Figure 3.5: Echocardiograms of adult mice perinatally exposed to Pb.

Significantly altered parameters in either sex were selected and graphed above, with n=8-12 per group, $p<0.05$ using two-way ANOVA. (BW= Body Weight; LV = Left Ventricle)

Comparison of gene expression between 4-month-old mice perinatally exposed to Pb and HFrEF gene signatures

Given the decreases in cardiac output and stroke volume in male mice with developmental Pb exposure, we examined changes in gene signatures associated with heart failure with reduced ejection fraction (HFrEF) phenotypes in human and mouse samples from a 2024 single cell sequencing study of HFrEF.[33] Venn diagrams show overlaps in genes with a p-value of < 0.05 in this study (combined, female, and male) and human and mouse DEGs from the HFrEF study, although none of these overlaps were statistically significant (**Figure 3.6**).

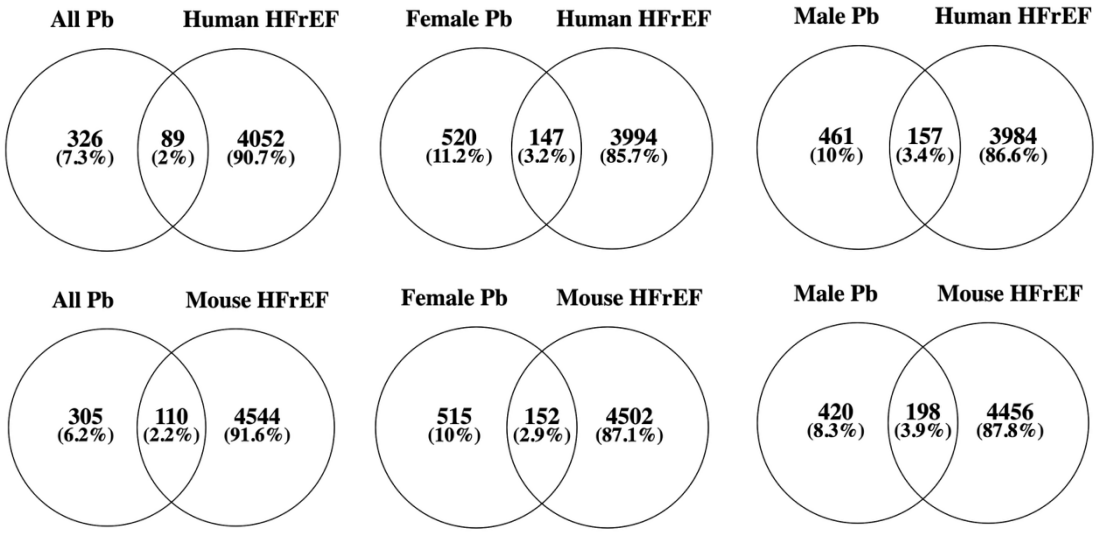


Figure 3.6 Overlaps in HFrEF gene signatures.

Venn diagrams show overlaps in gene expression of HFrEF associated genes from a 2024 study of mouse and human single cell heart gene expression and potential differentially expressed genes in this study (p-value < 0.05) for combined, female, and male mice.[33] The overlaps were not significant by hypergeometric enrichment testing.

3.5: Discussion

Pb-induced epigenetic pathway changes

Interestingly, perinatal Pb exposure affected epigenetic pathways in the heart in a sex specific manner, with significantly altered epigenetic pathways in male, but not female, 4-month samples (**Figure 3.3D**). These identified pathways were related to histone biology, which reflect changes in how tightly DNA is wrapped around histones and is regulated in an interconnected manner with DNA methylation and piRNA regulatory mechanisms in the germline.[34–36] These mechanisms may be first disrupted by Pb exposure during development and compensatory changes are later seen in adult heart tissue in a sex specific manner (only in males). This is

interesting as CVD is highly sexually dimorphic, and emerging work has found that altered histone regulation is involved in the development of different CVDs. Altered regulation of histones has been shown to be involved in heart failure, inflammation, and hypertrophy.[37,38] Importantly, H3K4 methylation is crucial for regulating gene expression during heart development and alterations in this have been implicated in congenital heart disease, myocardial infarction, and heart failure.[39–42] We found here significant upregulation of the GO pathway "histone methyltransferase complex," which included the gene *Wdr82*, a component of the Set1/COMPASS which is important in regulating H3K4 methylation and has been shown to regulate heart development in *Drosophila*.[43–45] Thus, Pb exposure may alter this epigenetic mechanism, and future mechanistic studies should investigate how Pb regulates *Wdr82* expression and function and how this dysregulation may relate to the development of cardiac abnormalities.

Histone regulation also has cross talk with DNA methylation, and so we also examined the normalized read counts of *Dnmt*s and *Tet*s (data not shown). However, we saw no significant changes in the expression of these genes. Future work will need to examine specific genomic targets of this altered epigenetic regulation, and how these are related to heart function and CVD. The final chapter of this dissertation will put these results into the context of the piRNA and associated gene expression changes discussed in Aim 1.

Pb-induced development, metabolism, and mitochondrial pathway changes

Other pathway changes induced by Pb included those related to metabolism and mitochondria (**Figure 3.3E and F**). Unsaturated fatty acid process was one of the pathways differentially regulated by Pb in the male hearts, and is important for cardiac function given that

the heart is a highly energetically demanding organ.[46] Mitochondria play a key role as the main source of energy in the heart, and eight mitochondrial related pathways were found dysregulated in female samples while only three were found dysregulated in male samples by Pb exposure. Previous studies show sexual dimorphism in how mitochondria in the heart respond to aging, with older females showing more significant decline in mitochondrial function.[47] Pathways related to mitochondrial processes were all upregulated in female mice here, which could indicate a compensatory mechanism to impaired mitochondrial bioenergetics, indicating Pb may accelerate this aging process in a sex dependent manner.[47] Pb is known to cause oxidative stress in the heart, but literature is limited in the heart relating Pb to mitochondrial disruption.[48] However, Pb is known to disrupt mitochondrial function in other tissues.[49] More studies are needed to define the mechanisms for how Pb disrupts mitochondrial function in the heart in a sex specific manner and potential relevance to the development of CVD.

Pb-induced pathway changes in cardiac development, structure, and function

Additional dysregulated pathways included those related to cardiac development, structure, and function (**Figure 3.3B and C**). Both males and females showed pathway changes involved in heart development, with males showing potentially dysregulated cardiac muscle cell proliferation (B), cardiomyocyte differentiation (C), females showing dysregulation of muscle cell proliferation and atrioventricular valve morphogenesis (B), and both sexes in a combined analysis potentially dysregulating smooth muscle tissue development, heart valve morphogenesis, and semilunar valve development (**Figure 3.3B and C**). Dysregulation of heart developmental pathways in the adult heart is especially interesting given that in certain CVDs including heart failure and cardiomyopathies, heart regulatory mechanisms revert to a fetal-like state.[50,51] Contradictorily, we examined markers of adult and fetal like states (*Myh6*, *Myh7*,

Nppa, and *Nppb*), and only found a change in *Myh6*, which was significantly upregulated in males only (p-value 0.036; data not shown). *Myh6* is known as a marker of adult-like phenotypes, but this change could be indicative of a compensatory mechanism induced by Pb exposure.[52] Other genes found in literature searches to be related to cardiac development were examined *(Bmp10, Bmp2, Bmp4, Bmpr1a, Bmpr2, Smyd1, Ctnnb1),* with no significant changes (data not shown).[53,54] It is possible heart developmental programs are regulated by Pb through epigenetic or post-translational mechanisms, and future work should examine ties between the altered histone regulation detailed above and developmental programs.

Nine pathways involved in heart structure and function were found to be significantly altered, with four of these uniquely in males and two uniquely in females (**Figure 3.3B**). Interestingly, pathways related to cardiac conduction and cardiac muscle cell action potential were altered by Pb in males only, while females showed a potential increase in expression of *Ryr2*, which releases Ca from the sarcoplasmic reticulum into the cytosol to cause cardiac contraction (**Figure 3.4**). Cardiac conduction can become dysregulated in CVD, with studies showing alterations of ECC in heart failure.[55] These studies do not show a direct role for increased *Ryr2* as a cause for this dysfunction, but suggest alterations in its phosphorylation and expression are a compensatory mechanism.[55,56] While potential changes in heart rate are examined below, future work should examine potential alterations in Ca handling by Pb. Aim 3 will examine how developmental Pb exposure influences action potential and Ca handling in human iPSC derived cardiomyocytes.

Pb-induced echocardiography changes

These molecular changes induced by Pb may have influenced phenotypes as exhibited by differences in echocardiograms. The decreases in cardiac output and stroke volume along with

decreases in left ventricular mass and volume in male mice (corrected to body weight) could be representative of a developmental defect caused by Pb exposure. This is particularly interesting given that these male mice showed dysregulation of pathways related cardiomyocyte differentiation and cardiac cell proliferation as detailed above.

Interestingly, the statistical test used only supports sex differences for the decrease in stroke volume seen in male mice. Studies have shown that at baseline, human and mouse male hearts have higher stroke volume and cardiac output than their female counterparts, but these differences are largely due to differences in overall body weight.[57,58] Here, stroke volume was corrected for body weight and so we saw a disproportionate decrease in stroke volume in male mice compared to females. While no changes in ejection fraction were seen (**Figure 3.S1 and S2**), these changes suggest a reduction in cardiac function in the male mice related to heart failure and could potentially indicate developmental Pb-induced sex differences that could contribute to long term disease risk.

Because of the decreases in cardiac output and stroke volume seen in male mice with Pb exposure, we examined gene expression changes pertaining to HFrEF by looking at overlaps between potentially altered genes in our datasets and those in a study of gene expression changes in HFrEF in mice and humans (**Figure 3.6**).[33] Although there were overlapping genes across analyses, hypergeometric tests indicated that these overlaps were not statistically significant (all $p > 0.05$). Additionally, the percentage of overlapping genes was only marginally increased in the male dataset compared to female (3-4%; **Figure 3.6**). This suggests that Pb exposure may alter molecular pathways that only partially overlap with HFrEF signatures, and that in the male mice there are likely other developmental alterations leading to the observed phenotypic

changes. Further work should be conducted to examine which genes and proteins are involved in dysregulating pathways related to the observed sex specific changes in echocardiography.

Limitations and future directions

This aim uniquely integrates transcriptomic analyses with *in vivo* cardiac phenotyping using a perinatal exposure model of Pb exposure, providing a systems level perspective of Pb's impact on the heart. It further examines sex-specific effects, advancing our understanding of sex as a biological variable. Unlike many DOHaD studies that focus on early developmental timepoints, this work examines mice at midlife, providing insight on how early life Pb exposure may program cardiac outcomes in later life and potentially uncovering changes that contribute to the later-life risk of cardiovascular disease.

Limitations of this work include the utilization of whole heart tissue that was not perfused, and so other cell types including blood were present for the gene expression analyses. Future work should examine specific cell types of the heart. Furthermore, only one time point was examined phenotypically, and as CVD is a disease of aging echocardiograms should be performed for older mice to further develop the causal link between the transcriptional changes shown and the potential development of cardiac pathology. Moreover, this work was broadly associative rather than causal, and future work should assess specific mechanisms underlying the gene expression and phenotypic changes shown here to develop potential prevention strategies, biomarkers, and treatment of CVD induced by Pb.

Conclusions

Through integration of transcriptomics and echocardiograms, we provide a comprehensive set of observations on how developmental Pb exposure disrupts heart biology

differently in male and female mice. These findings may be translatable to the sex disparities seen in CVD in humans and therefore may help develop targeted prevention and therapeutic strategies. Overall, this work shows that perinatal Pb exposure induces persistent and sex specific changes in both cardiac molecular pathways and functionality, highlighting the impact of early life Pb exposure on long term cardiovascular health and providing the foundation for future mechanistic studies dissecting the molecular drivers of developmental Pb-induced cardiotoxicity.

3.6: Supplementary Information

Supplementary information can be found at the repository here: https://doi.org/10.7302/5gs6-2b90

3.7: Acknowledgements

I would like to thank the DoGoodS-Pi Epigenetics Research Group, including Dr. Rachel Morgan and Junru Pan for leading the mouse exposure studies as well as the laboratory manager Tamara Jones (University of Michigan) for her laboratory and administrative support. I would also like to thank Anagha Tapaswi for her work on processing our RNA-Seq samples, and Dr. Tomoko Ishikawa for her contribution to bioinformatic analysis in this work. I would further like to thank University of Michigan Advanced Genomics Core for sample processing for this study.

3.8: References

1. Gao Z, Chen Z, Sun A, Deng X. Gender differences in cardiovascular disease. *Med Nov Technol Devices*. 2019;4:100025. doi:10.1016/j.medntd.2019.100025

2. Intapad S, Ojeda NB, Dasinger JH, Alexander BT. Sex Differences in the Developmental Origins of Cardiovascular Disease. *Physiology*. 2014;29(2):122-132. doi:10.1152/physiol.00045.2013

3. Shah M, de A. Inácio MH, Lu C, et al. Environmental and genetic predictors of human cardiovascular ageing. *Nat Commun*. 2023;14(1):4941. doi:10.1038/s41467-023-40566-6

4. Lanphear BP, Rauch S, Auinger P, Allen RW, Hornung RW. Low-level lead exposure and mortality in US adults: a population-based cohort study. *Lancet Public Health*. 2018;3(4):e177-e184. doi:10.1016/S2468-2667(18)30025-2

5. Dupont C, Armant DR, Brenner CA. Epigenetics: Definition, Mechanisms and Clinical Perspective. *Semin Reprod Med*. 2009;27(5):351-357. doi:10.1055/s-0029-1237423

6. Navas-Acien A, Guallar E, Silbergeld EK, Rothenberg SJ. Lead Exposure and Cardiovascular Disease—A Systematic Review. *Environ Health Perspect*. 2007;115(3):472-482. doi:10.1289/ehp.9785

7. Svoboda LK, Wang K, Jones TR, Colacino JA, Sartor MA, Dolinoy DC. Sex-Specific Alterations in Cardiac DNA Methylation in Adult Mice by Perinatal Lead Exposure. *Int J Environ Res Public Health*. 2021;18(2):577. doi:10.3390/ijerph18020577

8. Sala-Hamrick KE, Wang K, Perera BPU, Sartor MA, Svoboda LK, Dolinoy DC. Sex-stratified piRNA expression analysis reveals shared functional impacts of perinatal lead (Pb) exposure in murine hearts. *Epigenetics*. 20(1):2542879. doi:10.1080/15592294.2025.2542879

9. Parr DR, Harris EJ. The effect of lead on the calcium-handling capacity of rat heart mitochondria. *Biochem J*. 1976;158(2):289-294. doi:10.1042/bj1580289

10. Davuljigari CB, Gottipolu RR. Late-life Cardiac Injury in Rats following Early Life Exposure to Lead: Reversal Effect of Nutrient Metal Mixture. *Cardiovasc Toxicol*. 2020;20(3):249-260. doi:10.1007/s12012-019-09549-2

11. Parks RJ, Howlett SE. Sex differences in mechanisms of cardiac excitation–contraction coupling. *Pflugers Arch*. 2013;465(5):747-763. doi:10.1007/s00424-013-1233-0

12. Eisner DA, Caldwell JL, Kistamás K, Trafford AW. Calcium and Excitation-Contraction Coupling in the Heart. *Circ Res*. 2017;121(2):181-195. doi:10.1161/CIRCRESAHA.117.310230

13. Ferreira de Mattos G, Costa C, Savio F, Alonso M, Nicolson GL. Lead poisoning: acute exposure of the heart to lead ions promotes changes in cardiac function and Cav1.2 ion channels. *Biophys Rev*. 2017;9(5):807-825. doi:10.1007/s12551-017-0303-5

14. Gowda RM, Khan IA, Vasavada BC, Sacchi TJ, Patel R. History of the evolution of echocardiography. *Int J Cardiol*. 2004;97(1):1-6. doi:10.1016/j.ijcard.2003.07.018

15. Ozturk MT, Yavuz B, Ozkan S, et al. Lead Exposure Is Related to Impairment of Aortic Elasticity Parameters. *J Clin Hypertens*. 2014;16(11):790-793. doi:10.1111/jch.12414

16.Kasperczyk S, Przywara-Chowaniec B, Kasperczyk A, et al. Function of heart muscle in people chronically exposed to lead. *Ann Agric Environ Med AAEM*. 2005;12(2):207-210.

17.Zou HJ, Ding Y, Huang KL, et al. Effects of lead on systolic and diastolic cardiac functions. *Biomed Environ Sci BES*. 1995;8(4):281-288.

18.Yang WY, Zhang ZY, Thijs L, et al. Left Ventricular Structure and Function in Relation to Environmental Exposure to Lead and Cadmium. *J Am Heart Assoc*. 2017;6(2):e004692. doi:10.1161/JAHA.116.004692

19.Cheng S, Larson MG, McCabe EL, et al. Age- and sex-based reference limits and clinical correlates of myocardial strain and synchrony: the Framingham Heart Study. *Circ Cardiovasc Imaging*. 2013;6(5):692-699. doi:10.1161/CIRCIMAGING.112.000627

20.Svoboda LK, Wang K, Cavalcante RG, et al. Sex-Specific Programming of Cardiac DNA Methylation by Developmental Phthalate Exposure. *Epigenetics Insights*. 2020;13:2516865720939971. doi:10.1177/2516865720939971

21.Wang T, Pehrsson EC, Purushotham D, et al. The NIEHS TaRGET II Consortium and environmental epigenomics. *Nat Biotechnol*. 2018;36(3):225-227. doi:10.1038/nbt.4099

22.Svoboda LK, Neier K, Wang K, et al. Tissue and sex-specific programming of DNA methylation by perinatal lead exposure: implications for environmental epigenetics studies. *Epigenetics*. 16(10):1102-1122. doi:10.1080/15592294.2020.1841872

23.Faulk C, Barks A, Liu K, Goodrich JM, Dolinoy DC. Early-life lead exposure results in dose- and sex-specific effects on weight and epigenetic gene regulation in weanling mice. *Epigenomics*. 2013;5(5):487-500. doi:10.2217/epi.13.49

24.Perera BPU, Wang K, Wang D, et al. Sex and tissue-specificity of piRNA regulation in adult mice following perinatal lead (Pb) exposure. *Epigenetics*. 19(1):2426952. doi:10.1080/15592294.2024.2426952

25.Sala-Hamrick KE, Tapaswi A, Polemi KM, Nguyen VK, Colacino JA. High-Throughput Transcriptomics of Nontumorigenic Breast Cells Exposed to Environmentally Relevant Chemicals. *Environ Health Perspect*. 2024;132(4):047002. doi:10.1289/EHP12886

26.Babraham Bioinformatics - FastQC A Quality Control tool for High Throughput Sequence Data. Accessed September 2, 2025. https://www.bioinformatics.babraham.ac.uk/projects/fastqc/

27.MultiQC: summarize analysis results for multiple tools and samples in a single report | Bioinformatics | Oxford Academic. Accessed September 2, 2025. https://academic.oup.com/bioinformatics/article/32/19/3047/2196507

28.Dobin A, Davis CA, Schlesinger F, et al. STAR: ultrafast universal RNA-seq aligner. *Bioinforma Oxf Engl*. 2013;29(1):15-21. doi:10.1093/bioinformatics/bts635

29.Liao Y, Smyth GK, Shi W. featureCounts: an efficient general purpose program for assigning sequence reads to genomic features. *Bioinforma Oxf Engl*. 2014;30(7):923-930. doi:10.1093/bioinformatics/btt656

30.Sartor MA, Leikauf GD, Medvedovic M. LRpath: a logistic regression approach for identifying enriched biological groups in gene expression data. *Bioinformatics*. 2009;25(2):211-217. doi:10.1093/bioinformatics/btn592

31.Palpant NJ, Day SM, Herron TJ, Converso KL, Metzger JM. Single histidine-substituted cardiac troponin I confers protection from age-related systolic and diastolic dysfunction. *Cardiovasc Res*. 2008;80(2):209-218. doi:10.1093/cvr/cvn198

32.Garbincius JF, Merz LE, Cuttitta AJ, et al. Enhanced dimethylarginine degradation improves coronary flow reserve and exercise tolerance in Duchenne muscular dystrophy carrier mice. *Am J Physiol Heart Circ Physiol*. 2020;319(3):H582-H603. doi:10.1152/ajpheart.00333.2019

33.Jurado MR, Tombor LS, Arsalan M, et al. Improved integration of single-cell transcriptome data demonstrates common and unique signatures of heart failure in mice and humans. *GigaScience*. 2024;13:giae011. doi:10.1093/gigascience/giae011

34.Fu K, Bonora G, Pellegrini M. Interactions between core histone marks and DNA methyltransferases predict DNA methylation patterns observed in human cells and tissues. *Epigenetics*. 2019;15(3):272-282. doi:10.1080/15592294.2019.1666649

35.Tibben BM, Rothbart SB. Mechanisms of DNA Methylation Regulatory Function and Crosstalk with Histone Lysine Methylation. *J Mol Biol*. 2024;436(7):168394. doi:10.1016/j.jmb.2023.168394

36.Castañeda J, Genzor P, Bortvin A. piRNAs, transposon silencing, and germline genome integrity. *Mutat Res*. 2011;714(1-2):95-104. doi:10.1016/j.mrfmmm.2011.05.002

37.Zhang W, Song M, Qu J, Liu GH. Epigenetic Modifications in Cardiovascular Aging and Diseases. *Circ Res*. 2018;123(7):773-786. doi:10.1161/CIRCRESAHA.118.312497

38.Qin J, Guo N, Tong J, Wang Z. Function of histone methylation and acetylation modifiers in cardiac hypertrophy. *J Mol Cell Cardiol*. 2021;159:120-129. doi:10.1016/j.yjmcc.2021.06.011

39.Ang SY, Uebersohn A, Spencer CI, et al. KMT2D regulates specific programs in heart development via histone H3 lysine 4 di-methylation. *Dev Camb Engl*. 2016;143(5):810-821. doi:10.1242/dev.132688

40.Wan X, Liu L, Ding X, et al. Mll2 controls cardiac lineage differentiation of mouse embryonic stem cells by promoting H3K4me3 deposition at cardiac-specific genes. *Stem Cell Rev Rep*. 2014;10(5):643-652. doi:10.1007/s12015-014-9527-y

41.Li Y, Quan X, Li X, et al. Kdm6A Protects Against Hypoxia-Induced Cardiomyocyte Apoptosis via H3K27me3 Demethylation of Ncx Gene. *J Cardiovasc Transl Res*. 2019;12(5):488-495. doi:10.1007/s12265-019-09882-5

42.Dorsheimer L, Assmus B, Rasper T, et al. Association of Mutations Contributing to Clonal Hematopoiesis With Prognosis in Chronic Ischemic Heart Failure. *JAMA Cardiol*. 2019;4(1):25-33. doi:10.1001/jamacardio.2018.3965

43.Lee JH, Skalnik DG. Wdr82 Is a C-Terminal Domain-Binding Protein That Recruits the Setd1A Histone H3-Lys4 Methyltransferase Complex to Transcription Start Sites of Transcribed Human Genes. *Mol Cell Biol*. 2008;28(2):609-618. doi:10.1128/MCB.01356-07

44. Wu M, Wang PF, Lee JS, et al. Molecular Regulation of H3K4 Trimethylation by Wdr82, a Component of Human Set1/COMPASS. *Mol Cell Biol*. 2008;28(24):7337-7344. doi:10.1128/MCB.00976-08

45. Zhu J yi, Van De Leemput J, Han Z. Distinct roles of COMPASS subunits to *Drosophila* heart development. *Biol Open*. 2024;13(10):bio061736. doi:10.1242/bio.061736

46. Lopaschuk GD, Ussher JR, Folmes CDL, Jaswal JS, Stanley WC. Myocardial fatty acid metabolism in health and disease. *Physiol Rev*. 2010;90(1):207-258. doi:10.1152/physrev.00015.2009

47. Colom B, Oliver J, Garcia-Palmer FJ. Sexual Dimorphism in the Alterations of Cardiac Muscle Mitochondrial Bioenergetics Associated to the Ageing Process. *J Gerontol A Biol Sci Med Sci*. 2015;70(11):1360-1369. doi:10.1093/gerona/glu014

48. Babiker F, Al-Kouh A, Kilarkaje N. Lead exposure induces oxidative stress, apoptosis, and attenuates protection of cardiac myocytes against ischemia-reperfusion injury. *Drug Chem Toxicol*. 2019;42(2):147-156. doi:10.1080/01480545.2018.1429460

49. Han Q, Zhang W, Guo J, et al. Mitochondrion: a sensitive target for Pb exposure. *J Toxicol Sci*. 2021;46(8):345-358. doi:10.2131/jts.46.345

50. Mehdiabadi NR, Boon Sim C, Phipson B, et al. Defining the Fetal Gene Program at Single-Cell Resolution in Pediatric Dilated Cardiomyopathy. *Circulation*. 2022;146(14):1105-1108. doi:10.1161/CIRCULATIONAHA.121.057763

51.Razeghi P, Young ME, Alcorn JL, Moravec CS, Frazier OH, Taegtmeyer H. Metabolic Gene Expression in Fetal and Failing Human Heart. *Circulation*. 2001;104(24):2923-2931. doi:10.1161/hc4901.100526

52.Taegtmeyer H, Sen S, Vela D. Return to the fetal gene program. *Ann N Y Acad Sci*. 2010;1188:191-198. doi:10.1111/j.1749-6632.2009.05100.x

53.Wang Z, Schwartz RJ, Liu J, Sun F, Li Q, Ma Y. Smyd1 Orchestrates Early Heart Development Through Positive and Negative Gene Regulation. *Front Cell Dev Biol*. 2021;9:654682. doi:10.3389/fcell.2021.654682

54.Klaus A, Saga Y, Taketo MM, Tzahor E, Birchmeier W. Distinct roles of Wnt/β-catenin and Bmp signaling during early cardiogenesis. *Proc Natl Acad Sci*. 2007;104(47):18531-18536. doi:10.1073/pnas.0703113104

55.Scoote M, Poole-Wilson PA, Williams AJ. The therapeutic potential of new insights into myocardial excitation–contraction coupling. *Heart*. 2003;89(4):371-376. doi:10.1136/heart.89.4.371

56.Yamamoto T, Yano M, Kohno M, et al. Abnormal Ca2+ release from cardiac sarcoplasmic reticulum in tachycardia-induced heart failure. *Cardiovasc Res*. 1999;44(1):146-155. doi:10.1016/S0008-6363(99)00200-X

57.St. Pierre SR, Peirlinck M, Kuhl E. Sex Matters: A Comprehensive Comparison of Female and Male Hearts. *Front Physiol*. 2022;13:831179. doi:10.3389/fphys.2022.831179

58. Baumann PQ, Sobel BE, Tarikuz Zaman A k. m., Schneider DJ. Gender-Dependent Differences in Echocardiographic Characteristics of Murine Hearts. *Echocardiography*. 2008;25(7):739-748. doi:10.1111/j.1540-8175.2008.00680.x

Chapter 4: Aim 3: Evaluate Cell Line–Specific Gene Expression Changes and Functional Alterations Induced by Pb Exposure During Differentiation in Human iPSC-Derived Ventricular Cardiomyocytes

Goal: Characterize the dose-specific effects of Pb exposure during differentiation on gene, pathway, and functional alterations in human ventricular cardiomyocytes.

Aim 3A:

- *Hypothesis: Epigenetic regulatory genes as well as genes associated with cardiac development, structure, and function are affected by Pb exposure during differentiation in human iPSC-derived ventricular cardiomyocytes.*

Aim 3B:

- *Hypothesis: Pb exposure during differentiation impacts heart cell differentiation and beat characteristics in purified ventricular cardiomyocytes.*

4.1: Abstract

CVD disease etiology is known to be strongly influenced by Pb exposure and is highly sexually dimorphic, but the underlying sex specific molecular and functional mechanisms are unclear. Further, how epigenome modifying enzymes behave during heart development in both sexes in the absence or presence of Pb is yet to be fully understood. Using a new approach methodology, human induced pluripotent stem cell (iPSC) derived ventricular cardiomyocytes from one male and one female donor, we characterized how Pb exposure during cardiomyocyte differentiation impacts transcriptional as well as voltage and calcium (Ca) dynamics. In the absence of Pb, expression of *DNMT*s, *TET*s and *PIWIL*s were dynamic throughout differentiation and similar in expression patterns in both cell lines. Further, *PIWIL* levels were similar in unexposed iPSC-derived ventricular cardiomyocytes and human fetal heart samples. We also found cell line specific changes in *DNMT*s, *TET*s, and pluripotency markers in iPSCs exposed to a range of doses of Pb but that *DNMT* and *TET* expression was not affected by exposure to 0.5 and 5 μM Pb during differentiation. We conducted RNA-Seq in our Pb exposed female derived cell line and found significant Pb induced changes in expression of genes throughout differentiation and dysregulation of pathways related to heart development and function throughout differentiation in response to Pb, with particular emphasis on epigenetic and mitochondrial machinery. Upon benchmark dose modeling of this data, we found unique dose response gene expression changes induced by Pb in different days of differentiation. While the expression changes were unique, they corresponded to a similar median benchmark concentration of 0.2 μM for all days assessed. Gene ontology analysis of benchmark modeled genes showed changes in pathways related to heart development. Further, we characterized functional changes in Pb developmentally exposed (0.5 and 5 μM) female and male derived

ventricular cardiomyocytes through optical mapping of Ca transients and action potentials and found cell line specific effects of Pb. Overall, we characterized the transcriptional and electrophysiological changes induced by Pb in ventricular cardiomyocytes derived from iPSCs, opening the door to future mechanistic studies understanding how Pb exposure during differentiation may impact heart function.

4.2: Introduction

Building upon mouse studies that found potential alterations in piRNA, molecular pathways, and heart structure and function in mice exposed perinatally to Pb, we sought to understand how Pb exposure during human cardiomyocyte differentiation may alter developmental gene expression and cardiomyocyte function. Epidemiological studies of Pb exposure relating to adverse cardiovascular consequences in humans are well documented, and although fewer have focused on developmental Pb exposure, one found a relationship between maternal Pb levels and a significant increase in systolic blood pressure in young children, suggesting a relationship between *in utero* Pb exposure and adverse heart outcomes that could progress into CVD later in life.[1] In addition to the work presented in chapters 2 and 3, recent work from our lab has suggested perinatal exposure to Pb in mice relates to sex specific epigenetic changes in mice that are related to cardiac pathology, and so here we assess these potential changes in human cells.[2]

Pb at concentrations present during the Flint water crisis (0.5 μM to 1.5 μM) has been found to disrupt pluripotency factors in mouse embryonic stem cells, and has also been shown to alter DNA methylation, which plays an important role in maintaining a pluripotent state.[2,3] Therefore, we assessed changes in pluripotency markers *OCT4, SOX2* and *NANOG*, which give iPSCs

pluripotency characteristics, and *DNMT*s and *TET*s, which catalyze the addition or removal of methyl groups from DNA, respectively, in undifferentiated iPSCs exposed to Pb at human relevant doses.[4]

Pb exposure is also known to disrupt cardiac development in mice (including in chapters 2 and 3 of this study), as well as impair proper neuronal differentiation through epigenetic mechanisms.[5,6] To mimic an *in utero* exposure, we chose two human exposure relevant doses of Pb (0.5 μM and 5 μM) to treat human iPSCs during the first 8 days of their differentiation to ventricular cardiomyocytes, and examined epigenetic changes throughout differentiation (days 0-15). We chose this exposure window to capture the developmental period during which pluripotent cells commit first to mesodermal and then cardiac progenitor lineages, prior to the onset of spontaneous contraction and functional maturation of cardiomyocytes (days 8-30).[7,8] We assessed levels of *PIWIL* genes, as we saw changes in the piRNA and *Piwil* landscape with Pb exposure in our mouse model. We conducted this study in one male and one female derived stem cell line, as there are marked differences in heart disease between males and females.

Further, we conducted RNA-Seq of Pb exposed female derived iPSC ventricular cardiomyocytes and paid particular attention to pathways related to cardiac structure and function, development, epigenetics, energy metabolism, and mitochondria. Focus on energy metabolism and mitochondria was assessed because early life exposure to Pb is known to disrupt mitochondrial and metabolic function in the heart.[9,10] We also used benchmark dose modeling to look at genes responsive to Pb in a dose dependent manner and modelled the same pathway changes.

To assess how these epigenetic, gene, and pathway changes induced by Pb may be related to changes in cardiac function, we conducted optical mapping of action potentials and calcium

(Ca) transients. An action potential is the electrical signal that leads to the production of a rhythmic heartbeat, through a process called Excitation Contraction Coupling (ECC), leading to an influx of Ca in cardiomyocytes, which is ultimately results in contraction of these cells.[11,12] Importantly, Pb is known to mimic Ca and disruption of Ca signaling is one mechanism by which Pb exposure may lead to cardiac arrythmias.[13] Genes encoding ECC proteins are subject to epigenetic regulation during development, thus impacting heart beat characteristics later in life, and so ECC gene changes were also assessed in our unpurified cardiomyocytes.

Overall, this aim seeks to characterize how Pb exposure during differentiation of one female and one male iPSC-derived ventricular cardiomyocyte cell line impacts the gene expression and molecular pathways throughout differentiation as well as downstream function as purified cardiomyocytes.

4.3: Methods

Cell culture: iPSC maintenance

iPSC line PENN002i-442-1 from a 24-year-old Caucasian female and iPSC line PENN042i-258-12 from a Caucasian 21-year-old male, both reprogrammed from blood cells were obtained from WiCell (WiCell, Madison, WI, USA). In order to promote adhesion and growth, iPSCs were plated in 24 well or 6 well Corning plates on surfaces coated with Corning Matrigel Basement Membrane Matrix that was prepared in DMEM:F12 HEPES (#07-200-80, #09-761-146 #356234 and #11330032; Thermo Fisher Scientific, Waltham, MA USA). iPSCs were maintained on this matrix in StemMACS iPS-Brew XF Media or StemMACS PSC-Brew XF (#130-104-368 and #130-127-865; Miltenyi Biotec, Bergisch Gladbach, Germany) in feeder free conditions and incubated at 37°C in a 5% CO2 incubator. Media was changed regularly

according to the manufacturer's instructions (daily for iPS-Brew and every other day for PSC-Brew). Colonies of iPSCs that showed any signs of spontaneous differentiation were marked and removed via aspiration. Cells around 80% confluency were dissociated non-enzymatically with Versene (#15040066, Thermo Fisher Scientific, Waltham, MA USA) and seeded at low densities (1:24) for maintenance of iPSCs.

Cell culture: iPSC differentiation

To perform differentiation into ventricular cardiomyocytes, iPSCs from above were passaged with Versene and seeded at higher densities (80-100% cells used) into monolayers. When cells reached 80-95% confluency (1-3 days), differentiation into ventricular cardiomyocytes was commenced according to procedures outlined in prior studies (**Figure 4.1**).[7,8] In the first 8 days of differentiation, cells were maintained on "basal" media (RPMI medium with HEPES CAT# 22400-89 Gibco, Grand Island, New York, USA with supplements ascorbic acid #A8960 and BSA #A9418 Sigma Aldrich, St. Louis, MO, USA) and switched over to "B27" media on day 8 until purification. Modulation of Wnt/B-catenin signaling was utilized for differentiation as previously described (**Figure 4.1**).[7,8] To direct cells into a mesoderm state, iPSCs were treated on day 0 in basal media with CHIR99021 (#4423) which activates Wnt signaling, and after 2 days, cells were treated with IWP4 (#5214) in basal media, which inhibits Wnt signaling and drives cells towards a cardiac lineage (Tocris Bioscience, Avonmouth, Bristol, United Kingdom). After this, cells were given basal media without the addition of small molecules on days 4 and 6 and switched over to "B27" media on day 8 with B27 media changes every other day after this until purification (RPMI # 11875-093 and B27 supplement #17504-

044; Gibco, Grand Island, New York, USA).

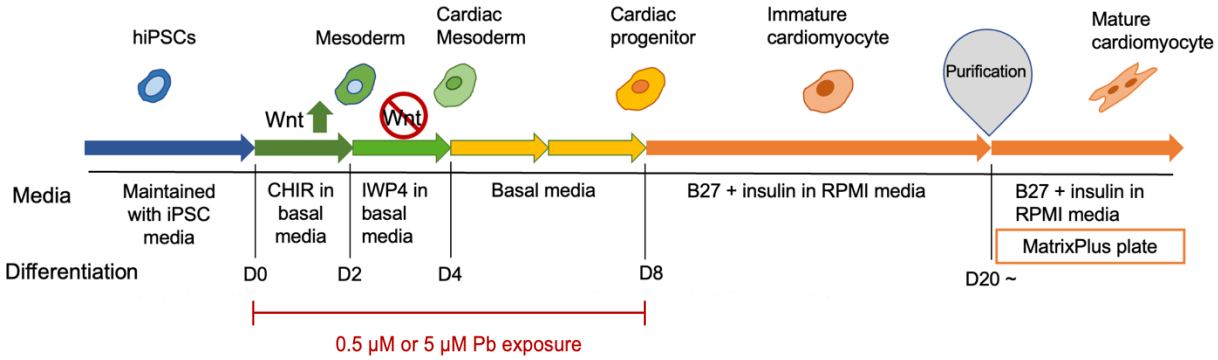


Figure 4.1: Protocol for differentiation of iPSCs into ventricular cardiomyocytes. Differentiation protocol and subsequent purification, with Pb treatment on the first 8 days of differentiation.

Cell culture: Pb exposure paradigm

As detailed in the figure above, Lead (II) Acetate Trihydrate (CAS: 6080-56-4 ; #215902, Sigma-Aldrich, St. Louis, MO, USA) was diluted in tissue culture grade water and iPSCs undergoing differentiation were treated for the first 8 days (days 0-8) at an environmentally and occupationally relevant dose of 0.5 µM and a higher toxic dose of 5 µM. For 6 well plates, 1-2 wells were used for each treatment (control and the two Pb doses), while for 24 well plates, 3 wells were used for each treatment and combined for subsequent extractions or purification. Additionally, iPSCs in 6 well plates not undergoing differentiation were treated with a range of doses of Pb (0, 0.4, 0.8, and 1.6 µM) for 72 hours before collection and RNA extractions.

Cell culture: cardiomyocyte purification

Ventricular cardiomyocytes derived above (both control and Pb exposed) were purified once beating was visualized throughout each well (days 10-20), with the intention of enriching culture with a highly pure population of cardiomyocytes and eliminating non-cardiomyocyte cell

populations. According to the cardiomyocyte isolation kit used from Miltenyi Biotec (#130-110-188, Bergisch Gladbach, Germany), this selective depletion strategy enhances the cardiomyocyte purity to 98%. First, cells were enzymatically dissociated with trypsin (#25200056, Thermo Fisher Scientific, Waltham, MA USA). After trypsin inactivation with EB20 media (reagents in **Table 4.1** below), cells were passed through 30 um pre-separation filters (#130-041-407 Miltenyi Biotec, Bergisch Gladbach, Germany), centrifuged, washed with magnetic-activated cell sorting (MACS) buffer (#130-091-221, Miltenyi Biotec, Bergisch Gladbach, Germany), centrifuged again, and then incubated in cardiomyocyte depletion primary antibody from the Miltenyi isolation kit for 10 minutes. Primary antibody was washed off with MACs before incubation with secondary antibody from the kit which attaches the non-cardiomyocyte cells to magnetic microbeads. After this, cells in MACs suspension were passed through magnetic separation columns attached to a magnet, where cardiomyocytes pass through and noncardiomyocytes remain attached to the column (LS columns #130-042-401 and magnetic separator #130-042-303, Miltenyi Biotec, Bergisch Gladbach, Germany). Cells were then spun down and redissolved in EB20 media. Finally, these purified cardiomyocytes were plated at 75,000 cells per well on a 96 well CELLvo™ Matrix Plus extracellular matrix coated plate (#30001.57, StemBioSys, San Antonio, Texas, USA). After 48 hours, cells were then maintained in EB20.

Reagent to make EB20 media	**Product Number, Company, Location**
80% DMEM:F12	#11-220-033, Gibco, Grand Island, New York, USA

20% FBS	#f2-442-500ml, Sigma-Aldrich, St. Louis, MO, USA
1 mmol/L L-glutamine	#25030-081, Gibco, Grand Island, New York, USA
0.1 mmol/L Nonessential amino acids	#11140-050, Gibco, Grand Island, New York, USA
0.1 mmol/L beta-mercaptoethanol	#21985-023, Invitrogen, Waltham, Massachusetts, USA
0.001% Blebbistatin	#13186, Cayman chemical, Ann Arbor, Michigan, USA

Table 4.1: Reagents in EB20 Media

Immature heart samples

Human immature heart and gonadal tissues were obtained via an NIH-supported biobank through the University of Washington (2R24 HD000836-47). Tissue samples were collected from healthy individuals electing pregnancy termination during the first or second trimester, as previously described.[14] For this study, samples from gestational days 90–105 were selected. Following informed consent and surgical procedures, tissues were flash-frozen in liquid nitrogen using polycarbonate-free polypropylene tubes and stored at –80°C. Samples were then shipped to the University of Michigan on dry ice. A total of five male and five female samples per tissue were included in the analysis.

RNA extractions

Cells were scraped off plates and pelleted before commencing RNA extractions. For iPSC analysis, cells were collected after 72 hours of exposure. For analysis during differentiation, cells were collected at days 0-6 and 15 for the female derived line and days 0, 1, 2, 6, and 15 for the male derived line. RNA extraction was performed using the AllPrep DNA/RNA Universal Kit (#80224 Qiagen, Aarhus, Denmark) according to the manufacturer's instructions with an additional DNAse incubation step (#79254, Qiagen, Aarhus, Denmark). Sample concentration and quality were assessed using a nanodrop microvolume spectrophotometer (Thermo Fisher Scientific, Waltham, Massachusetts, USA).

qRT-PCR

500 ng to 1 μg of total RNA was reverse transcribed into cDNA using the iScript cDNA Synthesis Kit (#1708890 BioRad, Hercules, California; the same amount of cDNA was used within each experiment). mRNA expression of genes whose primers are listed in the table below were quantified using the CFX Real-Time PCR using iTaq Universal SYBR Green Supermix according to manufacturer's protocols with all samples run in triplicate. mRNA expression was compared using the same method on the same plate to amplification of two reference genes (*ACTB and GAPDH*; primer information in **Table 4.2** below). All primer information is listed in **Table 4.2** below. For *PIWIL* primers, primers were designed and primer efficiency was confirmed using cDNA serial dilutions in a previous study.[15] All qRT-PCR reactions were carried out for 40 cycles under standard PCR conditions. ΔCq values were calculated by subtracting the Cq triplicate average of a target sample from that of the geometric mean of the reference genes. The relative difference in gene expression was then calculated using $2^{-\Delta Cq}$ and graphed using GraphPad Prism, where one way ANOVA and unpaired t-tests were used to determine statistical differences between control and treatment groups.

Gene name	**Primer Information**	**Company**
DNMT1	qHsaCID0021977	BioRad, Hercules, California
DNMT3A	qHsaCID0010863	BioRad, Hercules, California
DNMT3B	qHsaCID0016111	BioRad, Hercules, California
TET1	qHsaCID0007976	BioRad, Hercules, California
TET2	qHsaCID0014693	BioRad, Hercules, California
TET3	qHsaCID0010281	BioRad, Hercules, California
NANOG	qHsaCED0043394	BioRad, Hercules, California
SOX2	qHsaCED0036871	BioRad, Hercules, California
ATP2A2	Hs.PT.56a.39859858.g	Integrated DNA Technologies, Coralville, Iowa
CACNA1C	Hs.PT.58.14979004	Integrated DNA Technologies, Coralville, Iowa
RYR2	Hs.PT.58.502763	Integrated DNA Technologies, Coralville, Iowa
SLC8A1	Hs.PT.58.40534466	Integrated DNA Technologies, Coralville, Iowa

PIWIL1	F: ACGAAGTGCCACAGTTTTTGG R: AGTCTTCCTCCAGACTGAGC	Integrated DNA Technologies, Coralville, Iowa
PIWIL2	F: GCCTGGGTTGAACTAAAGGA R: CCATGATGATGCAAACAACC	Integrated DNA Technologies, Coralville, Iowa
PIWIL3	F: TCAGATGGCAGCAAAATCAC R: ACGTTGTGTACCCGTTAGGC	Integrated DNA Technologies, Coralville, Iowa
PIWIL4	F: ATGGCACCGAGATCACCTAT R: GCTGAGCCTCACTGTTGTCA	Integrated DNA Technologies, Coralville, Iowa
ACTB	qHsaCED0036269	BioRad, Hercules, California
GAPDH	qHsaCED0038674	BioRad, Hercules, California

Table 4.2: Primer Information

RNA sequencing: plexWell cDNA preparation and quality control assessment

RNA sequencing was performed using the plate-based plexWell method (SeqWell), following a modified version of our previously established protocol.[16] For cDNA synthesis, 1 µL of RNA at 10 ng/µL was added to a 96-well plate (Dot Scientific, Cat. #951-PCR-B) and subjected to oligo annealing at 72°C for 10 minutes. Reverse transcription was then carried out at 50°C for 30 minutes, followed by an initial denaturation at 98°C for 3 minutes. Amplification proceeded through 12 PCR cycles of 98°C for 20 seconds, 67°C for 20 seconds, and 72°C for 6 minutes using a C1000 Thermal Cycler (Bio-Rad, Cat. #1851196). Samples were held at 4°C until purification. cDNA was purified using MAGwise Paramagnetic Beads (SeqWell, Cat.

#MG10000), added in a 1:1 volume ratio with a 5-minute binding time. Samples were placed on a magnetic stand, the supernatant was removed, and beads were washed once with 80% ethanol (Spectrum, Cat. #E10258). Elution was performed in 20 µL of 10 mM Tris buffer (Thermo, Cat. #J22638-AE), and samples were stored at –20°C pending quantification.

cDNA concentration was measured using the Quant-iT PicoGreen dsDNA Assay Kit (Thermo, Cat. #P7589) following the manufacturer's instructions. Samples and standards were plated in a 96-well format, and 100 µL of PicoGreen solution was added to each well. After incubation at room temperature in the dark, fluorescence was measured using the SpectraMax M5e and SoftMax Pro software v5.4. A global dilution factor calculator provided by plexWell was used to determine the appropriate cDNA input volume, targeting a minimum of 5 ng per sample.

RNA sequencing: library preparation using plexWell and sequencing

For library construction, 6 µL of cDNA at ~1.7 ng/µL per sample was transferred to the sample barcode plate included in the plexWell LP384 Library Preparation Kit (SeqWell, Cat. #LP384X). Each sample was tagged with a unique i7 index using PCR conditions of 55°C for 15 minutes and 68°C for 10 minutes. After indexing, 18 µL of each barcoded sample was pooled, mixed with an equal volume of MAGwise beads, and incubated for 5 minutes to allow binding. Beads were pelleted on a magnetic stand and washed twice with 80% ethanol. Barcoded cDNA was eluted in 40 µL of 10 mM Tris.

Following pooling, sample concentration was re-quantified using the PicoGreen assay to ensure that the final concentration was within the recommended range (3.6–6 ng/µL). The pooled samples were then tagged with an i5 index (pool barcode) through a tagmentation reaction: 55°C

for 15 minutes and 68°C for 10 minutes. After tagmentation, samples were purified using the previously described method and eluted in 24 µL of 10 mM Tris.

Final library amplification was conducted with the following thermocycling conditions: 72°C for 10 minutes, 95°C for 3 minutes, followed by 8 cycles of 98°C for 30 seconds, 64°C for 15 seconds, and 72°C for 30 seconds, and a final extension at 72°C for 3 minutes. Amplified libraries were diluted with 205 µL of 10 mM Tris, and 200 µL was purified using 0.8× volume of MAGwise beads. After magnetic separation and two ethanol washes, libraries were eluted in 30 µL of 10 mM Tris and stored at –20°C for short-term use.

Library quality was assessed using the Agilent Bioanalyzer with the High Sensitivity DNA 5000 Kit at the University of Michigan (UM) Advanced Genomics Core. Libraries were sequenced on the Illumina NovaSeq 6000 S4 platform with 151-bp paired-end reads, targeting an average depth of >30 million reads per sample.

RNA sequencing: data processing and analysis

Raw reads were demultiplexed using i7 and i5 barcodes. Sequencing data were transferred to the University of Michigan Great Lakes High-Performance Computing Cluster for analysis. Quality control was performed using FastQC and MultiQC.[17,18] Reads were aligned to the GRCh38 human genome reference (splice-aware build) using STAR.[19] Gene-level counts per million (CPM) were calculated with featureCounts, excluding multi-mapped and multi-overlapping reads.[20]

Computational analysis: DEG and pathway analysis

The R package DESeq2 was used to conduct differential gene expression analysis comparing control to Pb exposed samples individually for each day (0, 1, 2, 6, and 15) in female

derived iPSCs undergoing differentiation into cardiomyocytes. DEG analysis examined genes with padj values of less than 0.05. Principal component analysis (PCA) plots were made using the plotPCA in DESeq2.

To assess for pathway enrichment, the LRPath function was utilized as previously described.[21] This function uses logistic regression using the p-value and fold change for each gene to test for enriched or depleted biological categories, and GOBP (biological processes), GOMF (molecular function) and GOCC (cellular compartment) were chosen as the MsigDB gene sets for this analysis.[21] Significant pathways were selected with and FDR cutoff of 0.05. To select for relevant pathways, terms were selected and sorted into 5 categories: cardiac (heart|cardiac|ventric|atrium|muscle|atrial|aorta), mitochondria (mitochondri|respiratory|electron transport|oxidative), metabolism (ATP|glycolysis|fatty acid|glucose|metabolism), development (development|differentiation), and epigenetics (epigenetic|chromatin|histone|methylation|acetylation). The top three terms for each category per day/treatment were selected and plotted in a dot plot and heat map of significance of all terms per category was plotted in a heat map using ggplot2.

Benchmark concentration analysis

Benchmark concentration analysis was performed as previously described for female derived RNA sequencing data comparing exposure to 0.5 and 5 µM Pb on days 1, 2, 6, and 15 of differentiation.[16] Gene-specific benchmark concentration and best fit benchmark concentration model were identified using BMDExpress version 3.2, a free software package developed by the National Institute of Environmental Health Sciences (NIEHS) and available for download (https://github.com/auerbachs/BMDExpress-3/releases). Best practices for dose-response modeling for each chemical were conducted according BMDExpress online documentation

(https://bmdexpress-2.readthedocs.io/en/feature-readthedocs/basic_workflow/). Normalized counts per million reads were imported into BMDExpress and prefiltered using one-way analysis of variance (ANOVA) for significance at a *p*-value of <0.05 to identify genes showing significant increasing or decreasing concentration responses. To determine concentration–response relationships, the filtered data were modeled in BMDExpress with hill, power, linear, polynomial (2°, 3°, 4°), and exponential (3 and 5) models and the best fit model was chosen. The benchmark response (BMR) was set to 1 standard deviation relative to control response, maximum iterations of the model was set to 250, a confidence level of 0.95 was used, and power was restricted to ≥1 for the power model. Best fit models were chosen for each concentration–response relationship per gene using nested chi square to select for the best model followed by lowest Akaike information criterion (AIC). Hill models were flagged if its "k" parameter was smaller than one-third of the lowest positive concentration and flagged hill models were included in the data. Directionality in response (upregulated/downregulated) was derived from the "Best adverseDirection" of the winning model for a given gene. Benchmark concentrations with values above the highest tested concentration (5μM) were excluded from individual gene and functional classification analyses. We conducted functional classifications analysis for the three Gene Ontology sets (Biological Process, Molecular Function, and Cellular Compartment) as well as for Reactome pathways. Pathway analysis results were filtered at a significance at a Fisher's exact two-tailed *p*-value of <0.05 for BMDExpress testing. We selected for key words as described above for these pathways, and results were visualized by dot plot using ggplot2. All original expression data, ANOVA filtered results, BMC results, and subsequent BMDExpress analysis for all chemicals are included in a .bm2 file available in the supplemental information link at the end of the chapter.

Optical mapping of action potentials and Ca transients

After cells recovered from purification (beating again throughout each well and matured after 7-10 days), optical mapping of action potentials and Ca transients was performed to measure electrophysiological changes in cells treated with Pb during differentiation. Two different fluorescent dyes were used: for action potentials, FluoVolt™ Membrane Potential Kit (#F10488 Thermo Fisher Scientific, Waltham, MA USA) and for Ca transients, Calbryte 520 AM (#50-224-9887 Thermo Fisher Scientific, Waltham, MA USA). Cardiomyocytes in a 96 well plate (purified as described above) were exposed to each reagent for 30 minutes and washed with HBSS++. After this, optical mapping was performed on a CARTOX/Nautilus plate reader within 5 minutes (Curi Bio, Seattle, WA, USA). Briefly, cells were placed in a motorized, temperature-controlled stage (37°C). This setup contained an LED array equipped with a 470nm excitation filter and an optical diffuser to stimulate dye fluorescence, and a high numerical aperture camera lens with a 525nm band-pass emission filter recorded the resulting fluorescence. Nautilis software purpose-built for the plate reader processed the data, and a custom developed parallel StemBioSys software was used to assess the resulting action potentials and Ca transients in each well (StemBioSys Optical Electrophysiology Analysis Tool (.oeat), StemBioSys, Inc./Southwest Research Institute, San Antonio, Texas, USA).[22] Together, this allows for comprehensive analysis of a range of parameters for both action potentials and Ca transients included in the tables below.

Action potential dynamics parameter descriptions (FluoVolt / Nautilus)

Parameter	**What It Measures**	**Physiological Significance**
Beat Frequency (Hz)	Number of spontaneous action potentials per second.	Reflects the intrinsic pacemaking activity of cardiomyocytes. Higher frequency indicates increased excitability; lower

		frequency reflects slower pacemaking or conduction defects.
Baseline Fluorescence (F0)	Resting membrane potential fluorescence before depolarization.	Indicates the relative resting membrane potential. Shifts suggest altered ion channel activity (e.g., K^+ currents, leak currents) or metabolic stress.
Action Potential Amplitude (dF/F0)	Peak fluorescence change from baseline during depolarization.	Represents the size of depolarization (Na^+ influx and membrane excitability). Larger amplitude = larger depolarization; reduced amplitude may indicate Na^+ channel dysfunction or fewer Na^+ channels
Action Potential Triangulation	Difference between two repolarization phases ($APD_{90} – APD_{30}$).	Indicates the balance of inward vs. outward currents. Increased triangulation is associated with prolongation of QT interval, a pro-arrhythmic risk.
Upstroke Slope	Maximum rate of change in optical signal during depolarization phase	Reflects activity of voltage-gated sodium channels
Conduction Velocity (mm/s)	Speed of action potential propagation across the monolayer.	Determines how rapidly impulses spread, a function of Na+ channels and gap junctions (Cx43). Slowed CV is a high risk for arrhythmias.

Table 4.3: Action potential parameters

Ca dynamics parameter descriptions (Calbryte/Nautilis)

Parameter	What It Measures	Physiological Significance
Beat Frequency (Hz)	Number of spontaneous contractions per second.	Reflects the intrinsic pacemaker activity of cardiomyocytes.
Baseline Fluorescence (F0)	Resting fluorescence intensity before Ca transients.	Indicates resting intracellular Ca levels. Changes suggest altered Ca homeostasis, buffering, or storage within the sarcoplasmic reticulum.

Ca Transient Amplitude (dF/F0)	The peak fluorescence intensity change from baseline during a Ca transient.	Represents the amount of Ca released from the sarcoplasmic reticulum, essential for contraction strength. Higher amplitude = stronger contraction.
Ca Transient Upstroke Slope	The rate of Ca influx into the cytoplasm during the transient.	Indicates the efficiency of Ca entry via L-type Ca channels and sarcoplasmic reticulum (RyR2) Ca release.
Ca Transient 80% Recovery (s)	Time taken for Ca levels to return to 80% of baseline after peak.	Indicates the balance between Ca influx and clearance. Prolonged recovery suggests impaired relaxation and may contribute to arrhythmias.
Ca Transient Triangulation	A measure of transient shape, calculated as the difference between time-to-peak and recovery duration.	Reflects Ca clearance mechanisms, including reuptake into the sarcoplasmic reticulum (via SERCA2) and extrusion via NCX.
Conduction Velocity (mm/s)	Speed of electrical signal propagation through the cardiomyocyte monolayer.	Determines how quickly electrical impulses spread.

Table 4.4: Ca transient parameters

4.4: Results

DNMT, TET, and pluripotency marker expression changes in a cell line specific manner in iPSCs exposed to human relevant doses of Pb

To determine how Pb may disrupt epigenetics and pluripotency at baseline, which could influence subsequent differentiation, cells were treated with a range of human relevant doses of Pb for 72 hours. These cells showed decreases in *DNMT3A* nearing significance in both cell lines with increasing Pb exposure, a significant decrease in *DNMT3B* only at 1.6 μM only in the female cell line, significant decreases in *NANOG* only in the female cell line at 0.4 and 1.6 μM, a significant decrease in *SOX2* in the female cell line at 1.6 μM (with a decrease approaching significance in the male cell line), a significant decrease in *TET1* at 0.4 μM in the male cell line

and 0.8 and 1.6 µM in the female cell line, and a significant decrease in *TET3* only in the female cell line at 1.6 µM (**Figure 4.2**).

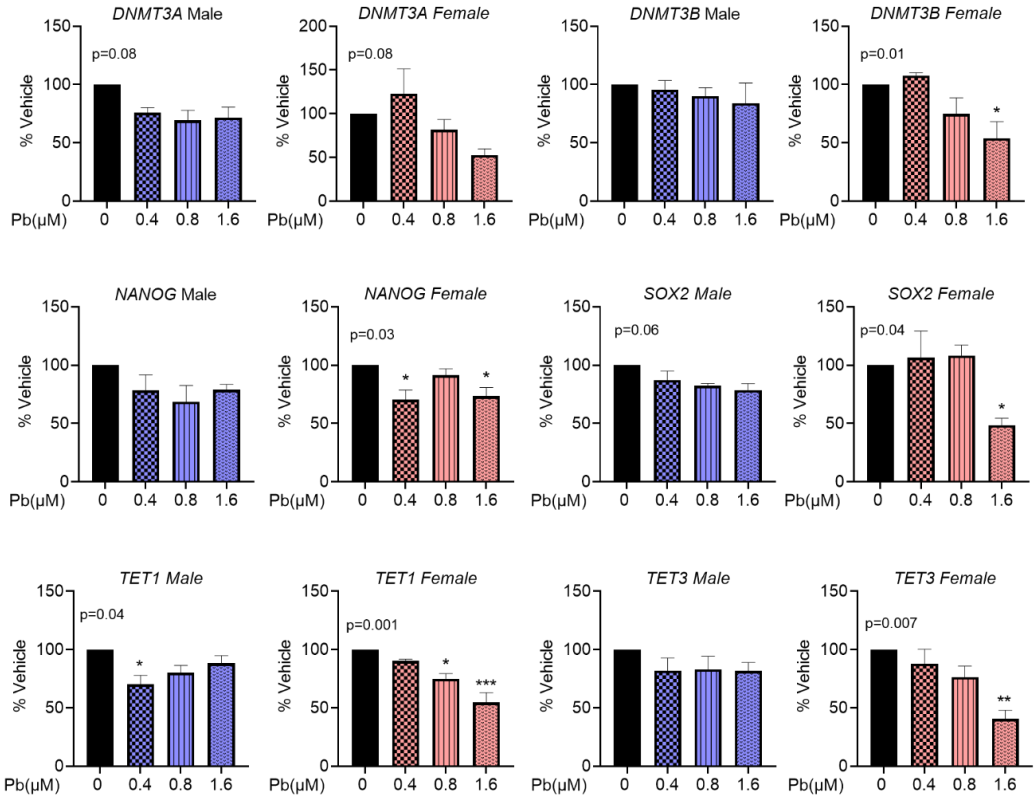


Figure 4.2: Epigenetic and pluripotency marker changes in iPSCs exposed to Pb. Undifferentiated female and male derived hiPSCs were exposed to a range of Pb doses for 3 days and showed cell line-specific differences in *DNMT*, *TET*, and pluripotency markers *NANOG* and *SOX2* (n=3 per cell line per treatment; % Vehicle indicates percent change in relative gene expression normalized to 0 µM Pb; one way ANOVA).

DNMT and TET expression is dynamic throughout differentiation and appears similar between different cell lines

DNMT and *TET* expression changes were also assessed for cells that underwent exposure to Pb during the first 8 days of differentiation in both cell lines. No effects of Pb were seen

(**Supplemental Figure 4.17**), but similar patterns in *DNMT* and *TET* expression changes were observed throughout differentiation, with a marked decrease in *DNMT3B* between days 6 and 15 in both cell lines (**Figure 4.3**).

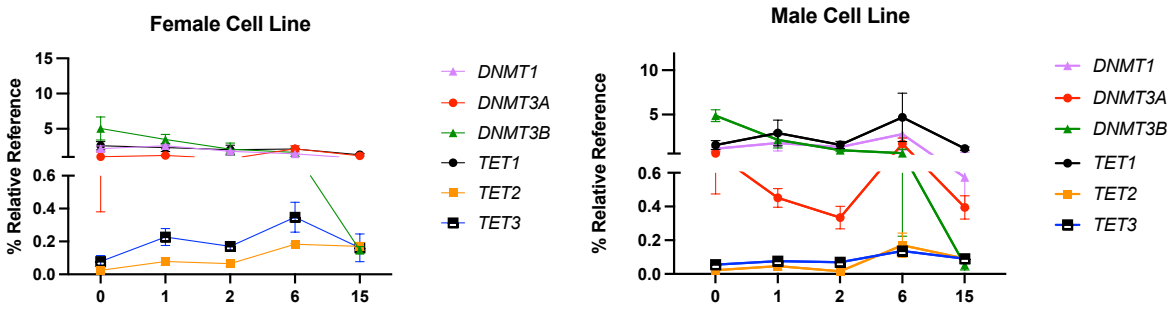


Figure 4.3: *DNMT* and *TET* expression changes throughout differentiation.

Female and male patient-derived iPSCs differentiating into ventricular cardiomyocytes (days 0-15 of protocol in **Figure 4.1**) showed similar patterns of *DNMT* and *TET* transcript expression (n=3 per cell line; % relative reference indicates relative gene expression normalized to housekeeping genes).

PIWIL expression is dynamic during development but is not impacted by Pb exposure

For both cell lines at days 0-15 of differentiation, transcript expression of all four human *PIWIL*s was examined, but only *PIWIL*s *2* and *4* showed expression in these cells (**Figure 4.4**). No significant expression differences were found between control and Pb exposure at any day, although D15 in the male cell line had p-values of 0.15 and 0.15 for each dose of Pb showing a trend towards decreased *PIWIL4* expression (**Figure 4.4**). Notably, *PIWIL2* significantly declined throughout differentiation between days 0 and 15, and *PIWIL4* showed a significant increase in the female line between days 6 and 15 and in the male line between days 0 and 15 (**Figure 4.4**).

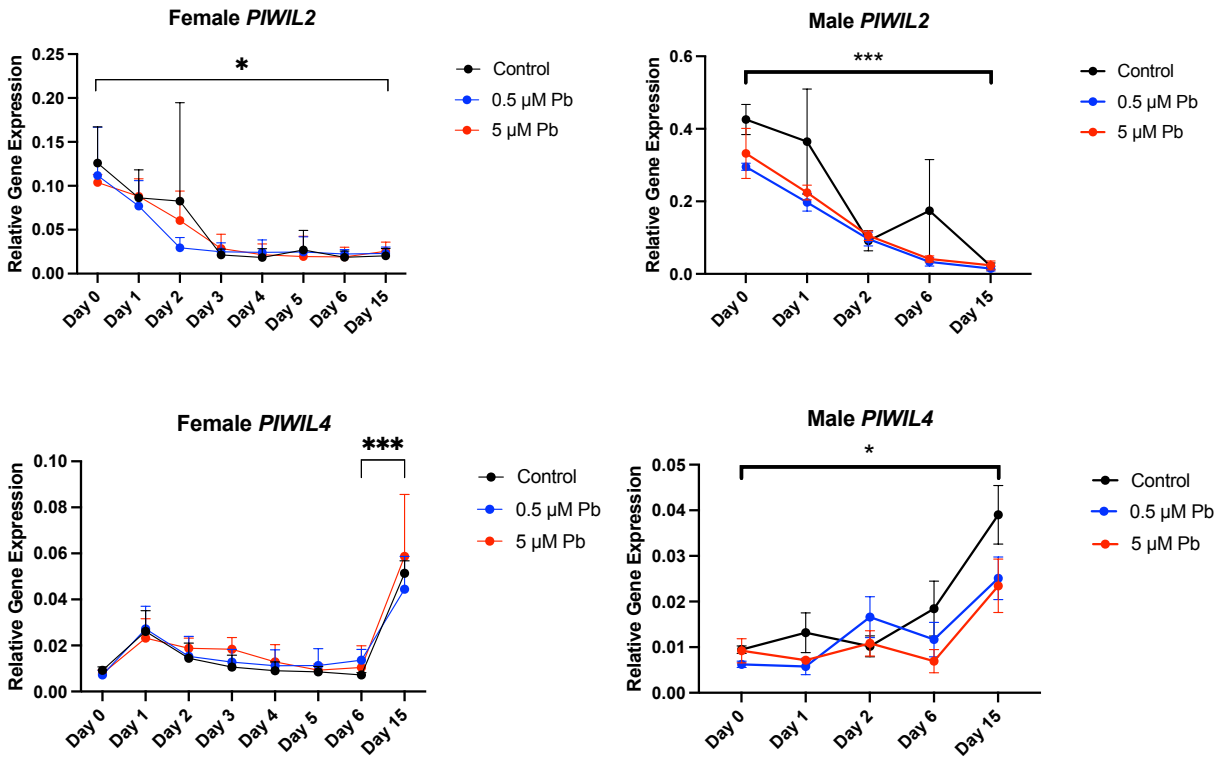
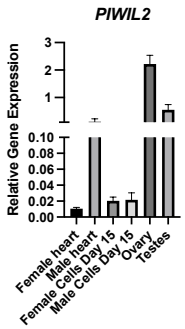


Figure 4.4: *PIWIL* expression is dynamic throughout differentiation in both cell lines.

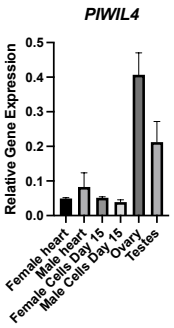
Both female and male cell lines were examined for PIWIL expression throughout differentiation, with zero or very little expression of *PIWIL*s *1* and *3* found for these samples (data not shown), and dynamic expression of *PIWIL2* and *4* found throughout differentiation but unchanged with exposure to Pb (female: *PIWIL2*: 6 fold decrease between D0 and D15, p-value of 0.01; *PIWIL4*: 7 fold increase between D6 and D15, p-value 0.0002; male: *PIWIL2*: 20 fold decrease between D0 and D15, p-value of 0.0007; *PIWIL4*: 4 fold increase between D0 and D15, p-value of 0.01; n=3 per cell line per treatment).

Comparison of PIWIL levels in Day 15 ventricular cardiomyocytes to immature human heart samples

Gestational day 90-105 male and female immature heart samples show similar expression of *PIWIL*s *2* and *4* as day 15 cell samples in both cell lines (**Figure 4.5** no significant differences by one-way ANOVA). Fetal ovaries, on the other hand, show significantly higher expression of both *PIWIL*s compared to fetal heart cells and day 15 ventricular cardiomyocytes (one-way ANOVA; **Figure 4.5**).



Tukey's multiple comparisons test	
Female heart vs. Male heart	ns
Female heart vs. Female Cells Day 15	ns
Female heart vs. Male Cells Day 15	ns
Female heart vs. Ovary	****
Female heart vs. Testes	ns
Male heart vs. Female Cells Day 15	ns
Male heart vs. Male Cells Day 15	ns
Male heart vs. Ovary	****
Male heart vs. Testes	ns
Female Cells Day 15 vs. Male Cells Day 15	ns
Female Cells Day 15 vs. Ovary	****
Female Cells Day 15 vs. Testes	ns
Male Cells Day 15 vs. Ovary	****
Male Cells Day 15 vs. Testes	ns
Ovary vs. Testes	****



Tukey's multiple comparisons test	
Female heart vs. Male heart	ns
Female heart vs. Female Cells Day 15	ns
Female heart vs. Male Cells Day 15	ns
Female heart vs. Ovary	***
Female heart vs. Testes	ns
Male heart vs. Female Cells Day 15	ns
Male heart vs. Male Cells Day 15	ns
Male heart vs. Ovary	***
Male heart vs. Testes	ns
Female Cells Day 15 vs. Male Cells Day 15	ns
Female Cells Day 15 vs. Ovary	**
Female Cells Day 15 vs. Testes	ns
Male Cells Day 15 vs. Ovary	***
Male Cells Day 15 vs. Testes	ns
Ovary vs. Testes	ns

Figure 4.5: Comparison of *PIWIL* expression levels between human immature heart samples and iPSC-derived ventricular cardiomyocytes.

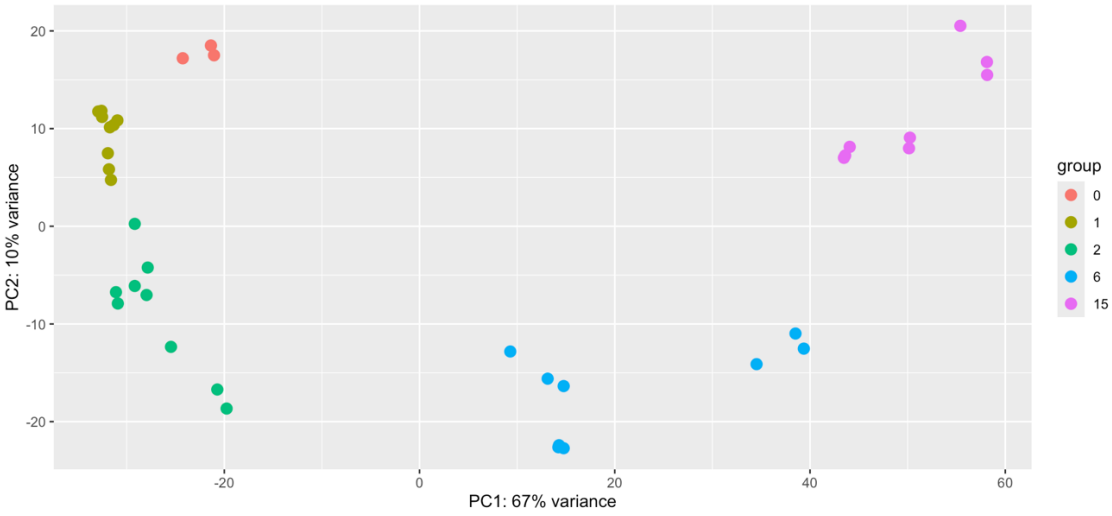
PIWIL levels were compared in immature human heart and gonadal RNA extracted from samples on gestational day 90-105 (n=5 per sex per tissue) to day 15 cardiomyocytes derived from one female and one male iPSC line (n=3 per cell line), and no significant differences were found between fetal heart samples and cells of either sex, while ovaries showed significantly higher expression of both *PIWIL*s compared to fetal heart and cell samples.

PCA plots show clustering by day of differentiation and replicate but not by Pb treatment

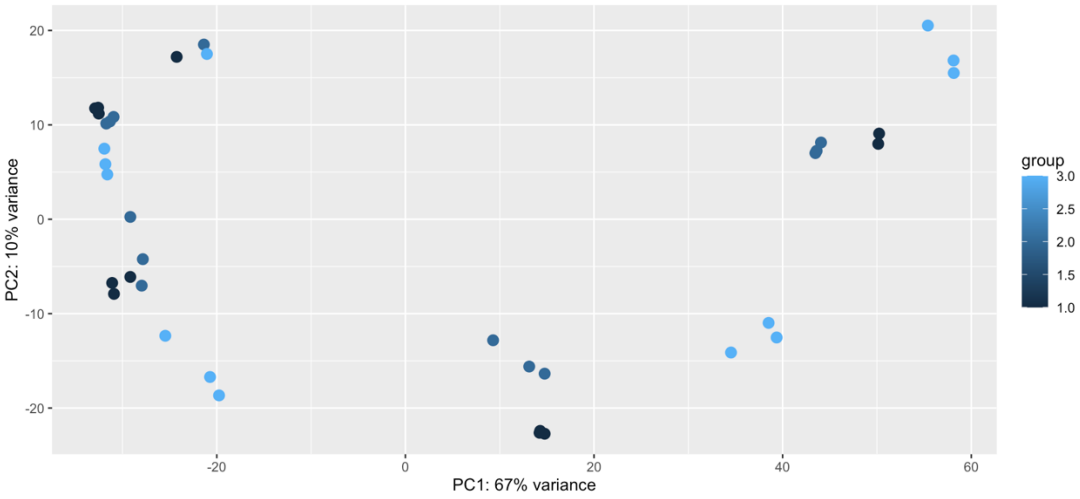
To examine gene and pathway changes, RNA sequencing was conducted for female iPSCs undergoing differentiation into ventricular cardiomyocytes on days 0, 1, 2, 6 and 15 of differentiation (n=3). Principal component analysis (PCA) plots were made across all days of

differentiation and all treatments, and showed clustering by day (**Figure 4.6A**) and replicate (**Figure 4.6B**), but not by Pb treatment (**Figure 4.6C**).

A: Day of Differentiation



B: Replicate Number



C: Pb Treatment

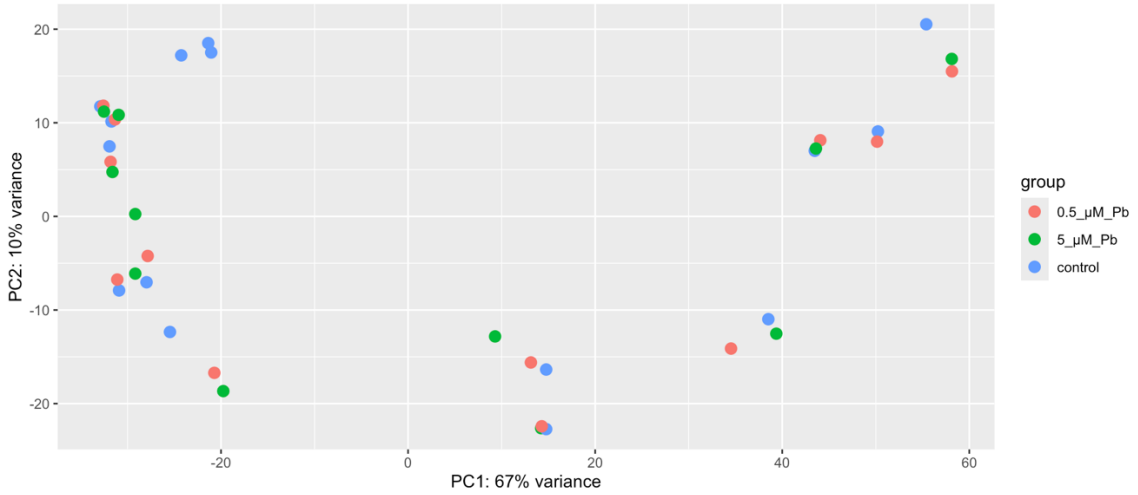


Figure 4.6: PCA plots reveal clustering by day and replicate number but not by Pb treatment.

PCA analyses for RNA sequencing data of female iPSCs undergoing differentiation into ventricular cardiomyocytes were plotted so each day (0, 1, 2, 6, 15) appears in a different color (A), replicate number (1, 2, or 3) in a different shade of blue (B), and Pb treatment (0, 0.5, 5 µM) in a different color (C) (n=3 per treatment).

Pb induces differential gene expression throughout differentiation

DESeq2 was run separately for each day, comparing Pb exposure to control for each day. We found a dynamic set of differentially expressed genes (padj > 0.05) on different days and treatments (**Table 4.S1**). Interestingly, 5 µM Pb showed the greatest number of differentially expressed genes, with day 6 showing 77 genes up or downregulated compared to control (**Table 4.5**). **Figure 4.7** shows overlaps in DEGs between all days and doses examined. Notably, the two DEGs overlapping between days 2 and 6 are *CCKBR* and *FOXA2*.

	D1_0.5	D1_5	D2_0.5	D2_5	D6_0.5	D6_5	D15_0.5	D15_5
Total	16	23	2	19	0	77	0	6
Up	8	11	0	1	0	7	0	0
Down	8	12	2	18	0	70	0	6
Overlap between 0.5 and 5μM	NA	8	NA	0	NA	NA	NA	NA

Table 4.5: Differentially expressed genes by Pb exposure in female iPSCs undergoing differentiation into ventricular cardiomyocytes.

Differentially expressed genes identified using DESeq2 with a padj cutoff of 0.05 for 4 days of differentiation (1, 2, 6, and 15) and 2 doses of Pb (0.5 and 5 μM) for cells treated during the first 8 days of differentiation. Overlap between 0.5 and 5 μM doses within the same day are shown in the last row.

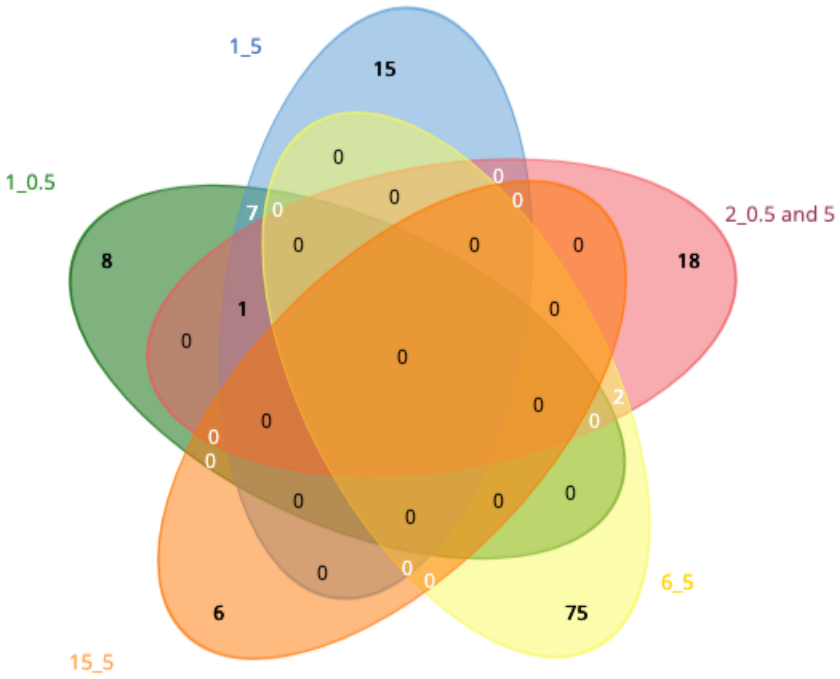


Figure 4.7: Overlap in DEGs by day and dose.

Venn diagram showing overlaps in DEGs by day and dose, with day 2 combined (no DEGs overlapped between day 2 for 0.5 and 5 μM).

Gene ontology analysis reveals Pb associated pathway perturbations dynamic throughout differentiation

We next wanted to investigate the pathways impacted by Pb exposure during differentiation of our female cell line using differential expression data. Inputting p-value and fold change DESeq2 data into LRPath, a function which uses logistic regression to test for enriched or depleted biological categories, we tested for gene sets GOBP (biological processes), GOMF (molecular function) and GOCC (cellular compartment) in our data and selected significantly altered pathways (FDR <0.05; all results shown in **Table 4.S2**). **Table 4.6** displays the top 30 unbiased pathways across all doses and days for all three analyses, and including repeats in

pathways between days/doses, 18/30 pertain to ribosomal function, while 8/30 pertain to mitochondrial pathways or function. Relevant cardiac, developmental, epigenetic, metabolic, and mitochondrial terms were further selected for our data and the top three terms for each day/treatment are shown in **Figure 4.8**. Interestingly, pathways related to cardiac differentiation were found to be changed by Pb exposure in later stages of differentiation (striated muscle cell tissue development for 5 μM on day 15, stem cell differentiation for 5 μM on day 6, and cardiocyte differentiation for 0.5 μM on day 6; **Figure 4.8A**). Heat maps of mean p-values for each pathway reveal dynamic pathway regulation throughout differentiation, with highly significant changes in mitochondrial pathways on days 1, 6 and 15, but not on day 2 (**Figure 4.8B**).

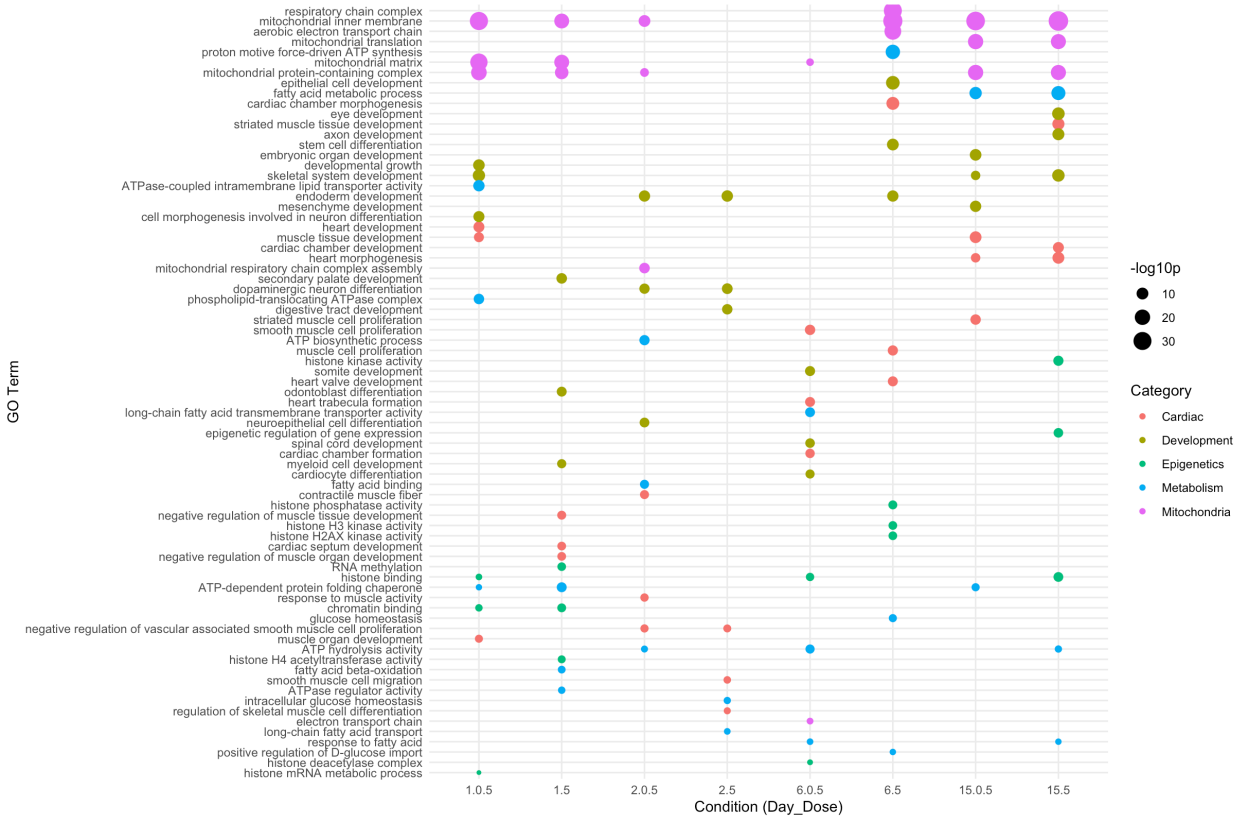
Description	**Day**	**Dose (μM)**	**FDR**
ribosomal subunit	1	0.5	3.81E-59
structural constituent of ribosome	1	0.5	6.67E-57
translation	1	0.5	1.59E-54
ribonucleoprotein complex biogenesis	1	0.5	7.94E-52
structural constituent of ribosome	6	5	2.05E-49
ribosomal subunit	6	5	1.19E-47
cytosolic ribosome	6	5	2.10E-42
ribosomal subunit	15	0.5	2.98E-37
mitochondrial inner membrane	15	5	3.96E-35
ribosomal subunit	1	5	1.20E-33
mitochondrial inner membrane	6	5	2.35E-33

structural constituent of ribosome	15	0.5	9.18E-32
mitochondrial inner membrane	15	0.5	3.40E-31
ribosomal subunit	15	5	3.64E-31
mitochondrial inner membrane	1	0.5	1.28E-29
cytoplasmic translation	6	5	1.64E-29
rRNA metabolic process	1	0.5	1.75E-29
respiratory chain complex	6	5	1.58E-28
structural constituent of ribosome	1	5	2.86E-28
mitochondrial matrix	1	0.5	3.28E-26
structural constituent of ribosome	15	5	4.33E-25
cell-cell junction	6	5	1.31E-24
spliceosomal complex	1	0.5	3.62E-24
translation	1	5	4.76E-24
RNA splicing, via transesterification reactions with bulged adenosine as nucleophile	1	0.5	7.56E-24
aerobic electron transport chain	6	5	1.98E-23
ATP synthesis coupled electron transport	6	5	2.33E-23
angiogenesis	6	5	3.24E-23
ribonucleoprotein complex biogenesis	1	5	5.05E-22
preribosome	1	0.5	4.06E-20

Table 4.6: Unbiased top 30 GOBP, GOMF, and GOCC pathway alterations across days and doses.

The top 30 pathways ranked by FDR for the LRPath results for GOBP, GOCC, and GOMF for days 1, 2, 6, and 15 of ventricular differentiation with two doses of Pb (0.5 and 5 µM).

A



B

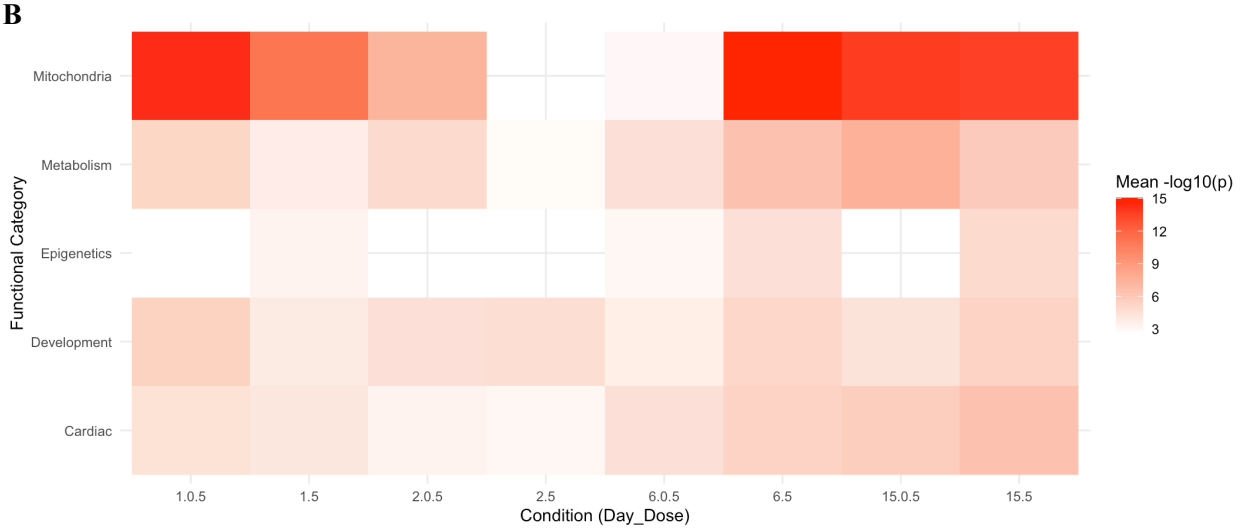


Figure 4.8: Pathways related to important cardiac processes were altered by Pb exposure in iPSCs from a female patient differentiating into ventricular cardiomyocytes.

LRPath results for GOBP, GOCC, and GOMF divided into the top 3 terms for cardiac, development, epigenetics, metabolism, and mitochondria relevant categories for days 1, 2, 6, and 15 of ventricular differentiation with two doses of Pb (0.5 and 5 μM). Dot plots of these pathways with size of dot representing -log10(p-value) and color corresponding to each category (A). Heat map of mean(-log10(p-value)) for each category (B).

Benchmark concentration modeling reveals unique gene and pathway expression patterns throughout differentiation at similar benchmark concentrations

To understand at which level of Pb exposure induces a meaningful gene expression or pathway responses during differentiation into ventricular cardiomyocytes, we performed benchmark concentration (BMC) modeling. This approach, detailed in the Methods section, fits dose–response models to expression data from our two Pb exposure concentrations and a control. It then determines a benchmark concentration at which there is benchmark response at a change equal to 1 standard deviation (SD) above or below the mean expression level in the control group**.** Genes with modeled responses meeting this BMR and showing statistically significant model fits (p-value <0.05) were retained for downstream analysis. Benchmark concentration modeling using BMDExpress3.2 on our RNA-Seq data for female derived iPSCs differentiating into cardiomyocytes revealed that of all genes altered in a benchmark response, there were similar median benchmark concentrations (BMCs) between days of differentiation of around 0.2 μM (**Figure 4.9** and **Table 4.7**). Further, each day showed differences in the total number of genes dysregulated and those that were upregulated or downregulated (**Table 4.8**), with no

overlap between days in the genes showing a benchmark concentration relationship (**Figure 4.10**).

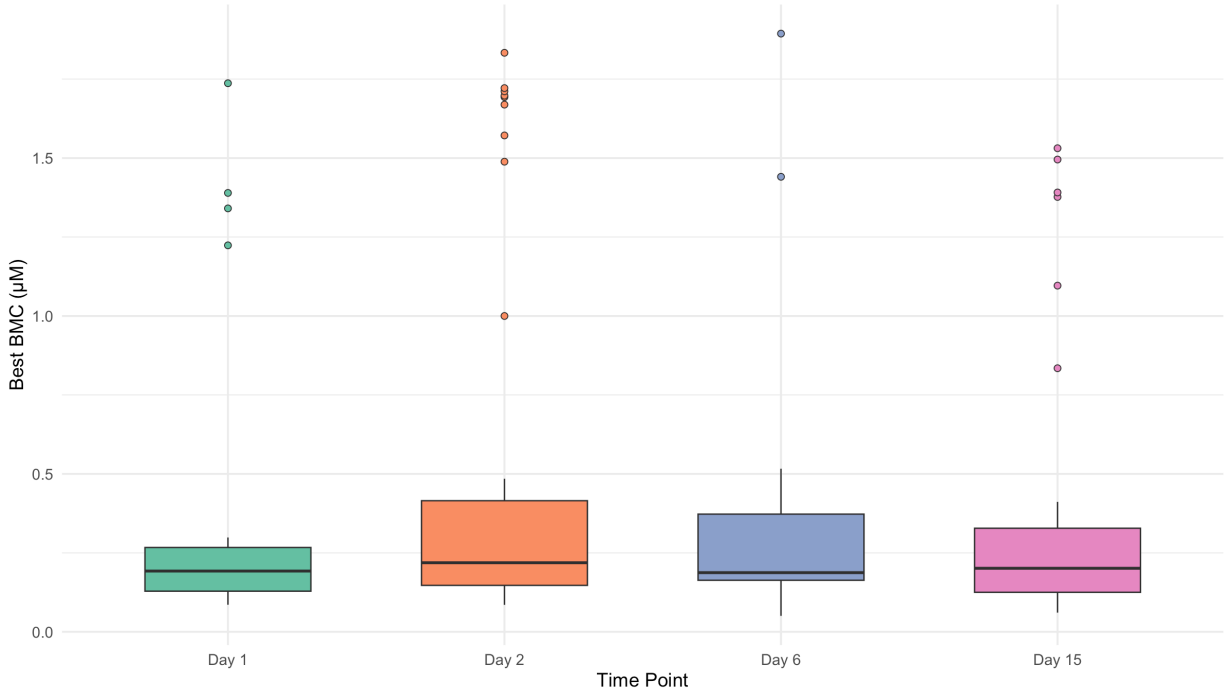


Figure 4.9: Best BMC across days of differentiation.

The best BMCs for each day of differentiation (1, 2, 6, and 15) were chosen for the best fit model for each concentration–response relationship per gene for a benchmark response (BMR) was set to 1 standard deviation relative to control response. Each boxplot (per day) represents all genes showing a benchmark response.

Day	**Median BMC (µM)**
1	0.19
2	0.22
6	0.19

15	0.20

Table 4.7: Median BMCs per day.

Median BMCs across all genes per day of differentiation.

Day	Downregulated	Upregulated	Total
1	10	18	28
2	23	25	48
6	5	8	13
15	14	17	31

Table 4.8: Upregulated and downregulated BMC genes per day.

Genes fitting a benchmark concentration response with directionality in response (upregulated/downregulated) derived from the “Best adverseDirection” of the winning model for a given gene.

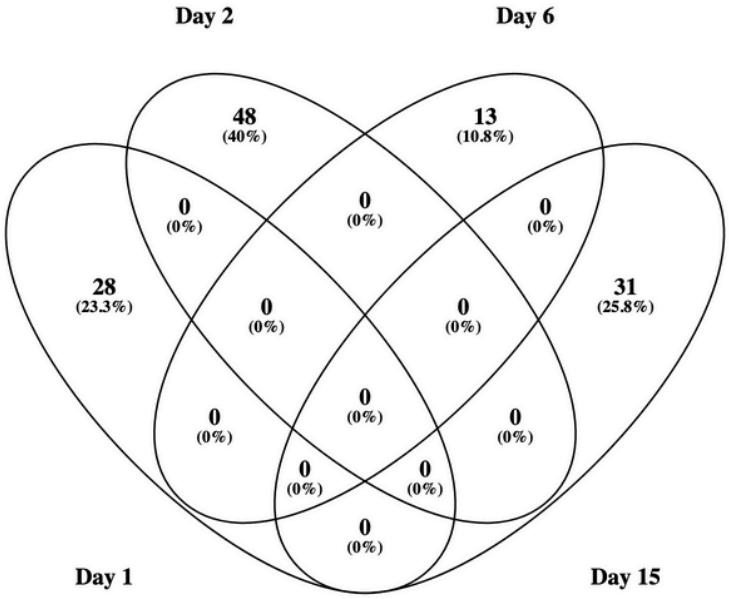


Figure 4.10: Overlap in BMC genes per day of differentiation.

Venn diagram of genes with a benchmark response made by Venny 2.1.0.

We further carried out functional classifications analysis on BMC data for the three Gene Ontology sets (Biological Process, Molecular Function, and Cellular Compartment) and for Reactome pathways. Accumulation plots were created to visualize the progressive increase in the number of potentially dysregulated pathways or gene sets exhibiting benchmark responses across Pb concentrations per day, showing how exposure level relates to the number of pathways affected (**Figure 4.11)**. This data was filtered at a significance at a Fisher's exact two-tailed p-value of < 0.05, all pathways are presented in **Table 4.S3**, and the top 30 terms across days are shown in **Table 4.9**. Key words were selected for as described above (cardiac, development, epigenetics, metabolism, and mitochondria). This selected data was plotted, showing changes only on days 1, 2, and 6, and notably showing downregulation of pathways cardiac myofibril assembly, muscle cell proliferation, and striated muscle cell proliferation for day 2 (**Figure 4.12**).

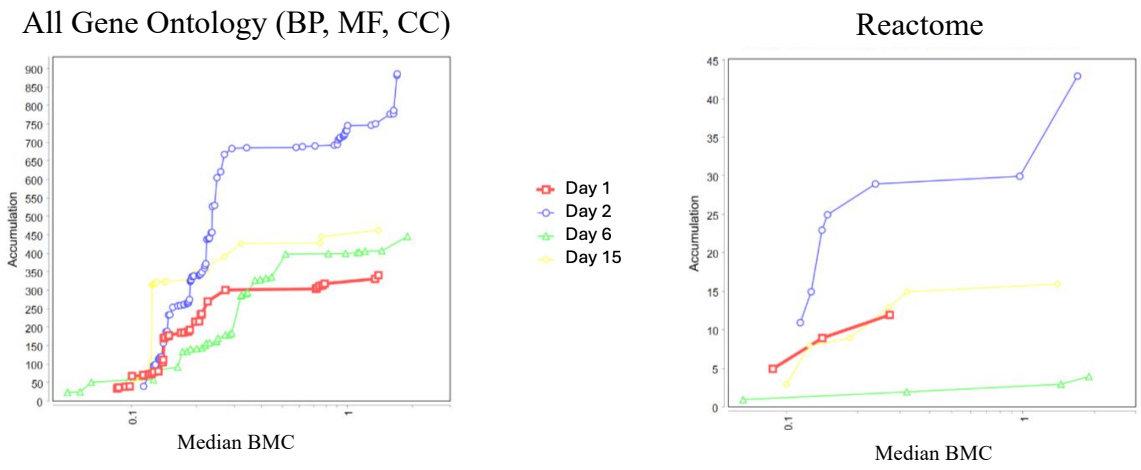


Figure 4.11: Accumulation plots for all GO (BP, MF, and CC) and Reactome pathways per day of differentiation.

BP = biological processes; MF= molecular function; CC= cellular compartment. Day 1 shown in red, day 2 shown in blue, day 6 shown in green, and day 15 shown in yellow.

Description	Fisher's Exact Two Tail	Overall Direction	Day
positive regulation of cytokine production	1.06E-04	DOWN	2
intracellular zinc ion homeostasis	1.24E-04	UP	15
positive regulation of lymphocyte migration	1.90E-04	CONFLICT	15
axonemal dynein complex	2.15E-04	DOWN	2
regulation of type I interferon production	2.61E-04	DOWN	2
regulation of lymphocyte migration	5.00E-04	CONFLICT	15
positive regulation of interferon-beta production	7.19E-04	CONFLICT	2

axonemal dynein complex assembly	7.19E-04	DOWN	2
Defective SLC5A5 causes thyroid dyshormonogenesis 1 (TDH1)	9.04E-04	UP	2
positive regulation of mononuclear cell migration	9.13E-04	CONFLICT	15
integrin-mediated signaling pathway	9.53E-04	CONFLICT	15
uropod organization	9.96E-04	UP	15
sodium:iodide symporter activity	9.96E-04	UP	2
cellular response to Thyroid stimulating hormone	9.96E-04	UP	2
dynein complex	0.0013085	DOWN	2
regulation of cytokine production	0.0013331	DOWN	2
3'-tRNA processing endoribonuclease activity	0.0013945	DOWN	1
thymocyte migration	0.0014939	UP	15
regulation of interferon-beta production	0.0015599	CONFLICT	2
response to type II interferon	0.0016712	DOWN	6
Drug-mediated inhibition of MET activation	0.0018082	DOWN	2
RAS signaling downstream of NF1 loss-of-function variants	0.0018984	DOWN	1
negative regulation of vesicle fusion	0.0019915	UP	15
response to erythropoietin	0.0019915	UP	15
cellular response to erythropoietin	0.0019915	UP	15
plasmacytoid dendritic cell differentiation	0.0019919	DOWN	2

iodide transmembrane transport	0.0019919	UP	2
response to Thyroid stimulating hormone	0.0019919	UP	2
regulation of mononuclear cell migration	0.0021547	CONFLICT	15
DNA-binding transcription repressor activity, RNA polymerase II-specific	0.002173	DOWN	2

Table 4.9: Top 30 GO Terms for BMC modeled data. `

The top 30 pathways ranked by Fisher's Two Tailed Exact p-value for the results for GOBP, GOCC, GOMF, and Reactome for days 1, 2, 6, and 15 of ventricular differentiation, including overall direction of regulation of the effect (UP, DOWN, or CONFLICT).



Figure 4.12: BMC modeled selected pathway changes.

Using pathway data for GO and Reactome, pathways related to cardiac, developmental, epigenetic, metabolic, and mitochondrial responses were selected for and plotted. Size of dot indicates relative significance (-log10(p-value)), with bigger circles indicating greater statistical

significance. Color indicates upregulation (orange), downregulation (blue) or conflict (both; yellow).

Exposure to Pb during differentiation affects cardiac action potentials in female and male cell lines

To connect the above transcriptional changes induced by Pb exposure to functional consequences on ventricular cardiomyocyte biology, we performed optical mapping of action potentials and Ca transients to examine changes electrophysiology induced by Pb exposure. Two cell lines were examined that were treated with 0.5 and 5 μM Pb during the first 8 days of differentiation, matured until day 10-15, purified, and recovered from purification and allowed to additionally mature for another 7-10 days. Therefore, upon optical mapping cells had not been exposed to Pb for 9-17 days.

Beat frequency, or the number of action potentials per second (Hz) was significantly upregulated at 5 μM Pb exposure during differentiation in the female line but downregulated at 0.5 μM Pb exposure in the male line (**Figure 4.13A**). Action potential duration triangulation (APD Triangulation), or the repolarization time, was increased in the female line at 5 μM Pb and increased in the male line at 0.5 μM Pb only (**Figure 4.13B**). Significant decreases in change in action potential amplitude (dF/F0; both doses) and upstroke slope (depolarization rate of change; 5 μM only) were observed in the male line only (**Figure 4.13C**). These parameters are defined in detail in **Table 4.3**.

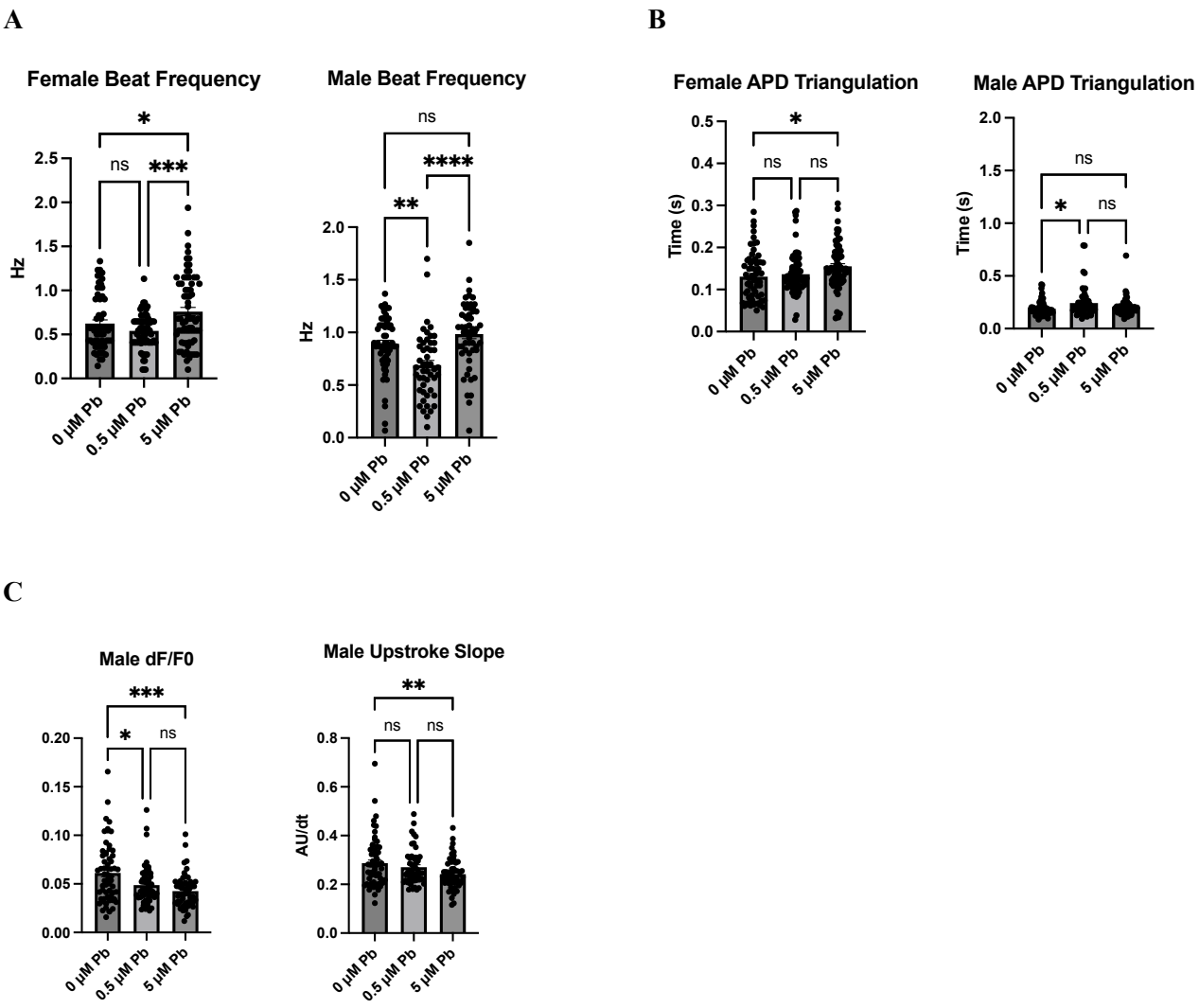
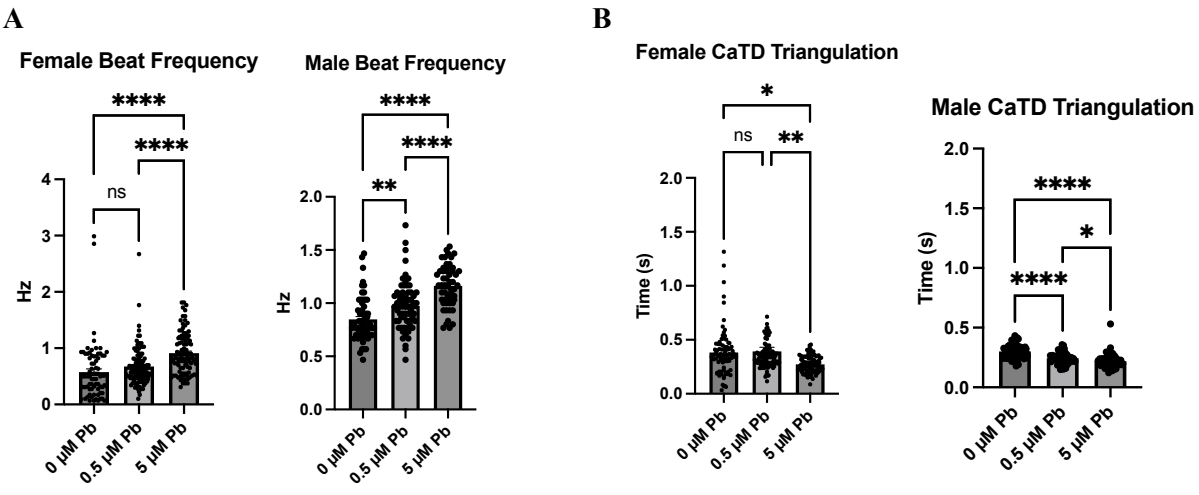


Figure 4.13: Action potential changes in female and male iPSC-derived ventricular cardiomyocytes treated with Pb during differentiation.

Significant changes in beat frequency (A) and APD Triangulation (B) were observed for both cell lines, while significant changes in dF/F0 and upstroke slope were observed for only the male line (n= 3 female and n=4 male replicates; one-way ANOVA; * p-value < 0.05, ** p-value < 0.01, *** p-value < 0.001, **** p-value < 0.0001).

Exposure Pb during differentiation affects cardiac Ca transients in female and male cell lines

Ca transient beat frequency, or the number of contractions per second, was significantly upregulated at both doses of Pb in both cell lines (**Figure 4.14A**). Ca transient duration triangulation (CaTD Triangulation) measures how efficiently Ca is cleared vs influx of Ca, specifically reflecting the kinetics of SERCA-mediated reuptake of Ca into the sarcoplasmic reticulum (SR) and the efflux via the Na/Ca exchanger. Longer or more triangulated CaTDs suggest slower Ca clearance, whereas shorter or more rectangular transients indicate more efficient Ca cycling. CaTD Triangulation was decreased in the female line at 5 µM and decreased in the male line both doses (**Figure 4.14B**). Also measuring Ca clearance, Ca Transient Duration at 80% Recovery (CaTD80) showed a significant decrease compared to control in the male cell line at both doses, and a significant decrease comparing 0.5 µM to 5 µM in the female cell line (**Figure 4.14C**). Other changes were observed included a significant increase in beat frequency standard deviation (Hz SD) at 5 µM in the female-derived cell line and significant decreases in the male line only at 5 µM in change in Ca transient amplitude (dF/F0) and upstroke slope (rate of Ca influx) (**Figure 4.14D**).



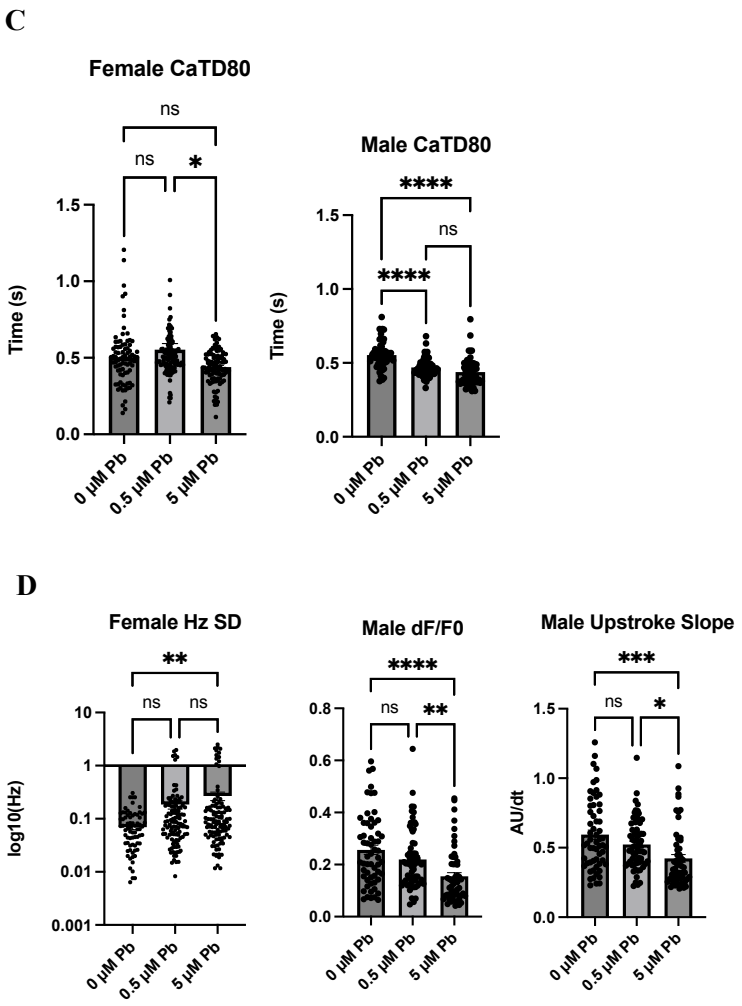


Figure 4.14: Ca transient changes in female and male iPSC-derived ventricular cardiomyocytes treated with Pb during differentiation.

Significant changes in beat frequency (A) and CaTD Triangulation (B), and CaTD80 (C) were observed for both cell lines, while significant changes in Hz SD was observed for the female cell line only and dF/F0 and upstroke slope changes were observed for only the male line (n= 4 female and n=3 male replicates; one-way ANOVA; * p-value < 0.05, ** p-value < 0.01, *** p-value < 0.001, **** p-value < 0.0001).

Differences in changes in action potential and Ca transient characteristics induced by Pb exposure during differentiation

Conduction velocity was evaluated for both action potentials as well as Ca transients in both cell lines (**Figure 4.15)**. Interestingly, in the female line there was a significant decrease in median conduction velocity for action potentials at both doses but not Ca transients, and in the male line there was a decrease in median conduction velocity at 0.5 μM for action potentials but an increase in conduction velocity at both doses for Ca transients.

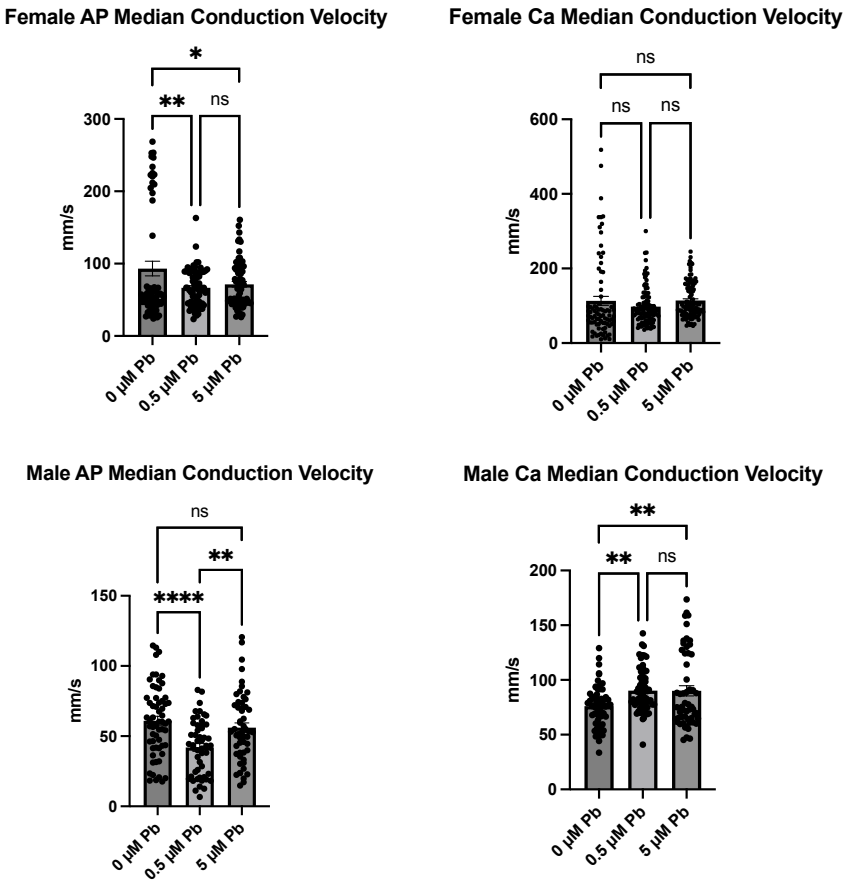


Figure 4.15: Comparison of median conduction velocity changes for each cell line for action potentials and Ca transients.

Significant changes in median conduction velocities across cell lines and doses of Pb exposure (n= 3-4 per cell line per parameter; one-way ANOVA; * p-value < 0.05, ** p-value < 0.01, *** p-value < 0.001, **** p-value < 0.0001).).

No significant Pb-induced ECC gene alterations in iPSC-derived ventricular cardiomyocytes

Given the changes in optical mapping shown above, changes in excitation-contraction coupling (ECC) genes were assessed by qRT-PCR. Four ECC genes assessed were: *ATP2A2* (SERCA2), which transports Ca from cytosol into sarcoplasmic reticulum, *CACNA1C* (Cav1.2) which transports Ca into cytosol, *RYR2* (ryanodine receptor), which transports Ca from sarcoplasmic reticulum into the cytosol, and *SLC8A1* (Na Ca exchanger) which transports Ca out of the cell. None of these genes showed any significant changes in either cell line across both doses of Pb exposure as unpurified (day 15) ventricular cardiomyocytes (**Figure 4.16**).

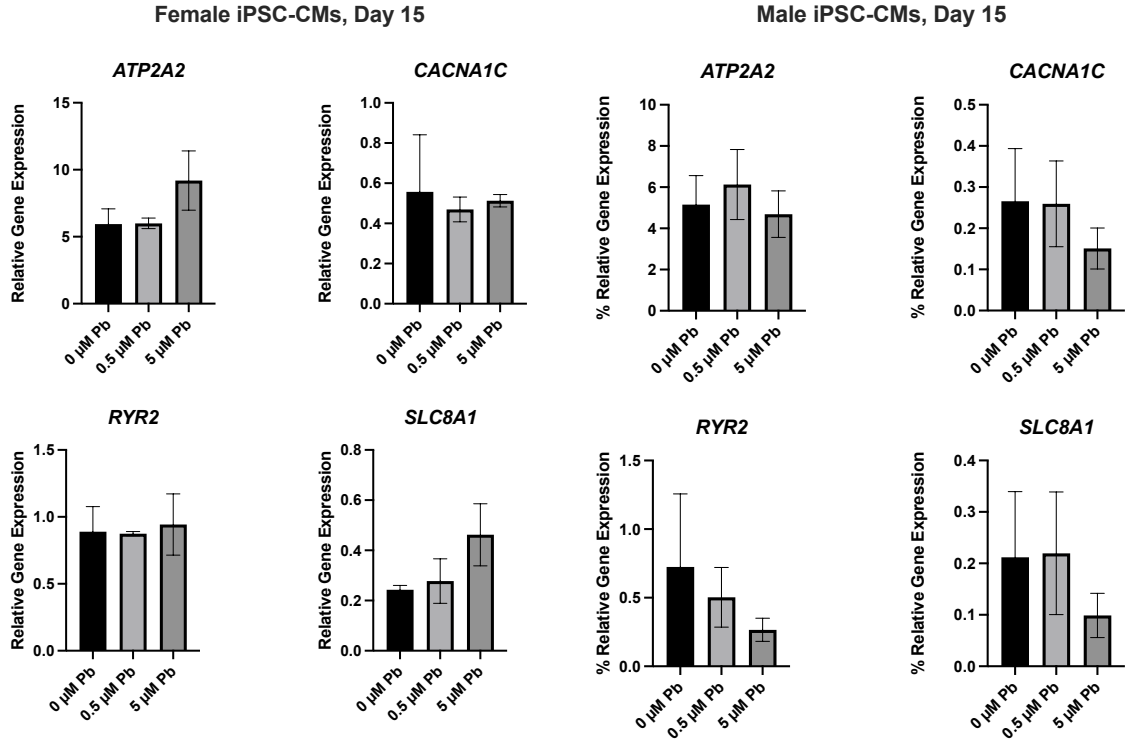


Figure 4.16: No Pb induced changes in ECC genes observed for either cell line at day 15 of differentiation.

For ECC genes *ATP2A2*, *CACNA1C, RYR2*, and *SLC8A1*, no significant changes were observed at day 15 of differentiation for either female or male cells treated with 0.5 and 5 μM Pb during the first 8 days of differentiation (n = 3 per cell line per treatment; one-way ANOVA p-value < 0.05).

4.5: Discussion

Epigenetic machinery in iPSC-derived ventricular cardiomyocytes is regulated by Pb

We found cell line specific changes in pluripotency markers and certain epigenetic regulators (*DNMT*s and *TET*s) after 72 hours of Pb (0.4-1.6 μM) in undifferentiated iPSCs (**Figure 4.2**), which corresponds to previous literature finding that 24 hours of Pb exposure at 0.5 μM to 2.5 μM altered expression of pluripotency factors in mouse ESCs and Pb exposure at 0.8 and 1.5 μM altering global 5hmC in human ESCs.[2,3] Future work should expose cells to Pb pre-differentiation only (rather than throughout) and examine how it alters trajectory of differentiation, and if these changes in expression persist, cause disruption in DNA methylation, and cause changes in cardiomyocyte function.

Upon differentiating iPSCs and treating them with Pb throughout the first 8 days of differentiation, we found no changes in *DNMT*, *TET*, or *PIWIL* expression in either cell line on any day examined, although this expression was dynamic throughout differentiation in both cell lines, highlighting the potential roles these genes may play in determining cell fate (**Supplemental Figure 4.17**, **Figure 4.3** and **Figure 4.4**). Interestingly, a marked decrease in *DNMT3B* was shown between days 6 and 15 in both cell lines supports existing work that

suggests *DNMT3B* is expressed highly in early cardiac progenitors but decreases in expression as cardiomyocytes mature.[23] Also of note for this body of work, one piRNA, piRNA-6426, has been found to work with DNMT3B to methylate *SOAT1* and thereby inhibit hypoxia-induced cardiomyocyte dysfunction and potentially improve heart failure.[24] While no Pb induced changes in *DNMT3B* expression were shown here, additional work is warranted to understand *DNMT3B*'s potential role in cardiac processes, and how Pb exposure may alter its protein expression or functionality.

The *PIWIL* expression changes throughout differentiation shown here (**Figure 4.4**) correlate to those found in a previous study in hESCs which discovered a downregulation in *PIWIL2* and upregulation of *PIWIL4* as cells shift from pluripotent into cardiac progenitor cells.[25] Further, the *PIWIL* levels in iPSC derived ventricular cardiomyocytes (day 15) show similar levels as seen in immature human heart samples, validating iPSC derived cardiomyocyte differentiation as a model for piRNA pathways during fetal development (**Figure 4.5**). While no changes in *PIWIL*s were found to be disrupted by Pb, this does not exempt the potential for Pb to dysregulate piRNA and associated pathways during cardiomyocyte differentiation, and future studies should be conducted that sequence piRNA in these cells, similar to the studies conducted here outlined in Chapter 2 as well as examine potential changes in PIWIL protein levels.

Additionally, in studies of only the female patient iPSC line, other epigenetic pathways were disrupted by Pb exposure throughout differentiation (**Figure 4.8**). Overall, 23 epigenetic pathways were found to be dysregulated, with 11 of these on day 1, 6 on day 6, and 6 on day 15 for either dose of Pb (with some pathways overlapping between days and exposures; data not shown). Over half of these (12) related to histone biology, and in our BMC analysis, similar epigenetic pathways were also disrupted, with two histone pathways upregulated on day 6.

Importantly, altered histone biology has shown to be involved in heart failure, inflammation in CVD, and cardiac hypertrophy.[26,27] Future work should examine whether these pathways are altered by Pb exposure in other male and female patient iPSC lines, as well as conduct CHIP-Seq or ATAC-Seq to examine gene protein binding and accessibility.

Exposure to Pb during differentiation alters expression of genes related to heart development and disease

DEG expression was dynamic throughout differentiation in female iPSC derived ventricular cardiomyocytes. Two genes of interest were found to be overlapped as DEGs between days 2 and 6: *FOXA2* and *CCKBR* (**Figure 4.7**). *FOXA2* (Forkhead box A2 transcription factor) was found downregulated at the 5 μM dose on both days and has been implicated as a factor in ventricular (vs atrial) cardiac differentiation.[28] This highlights the need to repeat this study in atrial cardiomyocytes in order to examine chamber specific differences in Pb cardiotoxicity. Interestingly, *CCKBR* (the cholecystokinin B/gastrin receptor) was also found to be downregulated on both day 2 and 6 by the 5 μM dose. Prior work has demonstrated *CCKBR* may be localized to the right atria in mice, although more work is needed to understand it's potential role in heart development or disease.[29]

The highest number of DEGs occurred on day 6 at the 5 μM dose, with 7 genes upregulated and 70 downregulated. Of those with a $|\log2FC| > 1$, a few genes related to cardiac dysfunction and disease. *FAS*, or fatty acid synthase, was upregulated with 5 μM Pb exposure on day 6. *FAS* is often upregulated in heart failure, plays a role in pathological cardiac remodeling, and has been identified as a potential therapeutic target for treating cardiac hypertrophy and heart failure.[30,31] In the context of our cardiac differentiation, on day 6 cells are cardiac progenitor cells, and upon investigating other signs of cardiac remodeling, we saw no changes in cardiac

lineage markers *TBX5* nor *NKX2-5* in these cells (analyzed by qRT-PCR; data not shown). *NQO1,* NAD(P)H: quinone oxidoreductase 1**,** was also upregulated by Pb in these cells, and plays a protective role of preventing the formation of reactive oxygen species and protecting against cardiovascular injury.[32] Thus, as Pb can induce oxidative stress, this upregulation of *NQO1* may be playing a protective role.[33] *PLVAP*, Plasmalemma vesicle associated protein, was downregulated in these cells, and it is an important endothelial factor known to play a critical role in heart development and repair, particularly in mouse models.[34] Taken together, DEGs present in day 6 cells exposed to 5 μM Pb indicate activation of regulatory mechanisms involved in cardiac pathology. Further mechanistic studies on how Pb dysregulates these genes during differentiation are needed in order to understand their roles and relationship with possible cardiac dysfunction.

Exposure to Pb during differentiation alters pathways related to ribosomal pathways and heart development

Of the top 30 pathways in the unbiased GO analysis, 18 related to ribosomal structure or function (**Table 4.6**). Given the essential role ribosomes play in protein synthesis, they are important in heart differentiation and function.[35] Furthermore, ribosomal dysfunction has been implicated in various CVDs, including hypertrophy, myocardial infarctions, and atherosclerosis.[35] Thus, this data calls for additional mechanistic investigation of ribosomal alterations induced by Pb exposure, including protein studies and functional assays of ribosome activity.

Both RNA-Seq pathway analysis and BMC data indicate that pathways related to heart development may be dysregulated by Pb exposure. Dysregulation in pathways included cardiac chamber morphogenesis (day 6 by 5 μM Pb), striated muscle tissue development (day 15 by 5

μM Pb), stem cell differentiation (day 6 by 5 μM Pb), heart development (day 1 by 0.5 μM Pb), cardiac chamber development (day 15 by 5 μM Pb), heart morphogenesis (day 15 by 0.5 and 5 μM Pb), cardiac chamber formation (day 6 by 0.5 μM Pb), and cardiocyte differentiation (day 6 by 0.5 μM Pb; **Figure 4.8A**). In our BMC analysis, cardiac myofibril assembly, muscle cell proliferation, and striated muscle cell proliferation were downregulated on day 2 of differentiation (**Figure 4.12**). This evidence shows Pb exposure causes both early and sustained disruption of cardiomyocyte differentiation, highlighting the potential for Pb to produce long lasting effects on cardiac development, with potential to increase risk of CVD later in life.

Mitochondrial pathways are significantly regulated by exposure to Pb during differentiation

Pb-induced changes in pathways related to mitochondria function were present throughout differentiation, and changes in mitochondrial pathways were more significant than any other set of selected pathways, with 47 mitochondria related pathways changed total and the most significant changes on days 1, 6, and 15 (**Figure 4.8B**). Pb is known to cause mitochondrial damage in various tissues, leading to oxidative stress, and CVD can be induced by high levels of oxidative stress, although literature connecting Pb, oxidative stress/mitochondrial dysfunction, and the heart is limited.[36] Interestingly, in the BMC modeled data, both positive and negative regulation of the release of cytochrome c from the mitochondria were downregulated on day 2, a process important in initiating apoptosis and known to be dysregulated by Pb in rat liver, rat kidney, and human neurons.[37–39] As the heart is a highly energetically demanding organ that relies on mitochondria for this energy, future work is warranted to understand Pb's induction of mitochondrial dysfunction, oxidative stress, and apoptosis in the heart and determine what this means in terms of cardiac pathology. Previous work has used a modified media, CDML3, on iPSC-derived cardiomyocytes to induce ischemia and mitochondrial dysfunction, and so future

studies could treat with Pb simultaneously in order to observe whether Pb enhances the metabolic stress induced by this media.[40]

Pb shows a similar level of dose-response effect but with different potential functional consequences throughout differentiation

BMC modeling of female derived iPSCs undergoing differentiation into ventricular cardiomyocytes revealed that a lower dose than was treated with has a significant effect on gene regulation, with benchmark concentrations of around 0.2 μM for all 4 days examined (**Table 4.7**). This gene regulation corresponded with cardiac, developmental, epigenetic, metabolic, and mitochondrial pathway regulation highlighted in the sections above, although these effects were not seen on day 15 (**Figure 4.12**). Interestingly, day 2 showed downregulated of BMC modeled pathways pertaining to heart cell development including cardiac myofibril assembly (driven by *MYLK3,* an essential gene in proper heart development and sarcomere formation) and striated muscle cell proliferation (driven by *HGF,* a gene that influences cardiomyocyte proliferation and differentiation in the developing heart).[41,42]

This early reprogramming could impact later cardiomyocyte function and highlights the importance of low dose effects. Importantly, the CDC's blood Pb reference value in children is 3.5 μg/dL and our BMC of 0.2 μM Pb is above this amount, around ~4.14 μg/dL.[43] Historical Pb exposure has been much higher, and recently during the 2014 Flint water crisis, children living in neighborhoods with the highest water Pb levels experienced a 6.6% increase in those with a blood Pb level above the then reference value of 5 μg/dL.[44] This highlights the public health relevance of our transcriptomic data; significant gene alterations that disrupt important pathways during cardiomyocyte differentiation occur at human relevant and historically common exposure levels.

Pb exposure during differentiation causes cell line specific changes in action potentials

Purified cardiomyocytes treated with Pb throughout differentiation showed changes in beat characteristics well after exposure had ended, suggesting that Pb exposure can have lasting impacts on heart function. Interestingly, these effects slightly varied between the two cell lines.

Action potential parameters were different between the two cell lines, with our findings showing an increase in beating rate in female 5 μM Pb dose but a decrease beat frequency in male 0.5 μM Pb dose (**Figure 4.13A**). At the same time, there was an increase in APD triangulation with Pb exposure at those same doses (**Figure 4.13B**). Both an increase and decrease in heart rate could be considered malfunctional, but an increase in heart rate with simultaneous increase in APD triangulation as seen in the female line shows prolonged repolarization despite increased firing rate, which is suggestive of potassium (K) efflux dysfunction.[45] In the male cell line, however, there were also decreases in change in action potential amplitude (dF/F0; both doses) and upstroke slope (depolarization rate of change; 5 μM only), which suggests possible sodium (Na) channel dysfunction (**Figure 4.13C**).[45] Pb's effect on K and Na channels in the heart has yet to be fully understood, but studies in other hippocampal neurons have shown Pb related effects on K and Na channels and currents. Pb ions can inhibit K efflux in hippocampal neurons, and so the prolonged APD triangulation seen here may indicate disrupted repolarization dynamics due to altered K channel function.[46–48] Chronic Pb exposure during rat development has been shown to cause a decrease in activation threshold and delayed activation of Na channels also in hippocampal neurons, which corresponds to the male data in our study.[49] It is also important to note that baseline fluorescence (F0), which reflects the resting membrane potential, was unchanged across conditions in both cell lines, suggesting that Pb exposure did not alter the cells' baseline electrical state but rather the activity

of Na and K currents during the action potential itself (see supplemental files for nonsignificant parameters). While these results allude to cell line specific disruptions in K and Na currents in cardiomyocytes, little is known about how Pb exposure during differentiation affects early developmental programming of these channels. More studies are needed on the mechanisms by which Pb exposure during differentiation may disrupt the expression and regulation of these channels well before cells begin to beat, and how these changes may relate to cardiac arrhythmias and pathology.

Pb exposure during differentiation causes cell line specific changes in Ca transients

Beat frequency as measured by Ca transients increased, with a corresponding decrease in CaTD and CaTD80, in both cell lines with Pb exposure, indicative of faster Ca handling (**Figure 4.14A-C**). Importantly, there was no change in baseline fluorescence (F0), suggesting Pb exposure did not alter resting intracellular Ca levels, but rather affected the Ca handling dynamics during transients (see supplemental files for nonsignificant parameters). This suggests alterations in the activity of channels that mediate the transients rather than pumps and exchangers that maintain resting Ca levels. Pb has been well characterized to mimic Ca as they are both divalent cations, and Pb is known to disrupt voltage-gated Ca channels and Ca homeostasis in the nervous system, leading to neurotoxicity.[50–52] In isolated guinea pig hearts, Pb (0-100 μM) has been shown to increase heart rate, block L-type Cav1.2 channels (which allows extracellular Ca into cardiomyocytes), and increase their fast inactivation, which could correspond to the decreases in decrease in CaTD and CaTD80 we see here.[13] The reduced amplitude we see with Pb here in the male cell line is also supported by this study (**Figure 4.14D**).[13] Interestingly, L-type Ca channels are known to play a role in embryonic development of the heart and modifications to them are associated a variety of arrhythmias such as atrial

fibrillation.[53] Pb exposure during differentiation could thus disrupt these channels during development, leading to lasting changes in cardiac electrophysiology. We examined the gene expression of *CACNA1C*, the gene that encodes for this channel in our day 15 unpurified ventricular cardiomyocytes and saw no changes in gene expression induced by Pb, but this does not preclude Pb from otherwise disrupting its protein expression or function (**Figure 14.16**).

Potential for action potential and Ca uncoupling in male ventricular cardiomyocytes exposed to Pb during differentiation

In the female derived cell line, there was an increased beat frequency measured by both action potentials and Ca transients at the higher dose, indicating faster pacing caused by Pb exposure. However, the action potential conduction velocity decreased in this cell line at both doses, suggesting the signal did not propagate effectively and potentially indicating disruption of gap junction functionality. Fasting firing combined with slower conduction in this cell line could reflect Pb causing faster depolarization but slower intercellular coupling.

In the male derived cell line, the effects of Pb during differentiation on electrophysiology were more complex. Action potential frequency decreased at the lower dose, while Ca transient frequency increased at both doses (**Figures 14.13** and **14.14**). Median conduction velocity decreased when measured by action potentials at the lower dose but increased as measured by Ca transients at both doses (**Figure 14.15**). This paradoxical shift indicates a slowing of electrical signal propagation with a simultaneous change in Ca kinetics, perhaps originating from an uncoupling of ECC. Slower action potential conduction velocity suggests possible gap junction dysfunction, which would impair coordinated depolarization across the cells, whereas faster Ca transient propagation may reflect compensatory changes in Ca handling machinery within individual cells to maintain contraction despite slowed electrical propagation.

Given these possible dysfunctions in ECC, we examined the gene expression of 4 channels/transporters related to ECC in our male and female lines on day 15 (unpurified cardiomyocytes) and saw no significant gene expression changes (**Figure 4.16**), but posttranslational effects or other mechanisms of functional disruption could be at play. Recent work in the heart has found little correlation between protein level changes and transcript expression changes, and so in addition to assessing gene expression of these channels/transporters in purified cardiomyocytes, future work should interrogate these cells' protein expression levels as well.[54] Furthermore, patch clamping of cardiomyocytes exposed to Pb during differentiation should be carried out to examine changes in ion channel function.

Limitations and future directions

This study represents a foundation for understanding the epigenetic and transcriptomic changes induced by human relevant Pb exposure in female and male derived ventricular cardiomyocytes but utilizing only one cell line per sex limits any conclusions that can be drawn about sex differences and could be representative of underlying individual variation. RNA-Seq was only carried out for one cell line, and further transcriptomic studies should be carried out in a representative sample from numerous male and female donors. While the RNA-Seq data clustered very nicely by day, representing expected differences in cell phenotype throughout differentiation, data also clustered by replicate, indicating replicate-to-replicate biological variation that could be due to differences in cell cycle state or other subtle differences in cellular conditions during differentiation (**Figure 4.6**). Additionally, optical mapping results are limited by experimental protocol—purifications occurred when cells began beating throughout their well, which varied in day from experiment to experiment, and optical mapping occurred at variable days past exposure cessation (between 9-17 days). Furthermore, the cardiomyocytes

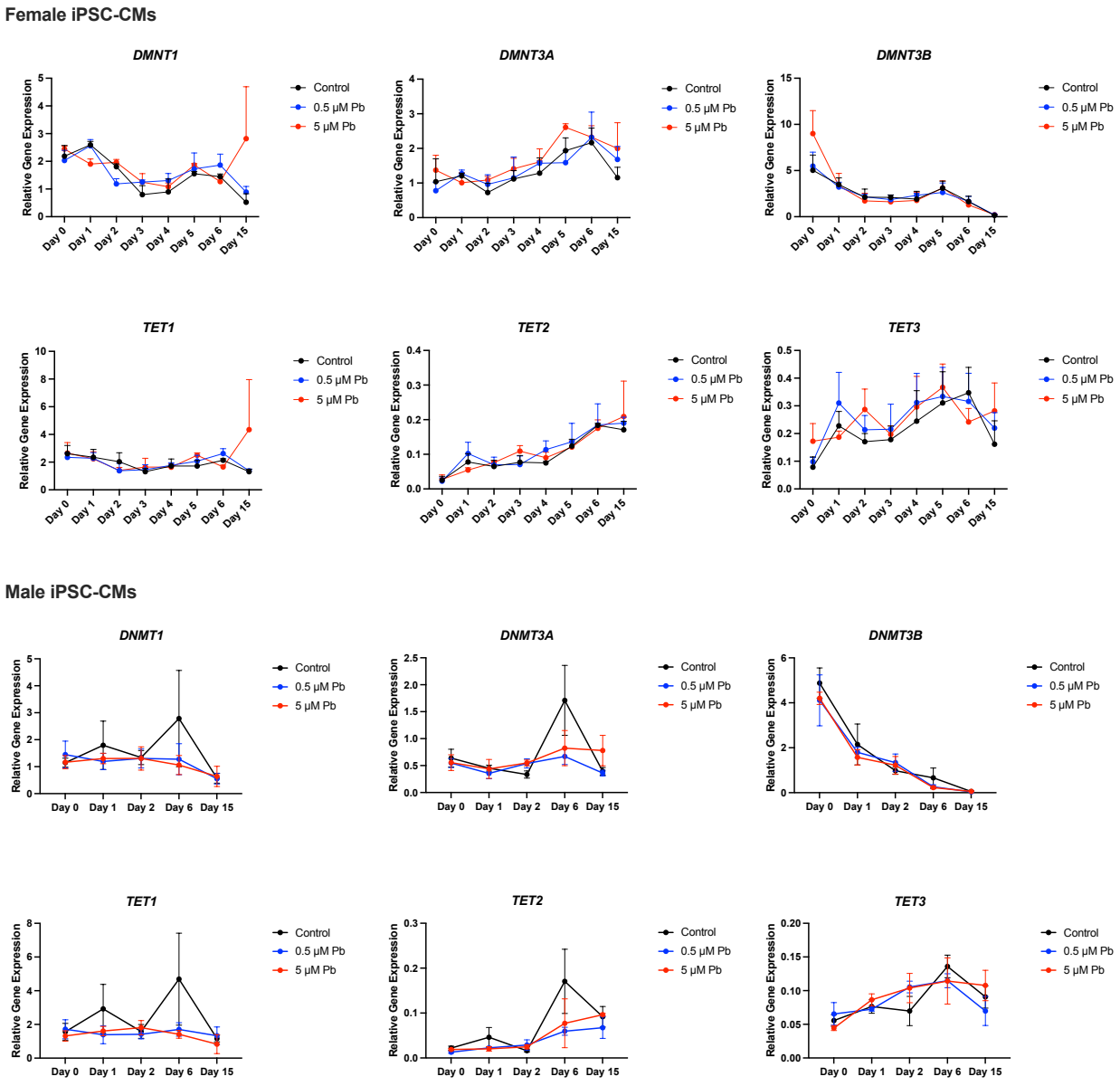
generated here represent a fetal like state, and so conclusions that can be drawn related to the development of cardiovascular disease in adults are limited.

Conclusions

Overall, we characterized transcriptomic changes induced by Pb throughout differentiation into ventricular cardiomyocytes in one iPSC line, with changes in epigenetic, developmental, and mitochondrial regulation as well as in genes related to the development of CVD. Further, these changes often showed a dose-response effect correlating to human relevant exposure ranges. Optical mapping in one female and one male derived iPSC ventricular cardiomyocyte cell line revealed some Pb induced changes in beat characteristics similar between the two cell lines and possible disruption of ECC in only the male cell line. Through a combination of transcriptomic and functional analyses, we found that Pb exposure during cardiomyocyte differentiation induces changes related to the development of cardiac pathology, paving the way for mechanistic studies to interrogate the molecular underpinnings of these effects.

4.6: Supplementary Information

Supplemental data for this chapter can be found in the figure below and at the repository here, including tables, bm2 file from BMDExpress, and optical mapping prism files: https://doi.org/10.7302/5gs6-2b90



Supplemental Figure 4.17: Female and male derived iPSC-CM expression of epigenetic enzymes during differentiation.

Transcript expression of *DNMT1*, *3A*, and *3B* and *TET*s *1-3* in both female (top) and male (bottom) patient derived iPSCs during differentiation into cardiomyocytes (days 0-15) with

exposure to 0.5 or 5 μM Pb during the first 8 days of differentiation. No significant changes with Pb exposure were seen on each day (one-way ANOVA).

4.7: Acknowledgements

I would like to thank the University of Michigan Cardiovascular Regeneration Core Laboratory, including Dr. Andre Monteiro da Rocha. I would also like to thank the DoGoodS-Pi Epigenetics Research Group and Svoboda labs, including Esha Shah, Isabelle Melis, and Dr. Tomoko Ishikawa for their cell culture support, as well as the laboratory manager Tamara Jones (University of Michigan) for her laboratory and administrative support. I would also like to thank Anagha Tapaswi and University of Michigan Advanced Genomics Core for RNA-Seq sample processing for this study.

4.8: References

1. Farzan SF, Howe CG, Chen Y, et al. Prenatal Lead Exposure and Elevated Blood Pressure in Children. *Environ Int*. 2018;121(Pt 2):1289-1296. doi:10.1016/j.envint.2018.10.049

2. Kim N, Filipovic D, Bhattacharya S, Cuddapah S. Epigenetic toxicity of heavy metals − implications for embryonic stem cells. *Environ Int*. 2024;193:109084. doi:10.1016/j.envint.2024.109084

3. Monear NC, Xhabija B. The effect of lead during the Flint water crisis on mouse embryonic stem cells self-renewal and differentiation markers. *Toxicol In Vitro*. 2020;63:104719. doi:10.1016/j.tiv.2019.104719

4. Yu J, Vodyanik MA, Smuga-Otto K, et al. Induced pluripotent stem cell lines derived from human somatic cells. *Science*. 2007;318(5858):1917-1920. doi:10.1126/science.1151526

5. Liu Q, Xu C, Jin J, et al. Early-life exposure to lead changes cardiac development and compromises long-term cardiac function. *Sci Total Environ*. 2023;904:166667. doi:10.1016/j.scitotenv.2023.166667

6. Senut MC, Sen A, Cingolani P, Shaik A, Land SJ, Ruden DM. Lead exposure disrupts global DNA methylation in human embryonic stem cells and alters their neuronal differentiation. *Toxicol Sci Off J Soc Toxicol*. 2014;139(1):142-161. doi:10.1093/toxsci/kfu028

7. Lian X, Hsiao C, Wilson G, et al. Robust cardiomyocyte differentiation from human pluripotent stem cells via temporal modulation of canonical Wnt signaling. *Proc Natl Acad Sci*. 2012;109(27):E1848-E1857. doi:10.1073/pnas.1200250109

8. Lian X, Zhang J, Azarin SM, et al. Directed cardiomyocyte differentiation from human pluripotent stem cells by modulating Wnt/β-catenin signaling under fully defined conditions. *Nat Protoc*. 2013;8(1):162-175. doi:10.1038/nprot.2012.150

9. Parr DR, Harris EJ. The effect of lead on the calcium-handling capacity of rat heart mitochondria. *Biochem J*. 1976;158(2):289-294. doi:10.1042/bj1580289

10. Davuljigari CB, Gottipolu RR. Late-life Cardiac Injury in Rats following Early Life Exposure to Lead: Reversal Effect of Nutrient Metal Mixture. *Cardiovasc Toxicol*. 2020;20(3):249-260. doi:10.1007/s12012-019-09549-2

11. Parks RJ, Howlett SE. Sex differences in mechanisms of cardiac excitation–contraction coupling. *Pflugers Arch*. 2013;465(5):747-763. doi:10.1007/s00424-013-1233-0

12. Ripa R, George T, Shumway KR, Sattar Y. Physiology, Cardiac Muscle. In: *StatPearls*. StatPearls Publishing; 2025. Accessed August 26, 2025. http://www.ncbi.nlm.nih.gov/books/NBK572070/

13. Ferreira de Mattos G, Costa C, Savio F, Alonso M, Nicolson GL. Lead poisoning: acute exposure of the heart to lead ions promotes changes in cardiac function and Cav1.2 ion channels. *Biophys Rev*. 2017;9(5):807-825. doi:10.1007/s12551-017-0303-5

14. Nahar MS, Liao C, Kannan K, Dolinoy DC. Fetal liver bisphenol A concentrations and biotransformation gene expression reveal variable exposure and altered capacity for metabolism in humans. *J Biochem Mol Toxicol*. 2013;27(2):116-123. doi:10.1002/jbt.21459

15.Morgan R. *Investigating the Impact of Lead Exposure on Epigenetic Regulation During Neural Differentiation and Neurodevelopment: Focus on piRNA and Transposable Element Regulation*. Thesis. 2023. doi:10.7302/8222

16.Sala-Hamrick KE, Tapaswi A, Polemi KM, Nguyen VK, Colacino JA. High-Throughput Transcriptomics of Nontumorigenic Breast Cells Exposed to Environmentally Relevant Chemicals. *Environ Health Perspect*. 2024;132(4):047002. doi:10.1289/EHP12886

17.Babraham Bioinformatics - FastQC A Quality Control tool for High Throughput Sequence Data. Accessed September 2, 2025. https://www.bioinformatics.babraham.ac.uk/projects/fastqc/

18.MultiQC: summarize analysis results for multiple tools and samples in a single report | Bioinformatics | Oxford Academic. Accessed September 2, 2025. https://academic.oup.com/bioinformatics/article/32/19/3047/2196507

19.Dobin A, Davis CA, Schlesinger F, et al. STAR: ultrafast universal RNA-seq aligner. *Bioinforma Oxf Engl*. 2013;29(1):15-21. doi:10.1093/bioinformatics/bts635

20.Liao Y, Smyth GK, Shi W. featureCounts: an efficient general purpose program for assigning sequence reads to genomic features. *Bioinforma Oxf Engl*. 2014;30(7):923-930. doi:10.1093/bioinformatics/btt656

21.Sartor MA, Leikauf GD, Medvedovic M. LRpath: a logistic regression approach for identifying enriched biological groups in gene expression data. *Bioinformatics*. 2009;25(2):211-217. doi:10.1093/bioinformatics/btn592

22.Allan A, Creech J, Hausner C, et al. High-throughput longitudinal electrophysiology screening of mature chamber-specific hiPSC-CMs using optical mapping. *iScience*. 2023;26(7):107142. doi:10.1016/j.isci.2023.107142

23.Gurrala C, Cohen M, Kubo H, et al. Abstract Thu096: DNMT3B-Mediated Epigenetic Reprogramming Induces Cardiomyocyte Dedifferentiation and Proliferation, Enhancing Post-MI Cardiac Regeneration. *Circ Res*. 2025;137(Suppl_1). doi:10.1161/res.137.suppl_1.Thu096

24.Zhong N, Nong X, Diao J, Yang G. piRNA-6426 increases DNMT3B-mediated SOAT1 methylation and improves heart failure. *Aging*. 2022;14(6):2678-2694. doi:10.18632/aging.203965

25.Greca AL, Scarafía MA, Cañás MCH, et al. PIWI-interacting RNAs are differentially expressed during cardiac differentiation of human pluripotent stem cells. *PLOS ONE*. 2020;15(5):e0232715. doi:10.1371/journal.pone.0232715

26.Zhang W, Song M, Qu J, Liu GH. Epigenetic Modifications in Cardiovascular Aging and Diseases. *Circ Res*. 2018;123(7):773-786. doi:10.1161/CIRCRESAHA.118.312497

27.Qin J, Guo N, Tong J, Wang Z. Function of histone methylation and acetylation modifiers in cardiac hypertrophy. *J Mol Cell Cardiol*. 2021;159:120-129. doi:10.1016/j.yjmcc.2021.06.011

28.Bardot E, Calderon D, Santoriello F, et al. Foxa2 identifies a cardiac progenitor population with ventricular differentiation potential. *Nat Commun*. 2017;8(1):14428. doi:10.1038/ncomms14428

29.Leigh RS, Ruskoaho HJ, Kaynak BL. Cholecystokinin peptide signaling is regulated by a TBX5-MEF2 axis in the heart. *Peptides*. 2021;136:170459. doi:10.1016/j.peptides.2020.170459

30.Bharati P, Burman P, Mahapatra S, et al. Fatty acid synthase inhibition offers protection against pressure-induced cardiac hypertrophy. *Biochem Pharmacol*. 2025;238:116962. doi:10.1016/j.bcp.2025.116962

31.Li Y, Takemura G, Kosai K ichiro, et al. Critical roles for the Fas/Fas ligand system in postinfarction ventricular remodeling and heart failure. *Circ Res*. 2004;95(6):627-636. doi:10.1161/01.RES.0000141528.54850.bd

32.Zhu H, Li Y. NAD(P)H: quinone oxidoreductase 1 and its potential protective role in cardiovascular diseases and related conditions. *Cardiovasc Toxicol*. 2012;12(1):39-45. doi:10.1007/s12012-011-9136-9

33.Lopes ACBA, Peixe TS, Mesas AE, Paoliello MMB. Lead Exposure and Oxidative Stress: A Systematic Review. *Rev Environ Contam Toxicol*. 2016;236:193-238. doi:10.1007/978-3-319-20013-2_3

34.Sui Y, Kou S, Ge K, Cao J, Liu C, Zhang H. Expression analysis of *plvap* in mouse heart development, homeostasis and injury. *Gene Expr Patterns*. 2023;50:119343. doi:10.1016/j.gep.2023.119343

35.Jiao L, Liu Y, Yu XY, et al. Ribosome biogenesis in disease: new players and therapeutic targets. *Signal Transduct Target Ther*. 2023;8:15. doi:10.1038/s41392-022-01285-4

36.Han Q, Zhang W, Guo J, et al. Mitochondrion: a sensitive target for Pb exposure. *J Toxicol Sci*. 2021;46(8):345-358. doi:10.2131/jts.46.345

37.Liu G, Wang ZK, Wang ZY, Yang DB, Liu ZP, Wang L. Mitochondrial permeability transition and its regulatory components are implicated in apoptosis of primary cultures of rat proximal tubular cells exposed to lead. *Arch Toxicol*. 2016;90(5):1193-1209. doi:10.1007/s00204-015-1547-0

38.Ma L, Liu JY, Dong JX, Xiao Q, Zhao J, Jiang FL. Toxicity of Pb2+ on rat liver mitochondria induced by oxidative stress and mitochondrial permeability transition. *Toxicol Res*. 2017;6(6):822-830. doi:10.1039/c7tx00204a

39.Ye F, Li X, Li F, et al. Cyclosporin A protects against Lead neurotoxicity through inhibiting mitochondrial permeability transition pore opening in nerve cells. *NeuroToxicology*. 2016;57:203-213. doi:10.1016/j.neuro.2016.10.004

40.Davis J, Chouman A, Creech J, et al. In vitro model of ischemic heart failure using human induced pluripotent stem cell–derived cardiomyocytes. *JCI Insight*. 2021;6(10). doi:10.1172/jci.insight.134368

41.Seguchi O, Takashima S, Yamazaki S, et al. A cardiac myosin light chain kinase regulates sarcomere assembly in the vertebrate heart. *J Clin Invest*. 2007;117(10):2812-2824. doi:10.1172/JCI30804

42.Gallo S, Sala V, Gatti S, Crepaldi T. HGF/Met Axis in Heart Function and Cardioprotection. *Biomedicines*. 2014;2(4):247-262. doi:10.3390/biomedicines2040247

43.Ruckart PZ, Jones RL, Courtney JG, et al. Update of the Blood Lead Reference Value - United States, 2021. *MMWR Morb Mortal Wkly Rep*. 2021;70(43):1509-1512. doi:10.15585/mmwr.mm7043a4

44.Hanna-Attisha M, LaChance J, Sadler RC, Champney Schnepp A. Elevated Blood Lead Levels in Children Associated With the Flint Drinking Water Crisis: A Spatial Analysis of Risk and Public Health Response. *Am J Public Health*. 2016;106(2):283-290. doi:10.2105/AJPH.2015.303003

45.Varró A, Tomek J, Nagy N, et al. Cardiac transmembrane ion channels and action potentials: cellular physiology and arrhythmogenic behavior. *Physiol Rev*. 2021;101(3):1083-1176. doi:10.1152/physrev.00024.2019

46.Madeja M, Binding N, Musshoff U, Pongs O, Witting U, Speckmann EJ. Effects of lead on cloned voltage-operated neuronal potassium channels. *Naunyn Schmiedebergs Arch Pharmacol*. 1995;351(3):320-327. doi:10.1007/BF00233254

47.Madeja M, Musshoff U, Binding N, Witting U, Speckmann EJ. Effects of Pb2+ on delayed-rectifier potassium channels in acutely isolated hippocampal neurons. *J Neurophysiol*. 1997;78(5):2649-2654. doi:10.1152/jn.1997.78.5.2649

48.Yu K, Ge SY, Dai XQ, Ruan DY. Effects of Pb2+ on the transient outward potassium current in acutely dissociated rat hippocampal neurons. *Can J Physiol Pharmacol*. 2003;81(8):825-833. doi:10.1139/y03-074

49. Yan D, Wang L, Ma FL, et al. Developmental exposure to lead causes inherent changes on voltage-gated sodium channels in rat hippocampal CA1 neurons. *Neuroscience*. 2008;153(2):436-445. doi:10.1016/j.neuroscience.2008.02.016

50. Atchison WD. Effects of toxic environmental contaminants on voltage-gated calcium channel function: from past to present. *J Bioenerg Biomembr*. 2003;35(6):507-532. doi:10.1023/b:jobb.0000008023.11211.13

51. Audesirk G. Electrophysiology of lead intoxication: effects on voltage-sensitive ion channels. *Neurotoxicology*. 1993;14(2-3):137-147.

52. Oortgiesen M, Leinders T, van Kleef RG, Vijverberg HP. Differential neurotoxicological effects of lead on voltage-dependent and receptor-operated ion channels. *Neurotoxicology*. 1993;14(2-3):87-96.

53. Shah K, Seeley S, Schulz C, Fisher J, Gururaja Rao S. Calcium Channels in the Heart: Disease States and Drugs. *Cells*. 2022;11(6):943. doi:10.3390/cells11060943

54. Dorr KM, Conlon FL. Proteomic-Based Approaches to Cardiac Development and Disease. *Curr Opin Chem Biol*. 2019;48:150-157. doi:10.1016/j.cbpa.2019.01.001

Chapter 5: Conclusions

5.1: Introduction

Cardiovascular disease (CVD) is the leading cause of death worldwide, is highly sexually dimorphic, and Pb exposure contributes substantially to CVD risk and mortality.[1–3] Lead (Pb) is also known to disrupt epigenetics in the heart, and certain piRNAs have been implicated in the development of CVD, but Pb's potential to impact piRNA pathways in the heart has yet to be characterized prior to my studies.[4–6] The overarching aim for this body of work was to fill knowledge gaps surrounding how developmental Pb exposure influences transcriptomic and functional processes in the heart in a sex specific manner using both murine as well as human models, with particular emphasis on piRNA expression and associated epigenetic machinery. Taken together, these gene expression and functional changes were put into the context of potential to increase CVD risk later in life.

To understand this, Aim 1 assessed piRNA expression changes induced by developmental Pb exposure in mice, Aim 2 looked at gene, pathway, and functional changes induced by developmental Pb exposure in mice, and Aim 3 assessed transcriptomic and functional changes caused by Pb exposure during differentiation of human iPSC-derived cardiomyocytes. The schematic of my research plan is shown below.

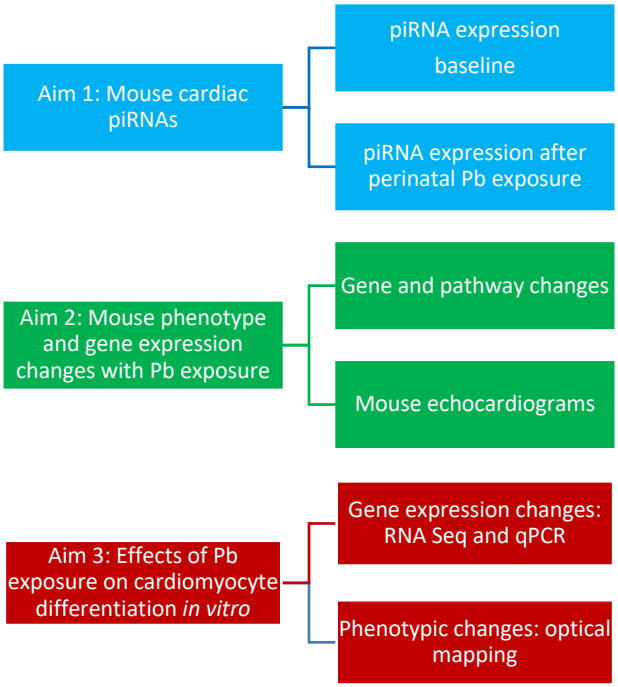


Figure 5.1: Schematic of Research Plan

This concluding chapter will first summarize key findings, followed by an in-depth synthesis of findings comparing the two models and examining sex differences, epigenetics, and functional consequences of developmental Pb exposure in the heart. The latter portion of this chapter will explore public health relevance, policy implications, and future directions.

5.2: Summary of key findings

Aim 1

Analyze Sex-Stratified piRNA Expression to Characterize Functional Impacts of Perinatal Pb Exposure in Murine Hearts

Goal: Establish sex-stratified baseline maps of all piRNAs expressed in murine heart tissue and examine effects of perinatal Pb exposure on piRNA expression in murine hearts.

Hypothesis: piRNAs are expressed in the heart, their expression is sex-specific, and their expression is affected by perinatal Pb exposure in a sex-specific manner.

Summary of Results: Combined and sex-stratified piRNA expression in both control and perinatally Pb-exposed adult murine hearts were characterized. A baseline 18,956 piRNAs were discovered in the murine heart in combined analysis, with sex differences in expression of piRNAs at baseline. Hundreds of piRNAs were found to be altered by developmental Pb exposure in a sex specific manner (847 in females and 187 in males with 23 overlapping in expression). These piRNAs were significantly enriched near genes involved in biological processes related to heart function and CVD development, including mitochondrial function, energy metabolism, and cardiac muscle structure (FDR < 0.05). We also found that Pb induced sex specific changes in *PIWIL* and ECC genes. In addition to providing a foundation for sex-specific piRNA expression in the heart, these findings suggest a novel epigenetic mechanism by which developmental Pb exposure may impact CVD risk later in life.

Aim 2

Determine the Sex-Specific Effects of Perinatal Pb Exposure on Murine Cardiac Gene Expression and Function

Goal: Examine the sex-specific effects of perinatal Pb exposure on gene and pathway alterations as well as phenotypic changes in adult mouse cardiovascular system.

<u>Aim 2A:</u>

- *Hypothesis: Perinatal Pb exposure alters transcriptional pathways associated with cardiovascular development and disease in a sex specific manner.*

<u>Aim 2B:</u>

- *Hypothesis: Perinatal Pb exposure causes structural and functional changes in the murine heart later in life in a sex specific manner.*

Summary of Results: We examined sex-specific gene and functional heart changes during midlife in mice that were perinatally exposed to Pb. We found changes induced by Pb in pathways related to cardiac function, development, epigenetics, mitochondria, and metabolism that differed by sex. Further, we found sex specific alterations in cardiac structure and function as assessed by echocardiograms. Overall, this aim provided a comprehensive analysis of how perinatal Pb influences cardiac biology differently in male and female mice, providing a foundation for future mechanistic investigations of mechanisms of Pb induced cardiotoxicity.

Aim 3

Evaluate Cell Line–Specific Gene Expression Changes and Functional Alterations Induced by Pb Exposure During Differentiation in Human iPSC-Derived Ventricular Cardiomyocytes

Goal: Characterize the dose-specific effects of Pb exposure during differentiation on gene, pathway, and functional alterations in human ventricular cardiomyocytes.

Aim 3A:

- *Hypothesis: Epigenetic regulatory genes as well as genes associated with cardiac development, structure, and function are affected by Pb exposure during differentiation in a cell line specific manner in human iPSC-derived ventricular cardiomyocytes.*

Aim 3B:

- *Hypothesis: Pb exposure during differentiation impacts heart cell differentiation and beat characteristics in purified ventricular cardiomyocytes.*

Summary of Results: In cardiomyocytes derived from one female and one male iPSC line treated with Pb during differentiation, we characterized epigenetic, molecular, and functional changes. We found changes in epigenetic, developmental, and mitochondrial regulation in the female patient cell line that showed a significant dose-response effect at human relevant concentrations. Further, electrophysiological changes in beat characteristics were discovered, with possible disruption of ECC in only the male patient cell line. Together, we characterized persistent transcriptomic and functional effects of Pb exposure during differentiation, providing a foundation for future mechanistic studies investigating potential links to cardiac pathology.

5.3: Comparison of mouse vs. human findings

It is important to note that the two exposure models in these studies differ in biological timing, therefore impacting what mechanisms are being interrogated. In the mouse exposure model, the parental germline cells are facing Pb exposure, while the stem cell models are reprogrammed *in vitro* to mimic a pluripotent state prior to Pb exposure. These *in vivo* vs. *in vitro* exposure differences have significant implications on epigenetic outcomes. Since in the mouse models assessed here, exposure began two weeks prior to fertilization, alterations in epigenetics of egg cells could be carried into the zygote. Further, widespread epigenetic reprogramming happens during early embryonic development, and as Pb exposure continued during this time frame, it could disrupt this reprogramming.[7] On the other hand, the stem cell model exposure window occurs after reprogramming, and thus epigenetic maintenance mechanisms are susceptible to the exposure during differentiation. By assessing these two models together, we can provide a comprehensive understanding of Pb exposure on epigenetics and transcriptomics relevant to development.

Both models in this study showed similarities in affected pathways, with sex specific changes in epigenetic regulation, cardiac development, mitochondrial regulation, and functional outcomes in the mouse model, and cell line specific changes in these factors in the human model. We can conclude that both models showed Pb's potential to impact CVD risk, but neither model perfectly mimics human CVD risk. Studies have found that gene expression, signaling pathways, epigenetics, and mechanisms of heart morphogenesis are similar between humans and mice, but there are substantial differences in processes of cardiac aging, lifespan, body size, and heart rate between humans and mice as well as minor differences in the contractile proteins expressed in humans and mice.[8–12] Further, mice exhibit differences in response to toxicants and metabolism which could impact the translatability of Pb exposure model to humans.[13] While human iPSC derived cardiomyocytes do not have these interspecies variables, there are nonetheless limitations to their usage as a model. Although our system induces important and robust maturation changes, iPSC-CMs are nonetheless limited to an immature state and lack surrounding tissue structures (3D architecture and vascularization).[14] Despite this, they are a great tool for examining transcriptomics, epigenetics, and electrophysiological parameters.[14–16] Together, these two models tell us different things: the mice give us a whole organism context, while the human cells give us context specific to human cardiomyocyte differentiation. Given that each model showed similarities in the pathways affected by Pb exposure, this work gives a comprehensive assessment of Pb's potential developmental cardiotoxicity in humans.

5.4: Sex differences in how the heart responds to Pb exposure

Significant sex differences in response to Pb exposure were present in the mouse model. In mice, piRNA expression varied both at baseline and in response to Pb, but interestingly the

functional consequences of these piRNAs may be similar between sexes. Both *Piwil* expression and ECC genes were only affected by developmental Pb in male mice. In transcriptomic analyses of mice, the male mice showed alterations in histone pathways, female mice showed more alterations in mitochondrial mechanisms, and both showed pathway disruption related to heart development. Echocardiograms further revealed sex specific changes, with heart rate impacted in female mice and potential diastolic dysfunction in male mice. These sex differences could be due to hormonal, epigenetic, or genetic factor differences, and future work should interrogate these possible mechanisms and relate them to potential risk for CVD development.

In our cell lines, only one female and one male line were assessed, but the differences in electrophysiology present between the female and male line may point to the potential for sex differences in how males and females respond to Pb. Interestingly, both cell lines showed increased beat frequency, but the male cell line showed potential dysregulation of ECC. Further examination with additional replicates of male and female lines are needed to make conclusions regarding sex differences. Using this model to assess sex differences will allow for interrogation of sex specific differences in genetics and epigenetics sans hormonal regulation that is present in a whole organism.

5.5: piRNA and epigenetic pathways altered by Pb exposure

Aim 1 of this study explores a largely unstudied regulatory mechanism in the heart both at base line and in the context of exposures –piRNA. The findings suggest Pb can alter piRNA and *Piwil* expression in a sex specific manner, and the piRNA changes map to regions significant to cardiac biology, including cardiac muscle structure, energy metabolism, and mitochondrial function. Given the significance of these pathways in heart processes, this suggests piRNA

dysregulation may thus contribute to cardiac pathology through developmental reprogramming. However, it is unknown whether Pb induced changes in piRNA expression are downstream or upstream of other molecular and functional changes in the heart.

Aims 2 and 3 show Pb caused changes in the pathways mentioned above and in other epigenetic pathways in both our mouse model of perinatal Pb exposure as well as in the human cardiomyocytes. A correlation can be drawn here suggesting that piRNA function upstream or in coordination with these pathways, thus underlying a potential developmental reprogramming that could contribute to CVD risk. This is further underscored by functional changes in heart mechanics in both models. However, without direct evidence of piRNA interplaying with these other cardiac processes, we cannot say definitively that piRNAs are playing this role, and so links between piRNA regulation and transposon or mRNA targets need to be further examined. piRNA sequencing will also be carried out in the human cell model of Pb exposure during differentiation as the piRNA changes may be different between models. This will answer the question of where Pb interferes with epigenetics—are these piRNA and epigenetic changes downstream compensatory mechanisms for Pb's interference with ECC or mitochondrial functions, do they work in concert, are they upstream effects, or some combination of these? Elucidating these relationships will be crucial in understanding Pb's developmental toxicity in the heart.

5.6: Functional alterations by developmental Pb exposure

Both aims 2 and 3 examine functional outcomes of Pb exposure, with echocardiograms in mouse perinatally exposed to Pb and electrophysiological parameters in cardiomyocytes exposed

to Pb during differentiation. The overall implications of both of these alterations suggest Pb induces changes in cardiac programming that affects heart functioning.

In mice, no change in heart rate was seen in either sex, which does not correspond to the increase in cardiomyocyte beat rates found in both sexes of cell lines through calcium (Ca) transient assessments. Importantly, in addition to model specific differences highlighted about, different doses of Pb were assessed between the two models. Additionally, as mice represent a systemic model of exposure, it is likely that Pb's known neurotoxic affects affect heart electrophysiology. Despite these differences, both models point towards Pb's potential to disrupt electrophysiology in the heart long after cessation of exposure.

Excitation contraction coupling genes were assessed in both models, with 3-week and 5-month male mice showing an increase in all 4 ECC genes, and 4-month female mice showing a potential increase in *Ryr2*. In unpurified cardiomyocytes, on the other hand, none of the ECC genes showed changes for either cell line. However, as highlighted in all three aims, changes in protein expression and posttranslational or other functional disruptions of their mechanics could be dysregulated by Pb exposure. This idea is underscored by recent work in the heart that found little correlation between protein level changes and transcript expression changes in disease models.[17] Future work should also examine the expression and function of one additional gene/protein of interest involved in ECC in Pb exposed cardiomyocytes: phospholamban (PLN), which regulates cardiac contractility through inhibition of the SERCA pump.[18,19]

Additional mechanistic underpinnings to functional changes caused by Pb exposure are alterations in Ca handling and mitochondrial function, which are interrelated. Mitochondria make up 30% of the volume of cardiomyocytes and are critical in maintaining Ca

homeostasis.[20,21] Pb is known to mimic Ca, and so could disrupt both ECC and mitochondrial function.[22] Importantly, mitochondrial pathways were found as potential targets of Pb altered piRNA (Aim 1) and as pathways differentially regulated by Pb in transcriptomic analysis (aim 2 and 3). Disruptions in mitochondrial pathways in the heart have been implicated in CVDs, including atherosclerosis, ischemia-reperfusion injury, hypertension, diabetes, cardiac hypertrophy, and heart failure through oxidative stress.[23] Studies on how Pb causes mitochondrial dysfunction in the heart are limited, but it is known to cause mitochondrial damage and oxidative stress in other tissues.[24] Therefore, this work points to the need for further mechanistic studies of how developmental Pb impacts mitochondrial development in the heart, with particular attention on both Pb's role in mimicking Ca as well how epigenetic processes (piRNA) may relate to disturbance of mitochondrial function. These studies should also seek to link mitochondrial disruption to changes in function of the heart or cardiomyocytes.

5.7: Relation to the Developmental Origins of Disease

The findings presented here indicate that Pb exposure during development/differentiation can disrupt cardiac epigenetics, development, electrophysiology, and mitochondrial pathways. Some or all of these pathways may be disrupted during development and work together to cause adverse consequences on heart function later in life. Alterations in all these mechanisms have been implicated in the development of different CVDs, so developmental Pb exposure could cause predisposition to adult disease. However, the molecular underpinnings of how Pb causes long term cardiac dysfunction need to be further elucidated by mechanistic studies. Future work should examine possible mechanisms, identify developmental windows of susceptibility, and assess the potential heritability of these changes.

5.8: Public health and policy implications

This body of work provides molecular insights on an environmental justice issue in the USA and world, as well as a context for sex-specific vulnerabilities to CVD. It highlights the importance of understanding how early life exposures alter heart biology in ways that could increase CVD risk. With these insights, policies can be initiated or adapted to both promote environmental justice as well as mitigate CVD risk.

Low income and marginalized communities are disproportionately affected by Pb exposure in the US, and worldwide Pb exposure is more severe in developing countries.[3,25] The molecular data presented here add to a body of work warning against the negative impacts of Pb exposure. Policies should be adapted which reduce the burden of Pb exposure, monitor vulnerable populations, and actively involve and educate the communities affected on the potential harms of Pb exposure. In particular, families and pregnant people should be educated about exposure risk.

In the US, the current CDC reference value of 3.5 μg/dL blood Pb level as a limit of identifying children with concerning levels of Pb exposure is supported by benchmark modeling in this work.[26] Identifying children and communities, often from low income or racial and ethnic minority groups, with higher blood Pb levels remains imperative. Worldwide, low and middle income countries have higher (greater than 5 μg/dL) blood Pb levels.[27] Only 48% of countries worldwide have regulations on the production and sales of Pb paints.[28] Therefore, better regulations worldwide are needed, and as in the US, monitoring, education, and community engagement efforts should be in place to alleviate this issue and therefore reduce Pb-induced CVD risk.

Further, the mouse studies in aim 1 and 2 show that developmental Pb has a different impact on female and male hearts. Therefore, sex specific monitoring data should be collected, studies examining human exposure risk should stratify by sex, and any safety testing of products should include both sexes. In addition to preventative measures, treatment for CVD in which Pb could have played a causal role should be tailored by sex.

Finally, as highlighted in the other sections of this chapter, this project shows the need for additional mechanistic studies on Pb exposure impact in the heart, and federal funding should be allocated for these investigations. These investigations would build on the studies presented here, leading to the development of both biomarkers to classify risk as well as potential intervention or therapeutic strategies.

5.9: Future directions

As explained so far in this chapter, deeper mechanistic studies are needed on how Pb affects particular piRNAs, other epigenetic pathways, and mitochondrial and metabolic pathways that link these changes to functional outcomes in the heart. Further, as CVD is an age related disease, longitudinal studies in mice should be carried out to assess later life cardiac outcomes. In iPSC models, additional replicates of both female and male lines are needed which include differing genetic backgrounds in order to make conclusions about sex differences. One additional opportunity to investigate sex differences in iPSC derived cardiomyocytes is the use of isogenic Klinefelter lines to examine the contributions of an XX vs XY genotype in the absence of patient-patient genetic variability.[29] Lastly, multi-omics strategies should be integrated into these studies to determine how epigenomics, transcriptomics, proteomics, and metabolomic changes are affected by Pb together to impact heart biology.

5.10: Concluding Remarks

Overall, this work increased our understanding of how exposure to Pb during development or differentiation influences epigenetics, transcriptomics, and functional processes in the heart in a sex specific manner. It is the first study to show how the piRNA landscape in the mouse heart is influenced by developmental Pb and the first to examine how Pb exposure during differentiation impacts later electrophysiological parameters as cardiomyocytes. Aim 1 shows a potential epigenetic mechanism (piRNA) by which Pb could cause changes in heart biology, which could lead to the development of targeted therapies. Aims 2 and 3 integrate transcriptomic changes with functional outcomes, paving the way for future mechanistic studies that put into context how developmental Pb increases CVD risk later in life. All together, these projects provide a novel and sex stratified framework for how developmental Pb exposure effects the heart.

Pb exposure was first identified as a problem in human antiquity, dating back to the second century BC, and since then humankind has made remarkable strides in science, medicine, and public health that have led to better qualities of life for humanity.[30] However, significant disparities in the US and world still exist regarding who is exposed to Pb, and Pb exposure contributes to an estimated 256,000 cardiovascular disease related deaths annually in the United States and 5.5 million adult deaths annually from cardiovascular disease worldwide in (2019; 10% of global deaths).[3,31,32] Further, development marks a critical window of exposure to Pb. Therefore, the studies conducted here aiming to understand how developmental Pb exposure affects heart biology is of imperative public health importance. By assessing Pb's impact on piRNA, transcriptomics, and function, we can better understand Pb's effects on the cardiovascular system, which will impact policies aimed at mitigating risk of Pb exposure.

Future research on how Pb impacts heart epigenetics, gene expression, and function in a sex specific manner should build off this work in order to elucidate underlying mechanisms and develop better policy, prevention, and therapeutic strategies to lessen the burden of Pb exposure for all.

5.11: References

1. World Health Organization. Cardiovascular diseases. Accessed August 9, 2023. https://www.who.int/health-topics/cardiovascular-diseases

2. Gao Z, Chen Z, Sun A, Deng X. Gender differences in cardiovascular disease. *Med Nov Technol Devices*. 2019;4:100025. doi:10.1016/j.medntd.2019.100025

3. Larsen B, Sánchez-Triana E. Global health burden and cost of lead exposure in children and adults: a health impact and economic modelling analysis. *Lancet Planet Health*. 2023;7(10):e831-e840. doi:10.1016/S2542-5196(23)00166-3

4. Svoboda LK, Wang K, Jones TR, Colacino JA, Sartor MA, Dolinoy DC. Sex-Specific Alterations in Cardiac DNA Methylation in Adult Mice by Perinatal Lead Exposure. *Int J Environ Res Public Health*. 2021;18(2):577. doi:10.3390/ijerph18020577

5. Rajan KS, Velmurugan G, Gopal P, et al. Abundant and Altered Expression of PIWI-Interacting RNAs during Cardiac Hypertrophy. *Heart Lung Circ*. 2016;25(10):1013-1020. doi:10.1016/j.hlc.2016.02.015

6. Yang J, Xue FT, Li YY, Liu W, Zhang S. Exosomal piRNA sequencing reveals differences between heart failure and healthy patients. *Eur Rev Med Pharmacol Sci*. 2018;22(22):7952-7961. doi:10.26355/eurrev_201811_16423

7. Zeng Y, Chen T. DNA Methylation Reprogramming during Mammalian Development. *Genes*. 2019;10(4):257. doi:10.3390/genes10040257

8. Hopper SE, Cuomo F, Ferruzzi J, et al. Comparative Study of Human and Murine Aortic Biomechanics and Hemodynamics in Vascular Aging. *Front Physiol*. 2021;12. doi:10.3389/fphys.2021.746796

9. Krishnan A, Samtani R, Dhanantwari P, et al. A detailed comparison of mouse and human cardiac development. *Pediatr Res*. 2014;76(6):500-507. doi:10.1038/pr.2014.128

10. Baccarelli A, Rienstra M, Benjamin EJ. Cardiovascular Epigenetics. *Circ Cardiovasc Genet*. 2010;3(6):567-573. doi:10.1161/CIRCGENETICS.110.958744

11. Uosaki H, Taguchi YH. Comparative Gene Expression Analysis of Mouse and Human Cardiac Maturation. *Genomics Proteomics Bioinformatics*. 2016;14(4):207-215. doi:10.1016/j.gpb.2016.04.004

12. Yutzey KE, Robbins J. Principles of Genetic Murine Models for Cardiac Disease. *Circulation*. 2007;115(6):792-799. doi:10.1161/CIRCULATIONAHA.106.682534

13. Absorption, Distribution, Metabolism, and Elimination: Differences Among Species | IVIS. August 9, 1999. Accessed September 17, 2025. https://www.ivis.org/library/veterinary-toxicology/absorption-distribution-metabolism-and-elimination-differences-among

14. Karakikes I, Ameen M, Termglinchan V, Wu JC. Human Induced Pluripotent Stem Cell-Derived Cardiomyocytes: Insights into Molecular, Cellular, and Functional Phenotypes. *Circ Res*. 2015;117(1):80-88. doi:10.1161/CIRCRESAHA.117.305365

15.Liang W, Gasparyan L, AlQarawi W, Davis DR. Disease modeling of cardiac arrhythmias using human induced pluripotent stem cells. *Expert Opin Biol Ther*. 2019;19(4):313-333. doi:10.1080/14712598.2019.1575359

16.Pozo MR, Meredith GW, Entcheva E. Human iPSC-Cardiomyocytes as an Experimental Model to Study Epigenetic Modifiers of Electrophysiology. *Cells*. 2022;11(2):200. doi:10.3390/cells11020200

17.Dorr KM, Conlon FL. Proteomic-Based Approaches to Cardiac Development and Disease. *Curr Opin Chem Biol*. 2019;48:150-157. doi:10.1016/j.cbpa.2019.01.001

18.Koss KL, Kranias EG. Phospholamban: a prominent regulator of myocardial contractility. *Circ Res*. 1996;79(6):1059-1063. doi:10.1161/01.res.79.6.1059

19.Silva MASC, de Oliveira TF, Almenara CCP, et al. Exposure to a Low Lead Concentration Impairs Contractile Machinery in Rat Cardiac Muscle. *Biol Trace Elem Res*. 2015;167(2):280-287. doi:10.1007/s12011-015-0300-0

20.Piquereau J, Caffin F, Novotova M, et al. Mitochondrial dynamics in the adult cardiomyocytes: which roles for a highly specialized cell? *Front Physiol*. 2013;4:102. doi:10.3389/fphys.2013.00102

21.Lai L, Qiu H. The Physiological and Pathological Roles of Mitochondrial Calcium Uptake in Heart. *Int J Mol Sci*. 2020;21(20):7689. doi:10.3390/ijms21207689

22.Kern M, Audesirk G. Stimulatory and inhibitory effects of inorganic lead on calcineurin. *Toxicology*. 2000;150(1-3):171-178. doi:10.1016/s0300-483x(00)00258-4

23.Siasos G, Tsigkou V, Kosmopoulos M, et al. Mitochondria and cardiovascular diseases—from pathophysiology to treatment. *Ann Transl Med*. 2018;6(12):256. doi:10.21037/atm.2018.06.21

24.Han Q, Zhang W, Guo J, et al. Mitochondrion: a sensitive target for Pb exposure. *J Toxicol Sci*. 2021;46(8):345-358. doi:10.2131/jts.46.345

25.Pirkle JL, Kaufmann RB, Brody DJ, Hickman T, Gunter EW, Paschal DC. Exposure of the U.S. population to lead, 1991-1994. *Environ Health Perspect*. 1998;106(11):745-750.

26.CDC. CDC Updates Blood Lead Reference Value. Childhood Lead Poisoning Prevention. January 31, 2025. Accessed September 22, 2025. https://www.cdc.gov/lead-prevention/php/news-features/updates-blood-lead-reference-value.html

27.Ericson B, Hu H, Nash E, Ferraro G, Sinitsky J, Taylor MP. Blood lead levels in low-income and middle-income countries: a systematic review. *Lancet Planet Health*. 2021;5(3):e145-e153. doi:10.1016/S2542-5196(20)30278-3

28.Legally-binding controls on lead paint. Accessed September 22, 2025. https://www.who.int/data/gho/data/themes/topics/indicator-groups/legally-binding-controls-on-lead-paint

29.Waldhorn I, Turetsky T, Steiner D, et al. Modeling sex differences in humans using isogenic induced pluripotent stem cells. *Stem Cell Rep*. 2022;17(12):2732-2744. doi:10.1016/j.stemcr.2022.10.017

30.Riva MA, Lafranconi A, D'Orso MI, Cesana G. Lead Poisoning: Historical Aspects of a Paradigmatic "Occupational and Environmental Disease." *Saf Health Work*. 2012;3(1):11-16. doi:10.5491/SHAW.2012.3.1.11

31.Lanphear BP, Rauch S, Auinger P, Allen RW, Hornung RW. Low-level lead exposure and mortality in US adults: a population-based cohort study. *Lancet Public Health*. 2018;3(4):e177-e184. doi:10.1016/S2468-2667(18)30025-2

32.Jha P, Brown PE, Ansumana R. Counting the global COVID-19 dead. *Lancet Lond Engl*. 2022;399(10339):1937-1938. doi:10.1016/S0140-6736(22)00845-5